The genetic and functional characterization of *ivp-3*

# The genetic and functional characterization the tumour suppressor *ivp-3* in *Caenorhabditis briggsae*

By Ramandeep Pabla,

*A Thesis Submitted to the School of Graduate Studies in the Partial Fulfillment of the Requirements for the Degree Master of Science*

McMaster University

Master of Science  (2017)

Hamilton, Ontario (Department of Biology)


TITLE: The genetic and functional characterization the tumour suppressor *ivp-3* in *Caenorhabditis briggsae*

AUTHOR: Ramandeep Pabla  (McMaster University)

SUPERVISOR: Dr. Bhagwati Gupta

NUMBER OF PAGES: xii, 100

# Abstract

*Caenorhabditis elegans* and one of its close relatives, *Caenorhabditis briggsae*, are animal models that are commonly used for comparative studies to understand the evolution of developmental mechanisms and gene function. Although the two species appear nearly identical morphologically, comparative genomic analyses have revealed interesting differences between the genomes. Whether such differences contribute to changes in developmental mechanisms and signalling pathways is an active area of research. One of the most well studied phenotypes associated with *C. elegans* signalling pathways are those that affect the specification of vulval tissue. Within the system of vuval development, mutants that exhibit the Multivulva (Muv) phenotype are important as they show inappropriate divisions of vulva cells, which model tumour formation. Comparing gene function in different species genetic backgrounds can lead to an understanding of how genetic differences contribute to different responses in cancer development. Genetic screens, conducted in our laboratory, yielded several genes whose loss of function results in a Muv phenotype and identified a novel regulator of *C. briggsae* vulval development, *Cbr-ivp-3*. Using the nematode *C. briggssae* as experimental system, we have characterized the tumour suppressor gene, *Cbr-ivp-3*, which impacts cell signalling and cell division. I have carried out molecular genetic analyses of *ivp-3* in both *C. briggsae* and *C. elegans* and have begun to characterize the functional role of *Cbr-ivp-3*. The findings in this thesis suggest that *Cbr-ivp-3* is functioning to negatively regulate EGF/*Cbr-lin-3*.

# *Acknowledgements*

I would first like to thank Dr. Bhagwati Gupta for giving me the opportunity to learn and grow under his supervision. I would like to thank my committee member Dr. Leslie MacNeil, for her support and invaluable advice, and Dr. Jonathan Stone for chairing my defence.

I would like to express my profound gratitude to to my colleagues in the Gupta Lab, for their help, encouragement and friendships. Looking back at my graduate career, the highlights will not only be the findings of my research but also the people I've worked with. Thank you for being a fantastic highlight in my research.

Finally, I am extremely appreciative to my family and to my better half for providing me with unfailing support and continuous encouragement throughout my years of study and through the process of researching and writing this thesis. This accomplishment would not have been possible without them. Thank you.

# Contents

# List of Figures

# List of Tables

# Acronyms

**AC** Anchor cell

**ALL** Acute Lymphoblastic Leukemia

**AML** Acute Myeloid Leukemia

**APC** Adenomatous *Polyposis coli*

**APL** Acute Promyelocytic Leukaemia

**Bag** Bag of Worms

**C/EBP$\alpha$** CCAAT/enhancer-binding protein-alpha

**Cbr** Caenorhabditis briggsae

**CDK** Cyclin-Dependent Kinase

**Cel** Caenorhabditis elegans

**CKI** Cyclin-Dependent Kinase Inhibitor

**CSL** CBF1, Suppressor of Hairless, LAG-1

**DIC** Differential Interference Contrast

**DSL** Delta/Serrate/LAG-2

**EGF** Epidermal Growth Factor

**EGFR** Epidermal Growth Factor Receptor

**Egl** Egg Laying Defective

**EMS** Ethyl Methyl Sulfonate

**ER** Estrogen Receptor

**ERK** Extracellular Signal-Regulated Kinases

**GRB-2** Growth factor Receptor-Bound protein-2

**GSK-3** Glycogen synthase kinase-3

**GSK3$\beta$** Glycogen Synthase Kinase 3 beta**Hh**Hedgehog

**Hyp** Hypodermis

**ivp** Inappropriate vulval cell proliferation

**JAK/STAT**Janus Kinase/Signal Transducer and Activator of Transcription

**MAML-1** Mastermind-like Protein

**MAPK** Mitogen Activated Protein Kinase

**MAPK** Mitogen Activated Protein Kinase

**MEC** Mammary Epithelial Cell

**MEK** Mitogen Activated Protein Kinase Kinase

**Muv** MultiVulva

**NHR** Nuclear Hormone Receptor

**NICD** Notch Intracellular Domain

**NRT** No Reverse Transcriptase Control

**NTC** No Template Control

**NuRD** Nucleosome Remodeling and Histone Deacetylase

**PCP** Planar Cell Polarity

**PML** Promyelocytic Leukemia

**PR** Progesterone Receptor

**Pvl** Protruding Vulva

**RT-qPCR** Reverse Transcription Quantitative PCR

**RAR** Retinoic Acid Receptor

**RB** Retinoblastoma

**RTK** Receptor Tyrosine Kinase

**SynMuv** Synthetic Multivulva

**TCF** T-cell factor

**TGF-$\beta$** Transforming Growth Factor Beta

**Utse** Uterine seam cell

**VPC** Vulva Precursor Cell

**VU** Ventral Uterine

**Vul** Vulvaless

**Wg**Wingless

# Declaration of Authorship

I, Ramandeep PABLA, declare that this thesis titled, "The genetic and functional characterization the tumour suppressor *ivp-3* in *Caenorhabditis briggsae*" and the work presented in it are my own. I confirm that:

**Chapter 3:Characterization of a novel vulva development gene *ivp-3***
I have performed the experiments for this thesis including *Cbr-ivp-3* sequencing to determine the open reading frame in AF16 and the nonsense mutation in the *Cbr-ivp(gu236)* mutant. The nonsense mutations in *Cbr-ivp(sy5216)* and *Cbr-ivp-3(sy5392)* were identified by Devika Sharanya. I have carried out phenotypic analysis for all three *Cbr-ivp-3* Muv mutants. Although *Cbr-ivp(sy5216)* had been analysed prior by Devika Sharanya, I have been able to reproduce her findings. I also analyzed the phenotypes of the MMP mutants, carried out molecular and phenotypic analysis of the *ivp-3* deletion strain *(gk3691)*, conducted qRT-PCR of *Cbr-lag-2* and *Cbr-lin-3* in *Cbr-ivp(sy5216)*, generated the *Cbr-lin-3* RNAi plasmid, and preformed RNAi knockdown of *Cbr-lin-3* in *Cbr-ivp(sy5216)*. Analysis of the RNAseq data was carried out by Ayush Ranawade and I carried out the Go Term enrichment analysis to identify potential target genes and validation of these target genes from the RNAseq dataset using qRT-PCR.

# Chapter 1

# Introduction

## 1.1 Cell Fate Specification and Cell Proliferation

The regulation of cell proliferation and cell fate specification plays a pivotal role in the development and maintenance of tissues. The early stages of metazoan development are characterized by the rapid proliferation of embryonic cells, followed by cell fate specification and differentiate to produce various specialized cell types, resulting in the formation of tissues and organs (Lambie 2002). Cell proliferation refers to an increase in the number of cells resulting from cell growth and cell division (Lambie 2002). The rate at which cells proliferate depends on cell growth and cell divisions, as well as the rate of cell loss, through apoptosis or differentiation (Lambie 2002). The process of cell fate specification requires that a particular subset of cells assumes a unique expression pattern such that their descendants adopt a definitive fate and carry out a specialized function (Maduro 2010). A balance between proliferation and specification is essential to ensure homeostasis.

In early embryos, cells increase in number through cell proliferation, which becomes restricted as an organism develops. Although some differentiated cells continue to proliferate, replacing cells when required, others lose their ability to do so after they have differentiated (Kim and Orkin 2011). Embryonic cells often display traits, distinct from adult cells, that provide them with a selective growth advantage. Such traits include rapid proliferation, extensive migration, and secreting factors that increase the local blood supply; all are also characteristic of

tumour cells (Kim and Orkin 2011). Embryonic cells can accumulate mutations in their DNA that can transform them into cancer cells. The mutated cells generally acquire abnormal proliferative capacity and cannot undergo the normal processes of differentiation (Kim and Orkin 2011). Such mutations in hematopoietic progenitor cells can promote proliferation by preventing cell death and producing a growth-promoting signal, which can lead to various types of leukemia (Lodish et al. 2000). Similarly, colon cancer is a result of mutations in proliferating cells that are constantly generated to replenish epithelial cells lining the colon (Lodish et al. 2000). Genetic or epigenetic alterations in mammary epithelial cells (MECs) can modify cell fate decisions during the earliest steps of tumour formation (Gross et al. 2016). In another example, the steroid hormones estrogen and progesterone play a role in the development of breast cancer, through the actions of their receptors. The majority of breast cancers ($\sim$70%) express estrogen receptors (ER) and progesterone receptors (PR) at the time of diagnosis. The hormones bind to these receptors, found on cancer cells, and promote cell proliferation (Lange and Yee 2008).

Throughout development, and in adult organisms, the ability of a cell to proliferate and its state of differentiation are closely connected. Adult tissues generally express factors, such as secreted molecules, transmembrane receptors, intracellular signalling molecules, and transcription factors, that act to maintain both the proliferation and the differentiation status of cells (Andreeff, Goodrich, and Pardee, 2003). The disruption of transcription factors that regulate these processes is commonly associated with cancer. An example can be seen in the genes involved in acute promyelocytic leukemia, PML and RAR (retinoic acid receptor) (Rousselot et al. 1994). RAR is a transcription factor often involved in differentiation. Its fusion to PML, due to chromosomal translocations, causes it to behave as a repressor of target genes related to differentiation, resulting in the disease (Rousselot et al. 1994). Furthermore, the transcription factor CCAAT/enhancer-binding protein-alpha (C/EBP$\alpha$) is required in stem cell differentiation (Khanna-Gupta et al. 2009). Dysfunction of C/EBP$\alpha$ causes differentiation to be hindered and as a result, the cells remain in a proliferative state, providing them with a growth advantage compared to the normal cells (Khanna-Gupta et al. 2009). A mutation in C/EBP$\alpha$ is found in $\sim$7-15% of acute myeloid leukemia (AML) cases and family

members with a predisposition to develop AML were found to have a germ line mutation in one allele of the transcription factor (Khanna-Gupta et al. 2009).

## 1.2 Cellular and Molecular Mechanisms of Cell Growth

Cancer is a disease of uncontrolled cell proliferation. The adverse effects of cancer are a result of the increase in the number of tumour cells. Reducing the number of tumour cells, thus preventing further accumulation of these cells is the goal of many cancer therapies. The mechanisms that underlie tumour and normal cell proliferation are very similar, therefore understanding the unique characteristics of tumour cell proliferation is made difficult. The following section provides a review of the current understanding of the complex molecular mechanisms involved in the regulation of cell proliferation.

### 1.2.1 Cell Cycle Control to Limit Cell Growth

A number of anti-proliferative signals are received by most mammalian cells, ensuring either temporary or permanent arrest of the cell cycle (Nishikawa et al. 2008). A resistance to the anti-proliferative growth signals must be developed by tumour cells in order to remain in a constant state of proliferation. Many tumour cells develop mutations in genes that regulate the cell cycle. In normal cells, the transition from one cell cycle event to the next is dependent on a series of checkpoints (Zetterberg et al. 1995). Entry into the next phase of the cell cycle is allowed only after completion of a particular cell cycle event. Any dysregulation of these vital checkpoints can contribute to cancer. For example, dysregulation of proteins controlling the spindle-assembly checkpoint, result in chromosomal imbalance and aneuploidy, a feature observed in almost all cancers (Zetterberg et al. 1995).

Passage of the cell cycle checkpoints requires the activation of serine/threonine kinases known as cyclin-dependent kinases (CDKs) (Bird 2003). The activation of

CDKs is the central event in cell cycle transitions and occurs when cyclin proteins bind to CDKs (Bird 2003). There are several mechanisms that control the activity of CDKs. The synthesis of cyclins is one level of control. Different cyclin proteins are synthesized depending on a particular stage of the cell (Bird 2003). For example, cyclin D production is initiated during G1 and is involved in the G1/S phase transition and cyclin E is synthesized in the late G1 and early S phase (Blomen and Boonstra 2007). In human cancers, alterations in cyclin D are detected more frequently than mutations in genes that regulate other cell cycle events (Sherr and Roberts 1999). The interaction between CDKs and different cyclins allows the corresponding CDKs to phosphorylate a number of downstream targets (Bird 2003). The degradation of cyclins also occurs at specific times during the cell cycle and is mediated by ubiquitin-dependent proteolysis (Bird 2003). Another mechanism in which CDKs can be regulated is through the phosphorylation and dephosphorylation of the ATP-binding site of CDKs by other regulatory protein kinases (Queralt and Uhlmann 2008). This kinase activity is unusual in that it has dual specificity, where phosphorylation of its ATP-binding site will deactivate the CDK and reactivation can occur by a phosphatase from the Cdc25 family (Hoffmann 2000). Another method of regulation involves the expression of cyclin-dependent kinase inhibitors (CKIs), which can block cyclin-CDK activity (Sherr and Roberts, 1999). Furthermore, cell cycle regulatory proteins can be targeted for degradation by the proteasome (Leuken et al. 2008; Kitagawa et al. 2009).

### 1.2.2   Tumour Suppressors and Proto-Oncogenes

In the event that DNA damage occurs, normal cells respond by activating cell cycle checkpoints, initiating the transcription of genes involved in DNA repair, and inducing apoptosis (Gartner et al. 2000). The p53 gene plays a key role in responses to damaged DNA as more than 50% of human tumors contain mutations in this gene (Sherr and McCormick 2002). The p53 protein functions as a transcription factor, affecting the transcription of a number of genes. In particular, p53 activates the p21 CKI gene in response to DNA damage (He et al. 2005). It has been found that the p21 gene is not transcribed in cells that experience a loss of p53 (He et al. 2005). This results in increased activity of numerous CDKs, normally

inhibited by p21 and thus leads to an increase in cell proliferation. In addition, p53 inhibits tumour formation by inducing apoptosis (Schumacher et al. 2001). Mutations that result in the complete loss-of-function of p53, lead to increased cell proliferation, decreased apoptosis, and tumour development. Such mutations are found in virtually every type of cancer, including breast cancer, colon cancer, and lung cancer (Sherr 2004). These findings signify the importance of the p53 gene and its prevention of the formation of tumours.

Genes such as p53 are known as tumour suppressors and are defined as genes which encode proteins that normally inhibit the formation of tumours. Mutations in tumour suppressor genes contribute to the development of cancer by inhibiting their inhibitory function (Sherr 2004). Another example of a tumour suppressor is the retinoblastoma (RB) gene (Knudsen and Knudsen 2006). Hundreds of mutations in this gene have been identified in individuals with retinoblastoma, a rare type of eye cancer that typically occurs in young children. The RB protein plays a key role in regulating the cell cycle (Knudsen and Knudsen 2006). The transcription factor E2F is responsible for the expression of the cyclin E gene (Nevins 2001). Cyclin E forms a complex with Cdk2, allowing for the transition from mitogen-dependent to mitogen-independent cell cycle progression (Yamasaki 2004). In normal cells, RB binds and inactivating the E2F transcription factor and therefore, loss of RB results in E2F activation (Nevins 2001). Because activation of the Cdk2-cyclin E complex allows for cell proliferation to occur in the absence of a mitogen, inactivation of RB can cause cells to remain in a constant proliferating state (Nevins 2001).

While tumour suppressor genes result in protein products that normally prevent cell division and promote apoptosis, proto-oncogenes produce protein products that normally enhance cell division and inhibit cell death. Oncogenes are the mutated, cancer-causing forms of proto-oncogenes, that increase the activity or expression of the normal gene, promoting uncontrolled cell proliferation (Rajalingam et al. 2007). One example of a proto-oncogene is cyclin D, which can be activated through several different mechanisms (Hunter and Pines 1994). Firstly, cyclin D normally functions to inactivate the RB protein by phosphorylating it (Narasimha et al. 2014). The gene is often amplified in cancers leading to reduced activity

of RB. It has been found that the cyclin D gene is often overexpressed in breast cancer (Narasimha et al. 2014). Cyclin D has also been found to play a role in tumours of the parathyroid gland, leading to uncontrolled release of calcium from bones (Vasef et al. 1999). A chromosome inversion can cause the transcriptional control region of the parathyroid hormone gene to be placed beside the cyclin D gene (Vasef et al. 1999). As a result, the cyclin D gene is expressed continuously, thus promoting proliferation. Myc is another example of an oncogene and is often found to be overexpressed in cancers. In Burkitt's lymphoma, Myc becomes over-expressed due to a chromosomal translocation where the promoter sequence, that normally drives the expression of large amounts of antibodies in B cells, is incorrectly placed next to the Myc protein coding sequence, producing large amounts of Myc mRNA (Boxer and Dang 2001). This results in mutant B cells which produce large amounts of the Myc protein and proliferate excessively, leading to the formation of tumours. Lastly, Ras is the most commonly activated oncogene in human tumours (Rajalingam et al. 2007). A large fraction of tumours carry mutations in one of the three Ras genes encoded by the human genome (H-ras, K-ras, N-ras) (Prior et al. 2012). It has been found that 70-90% of pancreatic cancer cases contain a mutation in the K-ras gene (Prior et al. 2012). A point mutation in Ras produces defective proteins that are unable to hydrolyze GTP thus the mutant Ras proteins remain in their active, GTP-bound state (Rajalingam et al. 2007). Constitutively active Ras continually activates the downstream MAP kinase pathway, which subsequently leads to cell proliferation (Rajalingam et al. 2007). The Ras pathway is one of several conserved oncogenic signalling pathways that play a potential role in the development of cancer cells. Ras and other signalling pathways, such as Wnt and Notch, are required for the promotion of cell division and alterations in components of these pathways are commonly observed in tumours.

### 1.2.3  Signalling Pathways

Many genetic alterations, that allow cancer cells to proliferate excessively and escape the normal regulation of cell survival, are found in signalling pathways. These pathways that control cell growth, cell death, cell fate, and differentiation decisions,

are also common causes of tumorigenesis. Mutations that convert proto-oncogenes to oncogenes can cause important signalling pathways to be over-activated, and mutations in tumour suppressor genes can result in the elimination of key negative regulators of signalling (Kobet et al. 2014). An examination of the Ras, Wnt, and Notch signalling pathways will be discussed to demonstrate how disruptions in such pathways can result in the formation of tumours.

The highly conserved signalling pathways involving Ras-ERK (extracellular signal-regulated kinases)/MAPK (Mitogen Activated Protein kinase) play a role in cell proliferation, differentiation, cell fate specification, and cell survival (Marshall 1995; Whelan et al. 2012). The pathway is activated when epidermal growth factor (EGF) ligands bind to the epidermal growth factor receptor (EGFR), activating the tyrosine kinase activity in the cytoplasmic domain of the receptor. The binding adaptor protein of EGFR, Grb2, binds to SOS, the guanine nucleotide exchange factor, forming the Grb2/SOS complex which can then bind to the phosphorylated EGFR (Schulze et al. 2005) (Figure 1.1). Once the complex is docked, SOS activates the small GTPase, RAS. RAS then stimulates a MAPK cascade consisting of the kinases RAF, MEK and ERK, where each kinase phosphorylates and activates the next, respectively (Sundaram 2006). The activated ERK can then positively or negatively regulate downstream targets via phosphorylation (Figure 1.1). Examples of downstream targets include transcription regulators such as GATA-1 (Towatari et al. 2004), translational regulators (Zhao et al. 1996), cell cycle regulators such as Cyclin D1 (Okabe et al. 2006), and apoptosis regulators (Tamura et al. 2004). Since the activation of Ras signalling regulates gene expression, cell cycle progression, proliferation, and survival, any alterations in this pathway can lead to abnormalities in these processes. This signalling pathway is found to be deregulated in nearly one-third of all human cancers (Dhillon et al. 2007). In addition to the Ras pathway, aberrant Wnt signalling is observed in many cancers.

The Wnt signalling pathway is necessary in many aspects of animal development, such as the self-renewal of stem cells, cell fate specification, cell differentiation, polarity, and cell migration (Katoh 2008). Wnt signalling is necessary for the proliferation of stem cells in the proliferative zones in the gut epithelium.

Most cases of colon cancer are associated with the hyperactivation of this pathway (Zhan et al. 2016). The canonical Wnt/$\beta$-catenin pathway, non-canonical Wnt/planar cell polarity (PCP) pathway, and non-canonical Wnt/calcium pathway are the three Wnt signalling pathways (James et al. 2008), all of which are activated when the Wnt ligand binds to a Frizzled family receptor (Figure 1.2). When this ligand is not present, $\beta$-catenin interacts with APC (adenomatous polyposis coli) and Axin scaffold proteins in the cytoplasm (Kobet et al. 2014). The $\beta$-catenin is then phosphorylated by CKI$\alpha$ kinase and GSK3$\beta$ (Glycogen Synthase Kinase 3 beta), leading to its ubiquitination and subsequent degradation by the proteasome (Kobet et al. 2014) (Figure 1.2). In the canonical pathway, CKI$\alpha$, GSK3$\beta$, APC, and Axin act as negative regulators (Kobet et al. 2014). For example, since APC is necessary to regulate $\beta$-catenin levels, loss or inactivation of APC is associated with development of colorectal cancer (Moon et al. 2014). In the presence of the Wnt ligand, the stabilized $\beta$-catenin is translocated into nucleus, where it interacts with T-cell factor (TCF) family transcription factors (Figure 1.2). This allows for the activation of the expression of target genes such as MYC, Cyclin D1 and other target genes that are involved in cell proliferation and cell differentiation (He et al. 1998; Chamorro et al. 2005). Dysregulation of such target genes have lead to the development of multiple types of cancer, including colon, breast ovarian, and thyroid (Zhan et al. 2016). Furthermore, the canonical Wnt/$\beta$-catenin pathway is vital for the regulation of stem cells (Nusse et al. 2008). For example, Wnt/$\beta$-catenin signalling controls mammary gland stem cell maintenance at different stages of development (Wend et al. 2010; Holland et al. 2013). These mammary gland stem cells can give rise to ductal, myoepithelial and alveolar components (Holland et al. 2013). Abnormalities in Wnt/$\beta$-catenin signalling lead to cancer in the mammary gland. Along with the Wnt pathway, Notch signalling is another important pathway in which aberrant signalling can result in tumour formation.

The Notch signalling pathway is highly conserved in most multicellular organisms. It plays a role in controlling proliferation, cell fate specification, cell differentiation, and apoptosis (Artavanis-Tsakonas et al. 1999). The Notch receptor and most of its ligands are transmembrane proteins. The Notch ligands, are expressed in the cells that are adjacent to the cells expressing Notch (Kobet et al. 2014).

The transcription factor CSL (CBF1, Suppressor of Hairless, LAG-1) is associated with co-repressors and prevents the expression of Notch target genes when Notch is not present (Andersson et al. 2011) (Figure 1.3). Interaction of Notch with a ligand, such as LAG-2, a transmembrane protein and a member of the DSL (Delta/Serrate/LAG-2) family, causes cleavage of the outside of the Notch receptor by an ADAM-family metalloprotease (Bray 2016). Cleavage of the remaining portion of the receptor, inside the cell membrane, then occurs by $\gamma$-secretase, releasing the intracellular domain of Notch (NICD) (Andersson et al. 2011) (Figure 1.3). NICD then enters the nucleus where it forms a complex with transcription factors CSL and mastermind-like protein (MAML-1), resulting in the transcription of target genes (Bray, 2016) (Figure 1.3). Abnormal activation of Notch signalling has been detected in a number of human cancers including pancreatic cancer (Ristorcelli and Lombardo 2010), colon cancer (Miyamoto and Rosenberg 2011), lung cancer (Galluzzo and Bocchetta 2011), and breast cancer (Reedijk 2012). Mutations in which human Notch1 becomes activated, are reported in approximately half of acute lymphoblastic leukemia (ALL) cases (Ferrando 2009). Studies have shown that Notch signalling is upregulated in pancreatic cancer stem cells (Abel et al. 2014). The reduction of Notch signalling either genetically or by treatment with $\gamma$-secretase inhibitor in human pancreatic cancer cell lines in tissue culture, showed a decrease in cancer stem cell populations and tumour formation (Abel et al. 2014).

### 1.2.4 The Role of Model Organisms in Understanding Cancer

Studies of model organisms have allowed for the identification of a number of highly conserved signalling pathways involved in the control of cell growth, cell death, cell fate decisions, and cell differentiation. Such pathways have been shown to play critical roles in the progression of tumours. Research in model systems has contributed to our knowledge of pathways involved in cancer and their application to human medicine.

Before the development of genetic mouse models, cancer was studied using cell culture systems of cell lines derived from human tumours (Goodspeed et al. 2016). The use of these systems are still used today and remain important in cancer research, however, limitations such as the inability to examine physiological interactions between other cells and their environment, resulted in the search for in vivo systems (Goodspeed et al. 2016). The mouse (*Mus musculus*) can be used as a model to overcome such limitations and has greatly facilitated our understanding human genetic disorders. The ability to make targeted gene knockouts makes the mouse model highly advantageous. For example, disruption of tumour suppressor genes and activation of oncogenes in mice often result in embryonic lethality or severe phenotypes (Gowen et al. 1996). Early embryonic lethality can be found in a knockout model of the tumour suppressor, *Brca-1*, which is commonly found to be mutated in human breast cancers (Gowen et al. 1996). The use of knockout models plays an important role in understanding how loss-of-function mutations in particular genes can result in the development of cancer. Furthermore, genetically engineered mouse models (GEMMs), have been utilized to study the function of human genes in diseases such as cancer. For example, acute promyelocytic leukaemia (APL) is a cancer of the bone marrow, occurring mostly in younger individuals (Pandolfi et al. 1991). Researchers used GEMMs to mimic the six types of APL, which are caused by different gene fusions (Pandolfi et al. 1991). Through clinical trials in both mice and humans, a cure was developed. Mouse models are an excellent vertebrate model for studying cancer genes and provide insights into the molecular mechanisms involved in tumorigenesis.

Invertebrates models are also extremely useful tools for understanding tumour biology and have lead to the discovery of a number of signalling pathways that play conserved roles in human development. For instance, many of the components essential in the cell cycle network are conserved from yeast (*Saccharomyces cerevisiae*) to mammals. In fact, CDKs, first discovered in yeast, can be derived from human cells and can be used to substitute CDKs in yeast (Wilson-Sanders 2011). The most commonly used invertebrate models are the fruit fly, *Drosophila melanogaster,* and the nematode, *Caenorhabditis elegans.*

Both *Drosophila* and *C. elegans* have contributed to numerous biological discoveries, such as the creation of the first chromosome maps, the one gene-one protein hypothesis, the temporal and spatial expression of genes to specify cell fates, and the identification of a number of genetic pathways implicated in human disease (Neidich 2005). Furthermore, genetic analyses of pattern formation in both models, have lead to the discovery of a number of signalling pathways and pathway components that are involved in cell fate development, including Notch, receptor tyrosine kinase (RTK), G protein-coupled receptor, Hedgehog (Hh), Wingless (Wg) and Janus kinase/signal transducer and activator of transcription (JAK/STAT) (Neidich 2005). Due to the high degree of evolutionary conservation between vertebrate and invertebrate genetic systems, mutations associated with a number of human diseases, have been identified in components of almost all of these pathways (Neidich 2005). Because most of these signalling pathways are associated with cell cycle regulation, aberrant signalling pathways can result in the failure to control cell proliferation, and subsequently lead to cancer. The genetic analysis of these invertebrate models has allowed for the discovery of a number of developmental pathways that are commonly conserved among most organisms. In this study, *C. elegans* and a close relative of the nematode, *Caenorhabditis briggsae*, were used to uncover the mechanism by which conserved signalling pathways regulate vulval development.

## 1.3 *C. elegans* as a Model Organism to Study the Genetic Bases of Development and Gene Function

Model organisms provide valuable tools to understand the genetic basis of animal development. Several *Caenorhabditis* species have been developed as models for comparative studies. These nematodes have been found to display an invariant cell lineage and developmental processes that are similar to each other, therefore allowing for comparative studies to take place (Sommer 2005). In the last decade,

developmental processes such as embryonic, gonad, vulva and male tail development, have been compared in up to five nematode families (Sommer 2005). These studies have provided insight into unique evolutionary changes in development. Studying developmental processes in multiple species are important in providing a comprehensive overview about variations, can help identify conserved genes and processes, and even have the potential to discover new genes that might not be present in one species. The identification of variations within developmental processes between species can help determine random fluctuations in the system i.e biological noise and environmental variations resulting from robustness (Félix and Wagner 2008).

*C. elegans* is a leading nematode animal model that allows for simplified studies of diverse and complex fundamental processes. Studies involving this model organism have provided a means for investigating the genetic basis of development and gene function and provide insights into the cellular and molecular basis of organ formation.

Since its establishment as a simple model for genetic and developmental studies, by Sydney Brenner, *C. elegans* has become the cornerstone of invertebrate model research. The use of the organism has lead to important discoveries in diverse fields such as development, signal transduction, cell death, aging, and RNA interference (RNAi). There are a number of useful features that make this nematode an attractive system for studies.

*C. elegans* feed on bacteria, such as *E. coli*, and are small (about 1- 1.5 mm) so they can be easily cultivated and housed in large numbers in the laboratory. The animals can be maintained in a frozen state for many years and can easily be re-grown by thawing (Brenner 1974). *C. elegans* have an invariant somatic cell lineage which has been completely characterized, thus the analysis of phenotypes that disrupt normal proliferation and patterning can be easily followed (Sulston and Horvitz 1977). Furthermore, the animals are transparent, thus the influence of genetic changes in cell fate, location, morphology and differentiation in an intact organism, can be observed using a dissecting microscope or a simple differential interference contrast (DIC) microscope (Sulston and White 1980). The nematode has a short life cycle (3 days) and can produce upwards of 300 progeny per mother,

making experiments relatively rapid and the production of numerous generations possible. Male and hermaphrodites are the two sexes present in a population. The hermaphrodites can self-fertilize or mate with males to produce offspring. Thus, crosses or self-fertilization can be manipulated as desired. Followinf fertilization, the egg is laid and hatch. The animal then proceeds through four larval stages (L1-L4) before becoming an egg-laying adult. *C. elegans* are able to survive in conditions of starvation or overcrowding by entering a dauer stage. The worms can survive in the dauer stage for months and return to a normal life cycle when the conditions become ideal again (Brenner 1974).

A large number of tools and resources are available in *C. elegans* that facilitate genetic studies that lead to new discoveries (WormMethods). *C. elegans* was the first multicellular organism to have its genome completely sequenced (Kimble and Hirsh 1979). New genetic and molecular tools that are constantly being developed and forward or reverse genetics approaches, can be used to clone or character-ize genes. Another intriguing feature that makes *C. elegans* a successful model organism is that they share many fundamental structures and developmentally conserved pathways with other organisms, including vertebrates such as mice and humans. These commonalities allow for the study of complex processes in a sim-pler system and enable researchers to apply their findings from one organism to others.

## 1.4 *C.briggsae* as a Model for Comparative Studies

*C. elegans* is a member of the genus *Caenorhabditis*, which includes a large number of diverse species. Although members of this genus seem morphologically simi-lar, the species show great ecological and genetic diversity (Kiontke and Sudhaus 2006). Several *Caenorhabditis* species are currently being utilized in laboratories for comparative studies, one of which is *C. briggsae*.

*C. briggsae* has been used extensively in comparative studies and is an attractive model system for studying the evolution of animal development and behaviour (Cutter 2008). It is frequently used in comparative studies to understand species-specific function of genes orthologous to *C. elegans* and can reveal evolutionary similarities and differences in the signalling and regulation of genes as well as developmental processes. The *C. briggsae* genome has been sequenced (Stein et al. 2003) and subsequent RNAseq analysis (Uyar et al. 2012) has made *C. briggsae* valuable in reverse genetics and genome-wide comparative studies. Such studies can provide insight into how conserved pathways are regulated in higher organisms.

Comparative analysis studies of *C. elegans* and *C. briggsae* to date have provided some insights into the evolution and role of particular sequences, genes, and pathways. Diverged from a common ancestor approximately 50 –120 million years ago (Coghlan and Wolfe 2002), the two species appear almost identical morphologically and occupy the same ecological niche (Stein et al. 2003). They are both soil-dwelling animals, containing self-fertilizing hermaphrodites and facultative males. They have genomes that are similar in organization and size, each containing six chromosomes, approximately 100 Megabases (Mb) in size (Stein et al. 2003). Studies, in which genes isolated in one species rescue mutant phenotypes in the other, demonstrate functional conservation between these species (Krause et al. 1994). It should be noted, however, that not all genes will rescue in a similar manner and thus not all genes are functionally conserved. Examination of differences between *C. elegans* and C. briggsae, such as vulva formation, sex determination, thermal sensitivity, RNAi uptake, excretory pore formation, and male tail development have revealed alterations in gene function (Gupta et al. 2007). For example, the uptake of ingested dsRNAs into intestinal cells requires the transmembrane protein SID-2 in *C. elegans*. Interestingly, *C. briggsae* encodes a divergent form of *sid-2*, and is unable to take up dsRNAs. The inability of *C. briggsae* to take up ingested dsRNAs can be rescued by expression of *C. elegans sid-2* in *C. briggsae* (Nuez and Félix 2012). These interspecific variations are indicative of evolutionary divergence resulting from alterations in the genome.

Comparative analyses have indicated that the genomes of *C. elegans* and *C. briggase* have diverged considerably (Stein et al. 2003). Despite having genomes

similar in organization and size, alignment of the nucleotide sequences of *C. elegans genome* with the wildtype C. briggsae genomic sequence shows a 52.3% alignment and 50.1% of the *C. briggsae* genome aligns with the *C. elegans* genome (Stein et al. 2003). It has also been found that 12 200 genes of the 19 500 protein-coding genes in the *C. briggsae* genome, ($\sim$60%) have clear *C. elegans* orthologs, a third of genes have one or more clearly detectable *C. elegans* homologs, and approximately 800 genes in *C. briggsae* have no matches with *C. elegans* (Stein et al. 2003). Analysis of 142 orthologous intergenic regions of *C. elegans* and *C. briggsae* indicates regions of up to 20% similarity, flanked with non-alignable sequence (Webb et al. 2002). It was also found that about 51% of operons are conserved in *C. elegans* while the remaining operons are divergent or specific to *C. briggsae* only (Stein et al. 2003; Uyar et al. 2012). Additionally, the slight difference in the genome size between *C. elegans* and *C. briggsae* (100.3Mbp and 104 Mbp, respectively) is mostly a result of sequence repeats, accounting for 22.4% of the *C. briggsae* genome and 16.5% of the *C. elegans* genome (Gupta et al. 2007). The role of alternative splicing is important in species specificity as it provides a means of regulating and diversifying gene function (Blencowe 2006). It has been found that there is limited conservation of genes with alternative splice forms however, further validated through comparison of transcriptomes of the nematodes at different developmental stages and environmental conditions is required (Uyar et al. 2012).

A comparison of the *C. elegnas* and *C. briggsae* genomes has revealed significant sequence differences. Whether such differences contribute to changes in developmental mechanisms and signalling pathways is an active area of research. More work is needed to fully understand the impact on gene networks. By studying developmental pathways in *C. briggsae*, similarities and differences to *C. elegans* can be uncovered, providing clues about gene evolution and its role in development.

# 1.5 Vulva development as a Model to Understand Mechanisms of Cell Fate Specification and Cell Proliferation

The formation of the *C. elegans* vulva is a powerful yet simple model for understanding how mechanisms of cell fate specification and cell proliferation are involved in the process of organogenesis. The simplicity of the vulva and the experimental tools available in *C. elegans*, make vulval morphogenesis a useful model to further our understanding of the mechanisms that build tissues and organs.

## 1.5.1 The Vulva as a Genetic Model Organ

The vulva is an excellent model to study developmental pathways and genes involved in cell signalling and cell division. This is due to that fact that the cell lineages that form the vulva and the effects of countless mutations on vulval development can be easily observed throughout the life of the animal. Furthermore, the vulva is not an essential organ, thus a number of mutations that cause vulval phenotypes are viable.

Within the system of vulval development, mutants that exhibit the Multivulva (Muv) phenotype are important as they show inappropriate division of vulva cells. The Gupta lab has a large collection of *C. briggsae* vulval mutants that have less than the normal number of cells (Vulvaless or Vul) or more cells Muv. In Muv mutants, multiple tumor-like protrusions, known as pseudovulvae, are present on the ventral surface of the animal (Fay and Yochem 2007). These pseudovulvae arise due to abnormal and uncontrolled cell division (Ferguson and Horvitz 1985). In Vul mutants, the vulva is not formed and eggs are not laid. As a result, the eggs hatch inside the mother, eventually escaping from the corpse, resulting in a bag of worms (Bag) phenotype. This Bag phenotype is also observed in mutations that cause an egg laying defective (Egl) phenotype (Trent et al. 1983). Vul genes promote vulval development (Ferguson and Horvitz 1985), where as Muv genes inhibit inappropriate division of vulva precursors (Fay and Yochem 2007). Other

mutations such the protruding vulva (Pvl) cause morphological defects in the vulva. Together, these mutant strains serve as valuable tools for comparative and evolutionary studies. Understanding and comparing the mechanism of gene function between *C. briggsae* to *C. elegans* can reveal how distinct processes form the nearly identical vulval structures in these two species.

## 1.5.2 The Cellular Events of Vulval Development

There are three main stages involved in vulval development. The first stage involves the formation and maintenance of the vulval competence group. In the *C. elegans* hermaphrodite, the animal is born with two rows of six P cells, some of which are the progenitors of all vulval cells, that are located in the mid-ventral region (Sulston and Horvitz 1977). During the L1 stage, migration of the P cells to the ventral midline of the animal occurs, followed by division where six daughters of the P cells become the vulval precursor cells (VPCs, P3.p-P8.p) (Sulston and Horvitz 1977). In the L2 stage, the gonadal anchor cell (AC) forms through interaction with Z1.ppp and Z4.aaa, the two gonadal cells, which become the AC and a ventral uterine (VU) cell (Hirsh et al. 1976). The formation of the AC allows for the competence of the VPC to be maintained (Wang and Sternberg 1999).

In the second stage of vulval development, the VPCs differentiate and proliferate. Inductive signals by the AC cause the VPCs to acquire the primary (1°), secondary (2°), or tertiary (3°) fates during the third larval (L3) stage (Sternberg and Horvitz 1989). The P6.p is induced by the AC to acquire a 1° fate, and both P5.p and P7.p adopt a 2° fate (Figure 1.4) (Sternberg and Horvitz 1986). A 3° fate is acquired by the VPCs that do not receive the inductive signal (P3.p, P4.p and P8.p) (Sulston and Horvitz 1977). Following induction by the AC, the VPCs divide longitudinally, and the daughters of the 3° VPCs fuse with a hypodermal syncytium (hyp7) (Figure 1.4). The 1° VPC P6.p undergoes cell division in a TTTT lineage (T is transverse axis of cell division) in the second round of divisions (Figure 1.4). Similarly, the 2° VPCs, P5.p and P7.p, undergo cell division, but in a NTLL lineage (N - no division, T – transverse and L – longitudinal axis) in opposite orientations (Figure 1.4). In the third round of cell divisions, eight

progeny (P6.pxxx) are generated with two adult cell types (vulE and vulF) in a mirrored pattern (Sternberg and Horvitz 1986) (Figure 1.4). The 2° VPCs produce seven progeny cells (P5.pxxx and P7.pxxx) and after the third round of cell division five cell types (vulA, vulB1, vulB2, vulC and vulD) are produced (Sternberg and Horvitz 1986) (Figure 1.4). It is these 22 cells that make up the functional, adult vulva.

Vulval morphogenesis is the last stage in vulval development and begins during the L3 stage, when the AC breaks the basement membrane that separate it from the descendants of the 1° P6.p cell (Sherwood et al. 2005). The descendants of the VPCs migrate towards the centre of the developing vulva and during the L4 stage, the vulval toroids form. Some of these cells fuse within the toroids. Subsequently, the vulva invaginates and the lumen of the vulva forms, the muscles attach to the vulva and are innervated. The AC then fuses with the eight pi cells of the uterus, forming the multinucleated syncytium, utse (uterine-seam cell). Lastly, the vulva undergoes eversion, turning inside out to form the adult vulva (Sherwood et al. 2005).

### 1.5.3   Signalling Pathways involved in Vulva Development

The formation of the vulva requires essential developmental processes which allow for cell fate specification, cell differentiation, cell migration, and cell fusion. Signalling pathways play a key role in coordinating such processes through crosstalk between other pathways and by regulating the expression and activity of several target genes. Conserved signalling pathways such as EGF-receptor/LET-23, Ras/LET-60 and ERK/MAPK, LIN-12 /Notch, and Wnt have been identified from studies based on the vulva mutant phenotypes discussed previously Fay and Yochem (2007).

Activation of the Let-23/Let-60/MAPK signalling pathway requires the secretion of the epidermal growth factor LIN-3/EGF by the AC (Hill and Sternberg 1992). During vulva development in *C. elegans*, Let-23/Let-60/MAPK signalling

is required to prevent ectopic cell fusion (Pellegrino et al. 2011; Alper and Podbilewicz 2008), for the division of the VPCs (Clayton et al., 2008), and for the 1° fate specification of P6.p (Wang and Sternberg 2000).

During vulval development in *C. elegans*, LIN-12/NOTCH signalling plays a role cell-cell communication and the formation of the vulva-uterine connection (Seydoux and Greenwald 1989). This signalling pathway also functions in the AC-VU decision process to generate the AC during the L2 stage. Additionally, LIN-12 signalling is involved in the acquisition of the 2° cell fate by P5.p and P7.p VPCs after the 1° fate of P6.p has been specified (Greenwald et al. 1983).

Mutations in Wnt pathway components result in defective cell proliferation and division during vulval development in both *C. elegans* and *C. briggsae*. Wnt signalling functions to maintain VPC competence, promotes 2° fate, and controls cell polarity through the regulation of the *lin-39* Hox gene (Eisenmann et al. 1998; Myers and Greenwald 2007). Additionally, Wnt signalling plays a role in changing the polarity of P7.p, resulting in the mirrored, symmetric patterns of P5.p and P7.p descendants (Deshpande et al. 2005)(Figure 1.4).

Vulva formation has been studied extensively in *C. elegans* and comprises of 22 cells generated by a series of signalling events involving the pathways discussed above (Sternberg 2005). Vulval development involves the induction of three VPCs (P5.p, P6.p and P7.p), located on the ventral surface of the worm. The AC, which lies dorsal to the VPCs, secretes LIN-3/EGF which initiates VPC induction (Hill and Sternberg 1992) (Figure 1.5). The VPC closest to the AC, P6.p, receives the most LIN-3 inductive signal via the RTK, LET-23/EGFR (Katz et al. 1996). Downstream of LET-23 is LET-60, the *C. elegans* ortholog of Ras (Aroian, Lesa, and Sternberg, 1994). LET-60 activates a MAPK cascade consisting of the kinases LIN-45/Raf (Han et al. 1993), MEK-2/MEK (Church et al. 1995) and MPK-1/ERK/MAPK (Lackner et al. 1994). In many cases, MPK-1 moves into the nucleus to phosphorylate transcription factors, thus leading to changes in gene expression (Lackner et al. 1994) (Figure 1.5). The series of signalling events following LIN-3 binding to LET-23 in P6.p results in the P6.p adopting the 1° cell fate and the subsequent production of eight vulval progeny (Ambros 1999). The two VPCs adjacent to P6.p, P5.p and P7.p, adopt the 2° fate and each produce

seven vulval progeny (Ambros 1999). Both P5.p and P7.p are located further away from the AC in comparison to P.6p and as a result, receive lower levels of LIN-3 in addition to receiving a repressive lateral signal from P6.p mediated by LIN-12 signalling (Simske and Kim 1995; Sternberg and Horvitz 1989) (Figure 1.5). As a primary VPC, P6.p is responsible for the production of LIN-12/Notch ligands, proteins of the DSL family, and the downregulation of the LIN-12 receptor. The ligands are either transmembrane proteins, such as LAG-2, or secreted ligands, such as DSL-1 (Chen et al. 2004). The ligands activate LIN-12 on the neighbouring P5.p and P7.p cells, promoting the 2° fate (Yoo et al. 2004). The VPCs P3.p, P4.p and P8.p, are located even further from the AC and as a result, remain uninduced, adopting a 3° cell fate (Hill and Sternberg 1992). The signalling pathways involved in vulval development may also be regulated by genes at the chromatin level.

## 1.5.4   Chromatin Mediated Regulation

The Synthetic Multivulva (SynMuv) genes control LIN-3/EGF signalling through chromatin mediated regulation. The SynMuv genes have been classified into three classes (A, B and C), based on their genetic interactions (Ferguson and Horvitz 1989). Interestingly, a mutation in a single SynMuv genes is not enough to cause the Muv phenotype, instead mutations in two SynMuv genes from two different classes are required (Ferguson and Horvitz 1989). Although this holds true for most SynMuv genes, the *lin-15* gene is the exception. In this gene, two transcripts (*lin-15A* and *lin-15B*) can be produced from a single promoter (Ferguson et al. 1987) and mutations affecting both transcripts result in the Muv phenotype (Clark et al. 1994). SynMuv genes function to inhibit vulval development by suppressing LIN-3 (Cui et al. 2006). In SynMuv double mutants, *lin-3* is ectopically expressed throughout the worm in comparison to wild type animals, where *lin-3* is restricted to the pharynx, anchor cell, gonad and tail. This ectopic expression results in the atypical activation of the signal cascade (Cui et al. 2006; Saffer et al. 2011). It is also known that SynMuv genes function throughout the animal, including the hyp7 syncytium to keep LIN-3 repressed (Saffer et al. 2011).

The molecular functions of the Class A SynMuv genes are not well understood (Fay and Yochem 2007). The molecular characterization of members of the large class B group of genes identified many genes involved in transcriptional regulation. Such genes include *efl-1*, the *C. elegans* ortholog of E2F Ceol and Horvitz 2001 and *lin-35*, which encodes the *C. elegans* RB protein ortholog Lu and Horvitz 1998. As previously discussed, RB complexes with E2Fs to inhibit the transcription of target genes (Nevins 2001). Other genes from this class include the nucleosome remodeling and histone deacetylase (NuRD) complex components (Fay and Yochem 2007). Furthermore, SET domain proteins, known to be involved in transcriptional repression, cell proliferation, transgene silencing, larval development and development of the pharynx (Cui et al. 2006) are also Class B members. Some of the Class C genes are also involved in transcriptional regulation at the chromatin level. Some of these genes encode components Tip60 chromatin remodeling complex (Ceol and Horvitz 2004). The Class C genes function redundantly with Class B genes and may be required to negatively regulate vulval development (Ceol and Horvitz 2004). The identification and characterization of a number of SynMuv genes that are involved in chromatin remodelling, suggests that SynMuv genes may play a critical role in the regulation of *lin-3* expression to control vulval differentiation in *C. elegans.*

## 1.6   Aim of the Thesis

The aim of this thesis is to dissect the molecular mechanism of *Cbr-ivp-3* function in vulval cell differentiation. To this end, I have carried out molecular genetic analyses of *ivp-3* in both *C. briggsae* and *C. elegans* to set the stage for comparative evo-devo analysis and have begun to characterize the functional role of *ivp-3*.

## 1.7   Previous Results

A set of 14 *C. briggsae* Muv mutants, obtained from previously conducted EMS ( ethyl methanesulfonate) experiments, were characterized and mapped to specific

regions of chromosomes using phenotypic markers and molecular polymorphisms (Sharanya et al. 2012). Three of the Muv genes were found to represent orthologs in the EGF-Ras pathway and the Wnt pathway of known *C. elegans* Muv genes. Four of the genes showed no known orthologs of Muv genes in *C. elegans* at that time. Of these four genes, 2 complementation groups (*Cbr-ivp(sy5216)* and *Cbr-ivp(gu102)*) were found to have more than one allele (Sharanya et al. 2012). Unpublished data showed that *Cbr-ipv(sy5216)* and *Cbr-ivp(sy5392* mutations are present on the *Cbr-ivp-3* gene present on chromosome 4 and both alleles were identified as nonsense mutations. The results of a complementation test conducted in Dr. Chamberlin's lab, lead to the speculation that a third mutant, *Cbr-ivp(gu236)*, may also an allele of *Cbr-ivp-3*. At this time, analysis of *Cbr-ivp(gu236)* had not been conducted.

Furthermore, Sharanya et al. (2015) examined *Cbr-ipv(sy5216)* and *Cbr-ivp(sy5392)* L4 animals using Nomarski optics to characterize defects in VPC induction. It was found that P5.p, P6.p, and P7.p were always induced, P8.p was almost always induced, P4.p was induced occasionally and P3.p was induced rarely in these mutants. In addition, Sharanya et al. (2015) examined L3 and L4 Muv mutant animals using Nomarski optics along with 1° and 2° lineage markers to determine defects in VPCs. In *Cbr-ipv(sy5216)* mutants, P3.p, P4.p and P8.p cells took on a 2° fate in 5%, 48.8% and 42.5% of the mutants respectively (Sharanya et al. 2015). Since VPC induction of the 2° cell fate is regulated by Notch signalling, the evidence suggested that *Cbr-ivp-3* may play a role in regulating Notch signalling. Work carried out in the Chamberlin Lab suggests that *C. briggsae* Muv mutants are less sensitive to pathway interference than *C. elegans*. Notch was tested as an alternative signalling pathway to identify the source of differences in EGF suppression seen between *C. elegans* and *C. briggsae*. The results suggested that the Notch pathway may be responsible for these differences. In addition, laser ablation studies, in which the gonad and therefore the precursor to the AC was removed, suggested that *Cbr-ivp-3* gene can bypass the normal dependence of vulval development on the AC (Sharanya et al. 2015).

Using RT-qPCR, Sharanya et al. (2015) looked at the expression level of *Cbr-lin-3* in *Cbr-ivp(sy5216)*. Their results suggested that the expression on *Cbr-lin-3*

in the Muv mutant did not significantly change in comparison to the wildtype (Sharanya et al. 2015). Since expression of the *Cbr-lin-3* was not unregulated in *Cbr-ivp(sy5216)*, Sharanya et al. (2015) concluded that *Cbr-ivp-3* is not a SynMuv gene. Lastly, *Cbr-ipv(sy5216)* was exposed to varying concentration of a MEK inhibitor during larval stage development. It was found that the Muv phenotype did not significantly become reduced when exposed to 10uM of the inhibitor and suggested that this mutation may act downstream of MEK in the EGF pathway (Sharanya et al. 2015). The previous work conducted by Sharanya et al. (2015), provided a basic understanding of some aspects of vulval formation in the *Cbr-ivp-3* Muv mutants and served as a basis to further understand the mechanisms to which *Cbr-ivp-3* regulates vulval development.

## 1.8   Major Findings of the Thesis

A thorough molecular genetic analyses of *Cbr-ivp-3* has been carried out. I have identified the gene expression profile of *Cbr-ivp-3* throughout larval development. Sequencing the cDNA of the entire *Cbr-ivp-3* gene to confirm the accuracy of the gene predictions provided by WormBase, has indicated the intron-exon boundaries were not correctly predicted upstream of the third exon. The speculation that a third mutant, *Cbr-ivp(gu236)*, is also an allele of *Cbr-ivp-3* has been confirmed through sequencing. I have found that a nonsense mutation is introduced at the fourth exon of the Cbr-ivp-3, located just upstream of where the RNase H-like domain begins. This finding further solidified the idea that *Cbr-ivp-3* plays a role in the negative regulation of vulval formation. Furthermore, the inappropriate divisions of VPCs in the *Cbr-ivp-3* mutants has been confirmed in *Cbr-ivp(sy5216)* and has been characterized in the other two mutants, *Cbr-ivp(sy5392)* and Cbr-lin(gu236). All mutants displayed ectopic division of VPCs as well as increased percentage of induced VPCs. Severe variations in the gonad morphology and guidance in all three mutants were also observed.

Similarly, I have identified the *C. elegans* ortholog of *Cbr-ivp-3*. This gene

had not been characterized earlier and thus a molecular genetic analyses of *ivp-3* in *C. elegans* was carried out. I have identified the gene expression profile of *ivp-3* throughout *C. elegans* larval development. Findings from the analysis of proteomics data indicate that 19 genes share a similar protein domain with *ivp-3* and are associated with processes such as nucleic acid binding activity, 3'-5' exonuclease activity, exonuclease activity and nuclease activity. The results of a phenotypic analysis of the *ivp-3(gk3691)* strain, suggest that animals homozygous for the deletion site, confer a protruding vulva phenotype and are sterile. Analysis of embryonic and larval lethality in *ivp-3(gk3691)* suggest that the loss of function of *ivp-3* in *C. elegans* likely prevents the production of fertilized eggs. Additionally, the findings suggest that in *C. elegans*, *ivp-3* is an important gene necessary for growth to a fertile adult.

By conducting molecular genetic analyses of *ivp-3* in both *C. briggsae* and *C. elegans*,I have provided an avenue in which comparative studies to understand evolution of gene function and developmental mechanisms can take place.

Lastly, I have attempted to understand the genetic pathway of *Cbr-ivp-3* and its function in vulval development through the identification of target genes. An RNAseq analysis, carried out in *Cbr-ivp(sy5216)*, allowed for the acquisition of gene expression profiles of thousands of genes from which candidate target genes can be identified and validated using RT-qPCR. It was also found that *Cbr-lin-3* is overexpressed in *Cbr-ivp(sy5216)*, contrary to the findings by Sharanya et al. (2015). The RT-qPCR findings also indicated that *Cbr-lag-2* transcript levels are not significantly changed in the Muv mutant, providing evidence against the hypothesis that *Cbr-ivp-3* may play a role in regulating Notch signaling. RNAi was utilized to knockdown *Cbr-lin-3* expression in *Cbr-ipv(sy5216)* and it was found that reduced *Cbr-lin-3* expression suppressed the Muv phenotype. Despite previous speculation that this may not be the case (Sharanya et al. 2015), the findings in this thesis suggest that *Cbr-ivp-3* is functioning in a manner similar to some SynMuv genes.
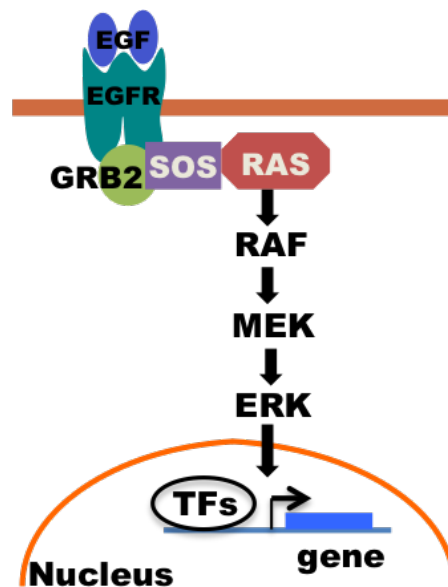
Figure 1.1: Receptor tyrosine kinases (RTKs) such as the epidermal growth factor receptor (EGFR) are activated and phosphorylated upon binding of the epidermal growth factor (EGF) ligands. This event causes the binding adaptor protein, GRB2 and the guanine nucleotide exchange factor, SOS to form a complex and bind to the phosphorylated EGFR. SOS then activates RAS, which activates the protein kinase activity of RAF kinase. RAF then phosphorylates and activates MEK, which phosphorylates and activates ERK. The activated ERK can translocate into the nucleus where it affects transcription factors (TFs) to positively or negatively regulate downstream target genes via phosphorylation. Adapted from Kobet et al. (2014)
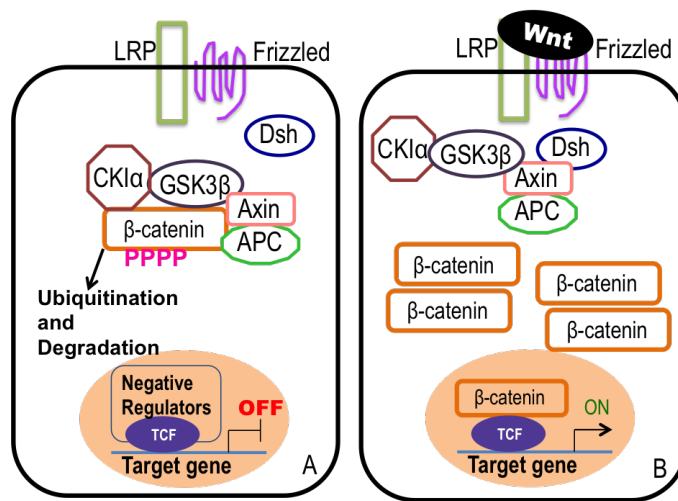
FIGURE 1.2: In all three Wnt signalling pathways, (A) in the absence of the Wnt ligand, $\beta$-catenin interacts with APC (Adenomatous *Polyposis coli*) and Axin scaffold proteins in the cytoplasm and becomes phosphorylated by CKI$\alpha$ kinase and GSK3$\beta$ (Glycogen Synthase Kinase 3 beta), leading to its ubiquitination and degradation by the proteasome. (B) the canonical pathway is activated when the Wnt ligand binds a Frizzled family receptor. The $\beta$-catenin is stabilized in the cytoplasm and is translocated into the nucleus where its interacts with with TCF family transcription factors, activating target gene expression. Adapted from Kobet et al. (2014)
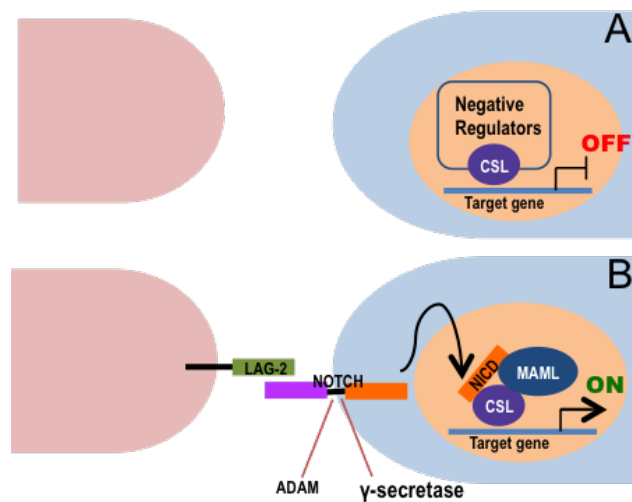
FIGURE 1.3: (A) In the absence of NOTCH, negative regulators inhibit the expression of Notch target genes; (B) When a ligand, such as LAG-2, is present, it interacts with the Notch receptor, causing the cleavage of the extracellular portion of the Notch receptor by ADAM-family and cleavage of the intercellular portion by $\gamma$-secretase. The released intracellular domain of Notch (NICD) then enters the nucleus where it forms a complex with the transcription factors CSL (CBF1, Suppressor of Hairless, LAG-1) and its co-activator, mastermind-like protein (MAML), resulting in the transcription of target genes. Adapted from Kobet et al. (2014)
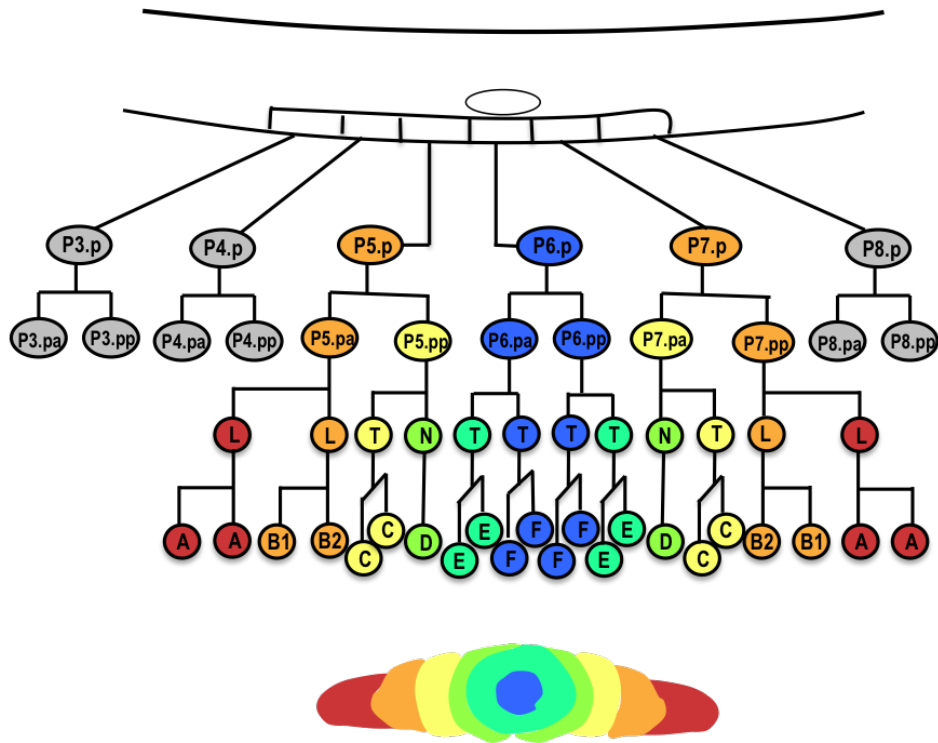
FIGURE 1.4: The fate of the VPCs is determined (1° fate - blue, 2° fate – orange, and 3° fate – gray), and then the VPCs divide. The daughters of tertiary fate VPCs fuse with hyp7. The daughters of the 1° VPC P6.p undergo cell division in a TTTT lineage (T is transverse axis of cell division), while the daughters of P5.p and P7. p form the pattern LLTN TTTT NTLL (T - transverse division, N - no division, and L - longitudinal division). The cells acquire adult vulval cell fates (vulA - red, vulB1 and vulB2 - orange, vulC - yellow, vulD - green, vulE – blue-green, vulF - blue). The VPCs migrate towards the center of the vulva, form a toroid and the cells fuse forming the adult vulva, consisting of 22 cells. Adapted from Weinstein and Podbilewicz (2016)
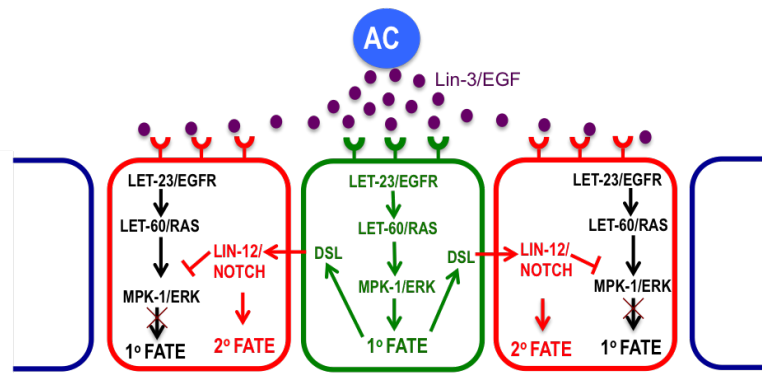
Figure 1.5: The anchor cell secretes the LIN-3/EGF inductive signal which binds to and activates LET-23 /EGFR receptors on nearby VPCs. Due to its proximity to the Anchor Cell (AC), the activation of LET-23 in P6.p, activates the 1° cell fate through the Ras–MAPK signalling pathway. LIN-3 forms a short-range gradient and is received by LET-23 receptors in P5.p and P7.p, where it promotes the 2°. Notch ligands are produced in P6.p following 1o cell fate specification and bind to the Lin-12/Notch receptors on P5.p and P7.p which also activates the 2° cell fate and inhibits the 1° cell fate. Adapted from Weinstein and Podbilewicz (2016)

# Chapter 2

# Materials and Methods

## 2.1 Strains and General Methods

Methods for culturing and maintaining nematodes have been followed as described previously (Brenner, 1974). Unless stated otherwise, all experiments have been carried out at 20°C.

The nematode strains used in this study are listed below.

Mutant Strains

C. elegans: N2 (wild type), *VC20274(gk197262)*, *VC40151(gk486330)*, *VC40672(gk756793)*, and *VC3731(gk3691)*

C. briggsae: AF16 (wild type), *lin-15AB(n309)*, Cbr-*ivp(sy5216)*, *Cbr-ivp(sy5392)* and *Cbr-ivp(gu236)*

Transgenic Strains C. elegans: *bhEx31[pRH51(hs::lin-3) + myo-2::GFP]* C. briggsae: *mfIs42[sid-2::GFP; myo-2::dSRed],bhEx31[pRH51(hs::lin-3) + myo-2::GFP]* *Cbr-ivp(sy5216);mfIs42[sid-2::GFP; myo-2::dSRed]*

## 2.2   Microscopy

The characterization of the Muv phenotype of the *Cbr-ivp-3* alleles and the examination of *C. elegans ivp-3* mutants were carried out using the Nikon Eclipse 80i microscope. Animals in L3 and L4 stages were mounted on agar pads and anaesthetized using 1M sodium azide.

The fates of VPCs P3.p to P8.p, were examined and were assigned an induced fate if the VPC was induced to give rise to more than 4 vulval progeny. Any gonad abnormalities including directionality defects, bulging anterior and/or posterior ends, abnormal length of gonad arms, and improper turning of arms were noted.

For GFP reporter expressing strains, the Zeiss Axioimager D1 microscope with the GFP filter HQ485LP (Chroma Technology). Images were taken using a Nikon DXM1200F digital camera and the Nikon ACT-1 software, and were processed using NIH Image J software.

## 2.3   Bleach Synchronization

To obtain synchronized worm populations, plates containing gravid hermaphrodites were bleached, using a hypochlorite solution consisting of 1N sodium hydroxide (NaOH) and sodium hypochloride (commercial bleach) in a 3:2 ratio. M9 buffer was used to wash animals off the plates and centrifuged in 15mL falcon tubes. The M9 buffer was discarded and new buffer was added to the tube, following centrifugation. The process was repeated until the M9 was clear. The bleach solution was added and the tube was vigorously shaken until all carcasses disintegrated and only eggs were visible. The eggs were pelleted and the bleach solution was discarded. This was followed by three to four washes with M9 buffer (Portman, 2005). The eggs were placed in a 1.5ml eppendorf tube and placed on a rotisserie overnight at room temperature, where the eggs were allowed to hatch and remain in the L1 stage until plated.

## 2.4  RNA Extraction

Staged worms were obtained by growing L1 larvae on NGM plates for 24 hours at 20°C following bleach synchronization. The developmental stage of animals was confirmed by observing gonad size and presence of the anchor cell in a sample of animals using Normarski optics. Worms were grown on 100mm agar plates and collected by washing with M9 buffer. Additional washes with M9 buffer were carried out to remove residual OP50 bacteria and other debris. Approximately $100\mu$l of pelleted worms were collected in eppendorf tubes. Using the TRIZOL method, total RNA was extracted from the staged worms. Four times the volume of TRIzol (Invitrogen, cat. no. 15596-026) was added to the volume of the pelleted worms. The pellet was then resuspended by vortexing, followed by freeze cracking, which disrupts the worm's cuticle to allow for rapid RNA solubilization. Freeze cracking was achieved by flash freezing the sample in liquid nitrogen, thawing at 37°C, vortexing and repeating two to three additional times. Three additional volumes of TRIzol to the amount of starting worms was added and vortexed for 30 seconds. The mixture was allowed to sit at room temperature for 5 minutes to disrupt RNA-protein complexes, followed by the addition of 2 volumes of the original worm pellet of chloroform. The sample was then left to stand at room temperature for 3 minutes and centrifuged at 12 000g for 15 minutes at 4°C. The upper aqueous layer containing the RNA was transferred to a new tube, and an equal volume of isopropanol was added. This solution was allowed to stand at room temperature for 10 minutes and was then centrifuged at 4°C at 12 000g for 10 minutes. The supernatant was pipetted off, the visible pellet of RNA was washed in $500\mu$l of 75% ethanol, and centrifuged at 12 000g for 5 minutes at 4°C. The supernatant was removed and the pellet was air-dried so that the ethanol evaporated (two to three minutes). The pellet was dissolved in nuclease free water that had been preheated to 55°C.

RNA samples were treated with RNaseOUT Recombinant Ribonuclease Inhibitor (Invitrogen cat. no. 10777-019) and DNase (Thermo Scientific DNase I, RNase-free, #EN0521). The RNA concentration of RNA was determined using the NAnodrop and RNA integrity was determined by running a 0.8% agarose gel.

The presence of two bands (28s and 18s) is indicative of intact RNA.

## 2.5 Heat-Shock Protocol

The *C. briggsae* strain, *bhEx31[pRH51(hs::lin-3) + myo-2::GFP]*, displays Muv phenotype due to elevated levels of *Cbr-lin-3* following induction by heat-shock. In order to isolate the RNA from the heat-shocked strain at L1+ 24 hours, the strain was removed from 20°C at L1 + 22 hours, and heat-shocked in a 37°C water bath for 1 hour. After the 1 hour, the strain was allowed to recover at 20°C for another hour. At L1 + 24 hours, the Normarski microscope was used to confirm the L3 stage by observing the size of the gonad and presence of the anchor cell. Using the TRIZOL method, total RNA was extracted from the staged worms. Some worms were kept aside so that the vulval morphology could be analyzed at the adult stage using Nomarski imaging to ensure that the heat shock was successful.

## 2.6 RT-qPCR

Quantitative real-time PCR (RT-qPCR) was used to quantify and compare changes in gene expression levels and for validation of RNAseq results. RNA was isolated from AF16 and *Cbr-ivp(sy5216)* animals at the L1+ 24hour stage (See Material and Methods 2.4). Primers for the candiate gene targets were designed and optimized (Table 2.1).

Expression levels of *Cbr-lag-2* and *Cbr-lin-3* in *Cbr-ivp(sy5216)* was also investigated. Primers for *Cbr-lag-2* were designed and optimized (Table 2.1). In addition, AF16 and BhEx31(hs::lin-3) were used as controls.

Using the SensiFAST$^{\text{TM}}$ cDNA Synthesis Kit (Bioline cat. no. BIO-65053), cDNA was made from the isolated RNA, making sure the final concentration of RNA was 800ng/$\mu$l for each strain. Using the SensiFAST$^{\text{TM}}$ SYBR® Hi-ROX Kit (Bioline cat. no. BIO-92005), qPCR was performed. The reference gene, pmp-3,

was used for normalization in gene expression data analysis to correct for differences in the amount of cDNA template between wild type and mutant reactions. At least three biological and three technical replicates were run along with the No Template Control (NTC) and No Reverse Transcriptase Control (NRT).

Data was analyzed using BioRad CFX manager software 3.1. The reaction mix and cycling conditions and were followed as recommended by SensiFAST™ SYBR® Hi-ROX Kit.

## 2.7 RT-qPCR Primer Design and Optimization

All primers that were used for Quantitative real-time PCR experiments were designed so that the primers spanned an exon-exon junction to avoid any genomic DNA contamination (Table 2.1). The primers were designed using the NCBI Primer Blast tool (found at https://www.ncbi.nlm.nih.gov/tools/primer-blast). Primer pairs were optimized for annealing temperature and product specificity, which was based on melt curve analysis. Furthermore, the identity of the amplicon was examined by running the PCR products on an agarose gel to ensure that the appropriate amplicon size was produced.

## 2.8 Constructing RNAi Plasmid

The *Cbr-lin-3* RNAi plasmid, used for knocking down *Cbr-lin-3* expression in the *Cbr-ivp(sy5216)*, was generated using PCR based cloning. This method allowed for a fragment from the *Cbr-lin-3* gene to be placed into the L4440 empty vector (Addgene plasmid # 1654). The primers GL1242 and GL1243 (Table 2.1) were used to amplify the 885bp fragment. The primers were designed to be roughly 21bp each, the respective restriction site sequence was added to the end of each primer, 3 to 5 bases were added upstream or downstream of restriction site, since many restriction enzymes do not cut DNA efficiently at the end of a linear piece. The fragment was PCR amplified using AF16 genomic DNA and extracted using a

standard Phenol Chloroform extraction method. The L4440 plasmid was extracted from a culture, from the RNAi library, that was grown overnight in 3ml of LB media and 3$\mu$l of Carbenicillin (100 $\mu$g/ml). A double digest, using PstI and XhoI restriction enzymes, was carried out overnight at 37°C for both the PCR fragment and L4440 vector. The digested DNA was run on A 0.8% agarose gel and gel purification was conducted to isolate the DNA. A DNA ligation was conducted to fuse the insert to the recipient plasmid. A total of 100ng of DNA was used in the ligation reaction with a recipient plasmid to insert ratio of 1:3. A negative control was set up in parallel which contained the digested L4440 vector but not the insert. The ligation reaction was carried out overnight, at room temperature. 2$\mu$l of the ligation reaction were transformed into MAX Efficiency® DH5$\alpha$™ Competent Cells (cat no. 18258012), according to the manufacturer's instructions. Individual bacterial colonies were picked and overnight cultures were grown for DNA purification. Following purification, a diagnostic restriction digest using SpeI and then run on an agarose gel. The plasmid was verified by sequencing before being transformed into HT115 electro-competent cells by means of electroporation.

## 2.9 Genetic Crosses

Since *C. briggsae* is resistant to RNAi introduced by bacterial feeding methods, transgenic strains, carrying a wild type copy of the *C. elegans sid-2* gene, were used for RNAi experiments involving the knockdown of *Cbr-lin-3* in the *Cbr-ivp(sy5216)* mutant. *C. elegans sid-2*, non-functional in *C. briggsae*, is an intestinal luminal transmembrane protein and is required for RNA uptake. The introduction of *cel-sid-2* enhances RNAi uptake in *C. briggsae* (Winston et al. 2007).

The transgenic strain *mfIs42[sid-2::GFP; myo-2::dSRed]*, which carries the wild-type copy of the *C. elegans sid-2* gene was used in a cross to generate strains sensitive to environmental RNAi in the *Cbr-ivp(sy5216)* mutant background. The genetic cross consisted of crossing males of the *mfIs42[sid-2::GFP; myo-2::dSRed]* strain with *Cbr-ivp(sy5216)* young adult hermaphrodites in a 5:1 ratio on agar plates. Animals were allowed to mate for 3 to 4 days to produce F1 animals.

F1 animals, expressing dSRed in the pharynx were cloned onto separate plates at the young adult stage and allowed to self fertilize. It was previously found that *Cbr-ivp(sy5216)* mutants exhibit a maternal rescue phenotype when the alleles segregate in a self-cross from a heterozygous mother, thus the F2 animals from this cross were not expected to display any Muv phenotype. The probability of obtaining an F2 animal homozygous for both *mfIs42[sid-2::GFP; myo-2::dSRed]* and *Cbr-ivp(sy5216)*, resulting from a self-mating heterozygous F1, is 1/16. To increase the chances of obtaining the desired genotype, 32 young adult F2 hermaphrodites, displaying no Muv phenotype but expressing dsRed were cloned singly onto plates and allowed to produce F3 progeny. The F3 progeny were screened for animals expressing dsRed and the Muv phenotype. A plate in which all of the F3 progeny were Muv and expressing dsRed was an indication that the F2 animal was homozygous for both *mfIs42[sid-2::GFP; myo-2::dSRed]* and *Cbr-ivp(sy5216)*. The penetrance of the Muv phenotype was monitored over the next several generations.

## 2.10    RNA Interference

RNAi agar plates containing 0.0005% cholesterol, 0.1% $NH_4Cl$, 0.2% $\beta$-lactose, 0.3% $KH_2PO_4$, 0.5% Casamino Acids, 0.6% $Na_2HPO_4$, 2% Agar, 1mM $MgSO_4$, 1mM $CaCl_2$, and 100$\mu$g/ml Carbenicillin were used to carry out all RNAi experiments. These plates were seeded with 100$\mu$l of the HT115 bacterial culture that produces dsRNA of the gene of interest. The culture had been grown overnight in 3ml of LB media and 3$\mu$l of Carbenicillin (100$\mu$g/ml). Bleach Synchronized L1 worms were plated on plates containing RNAi bacteria. The L4440 empty vector was used as a negative control and *pop-1* as the positive control. The L1-stage worms were allowed to grow until the desired stage and collected for analysis. RNAi experiments were performed in triplicate batches and only batches that produced consistent results were analyzed.

For RNAi knockdown of *Cbr-lin-3* in *Cbr-ivp(sy5216)*, the transgenic strain *mfIs42[sid-2::GFP; myo-2::dSRed]*, which carries the wild-type copy of the *C. elegans sid-2* gene was used in a cross to generate strains sensitive to environmental

RNAi. The HT115 bacterial culture containing the *cbr-lin-3* RNAi plasmid was used.

## 2.11  Constructing the *ivp-3* Rescue Fragment

The primers GL1228 and GL1229 (Table 2.1) were used to amplify a 9357bp fragment using long range PCR for the rescue experiment. The fragment consisted of the entire *Cel-ivp-3* gene including introns as well as 1899bp of the 5' UTR and 1227bp of 3'UTR.

N2 genomic DNA ($\sim$200ng/ul) was used as the template and the reaction mix was prepared as recommend by the QIAGEN LongRange PCR Kit (cat no. 206401). The thermal cycling conditions were followed as recommended by QIA-GEN. For the first ten cycles, an extension time of 1 minute per kilobase DNA was used. The remaining 28 cycles, the extension time was increased by increments of 20 seconds in each cycle.

For analysis of the PCR product, gel electrophoresis was carried out using a 0.6% agarose gel and Invitrogen1 kb Plus DNA Ladder (cat no. 10787018). The sample ran for 6 hours at 40 V. A restriction enzyme digestion using SpeI was carried out for 4 hours at 37°. The digested sample was run on a 0.6% agarose for 6 hours at 40 V. The PCR product was isolated using a standard Phenol Chloroform extraction method. The $\sim$9kb fragment of *C.elegans ivp-3* was microinjected into *Cbr-ivp(sy5216)* Muv mutants using the microinjection technique was followed as described in Mello et al. (1991). The injection mix contained 70ng/$\mu$l of the PCR product, 30ng/ul of Myo-2::GFP and nuclease free water. F1 animals were screened for Myo-2::GFP fluorescence. Fluorescing F1 animals were picked onto individual agar plates and allowed to produce F2 animals which were then screened for Myo-2::GFP fluorescence. The penetrance of the Muv phenotype was monitored over the next several generations.

## 2.12   Phenotypic Analysis of *ivp-3(gk3691)*

To carry out a phenotypic alanlysis of *VC3731(gk3691)*, a young adult hermaphrodite, that had GFP fluorescence and appeared wild type, was allowed to mature and lay eggs for 24 hours. The hermaphrodite was then transferred to a new plate to lay eggs for another 24 hours and this was repeated, 24 hours later, for a third time. The F1 progeny were scored when they reached adulthood presence of Pvl and GFP fluorescence and any other observations were noted. All animals that appeared Pvl and also happened to be GFP-fluorescing were cloned onto individual plates and monitored to observe if they produced F2 progeny 3 to 4 days later or until they died. The populations from two hermaphrodites were analyzed, a total of 415 animals were scored.

To test embryonic and larval lethality in the *VC3731(gk3691)* strain, a young adult hermaphrodite, that had GFP fluorescence and appeared wild type, was allowed to lay eggs for 24 hours. The hermaphrodite was then transferred to a new plate to lay eggs for another 24 hours and this was repeated, 24 hours later for a third time. The eggs were counted 24 hours after the hermaphrodite was allowed to lay eggs and the worm had been transferred to a new plate. The eggs were counted by placing the eggs in a single-file line which allows for efficient analysis following hatching. This was gently to avoid damaging the eggs. Any eggs that looked already dead or that were thought to be damaged during transfer to the line were flamed and not counted. The eggs were given 24 hours to hatch and then any unhatched eggs were counted. The larvae on these plates were then scored when they reached adulthood, 3 days later. The populations from two hermaphrodites were analyzed. The wild type *C. elegans* strain, N2, was analyzed as a control.

## 2.13   Identifying *ivp-3* Gene Interactions

Gene Multiple Association Network Integration Algorithm (GeneMANIA) is a large collection of interaction networks from several data sources which identify

genes and networks that are functionally associated with the query gene or gene sets. GeneMANIA searches many large, publicly available biological data sets to find related genes. These include protein-protein, protein-DNA and genetic interactions, pathways, reactions, gene and protein expression data, protein domains and phenotypic screening profiles.

To generate the gene network, showing gene interactions, the gene of interest was processed through the GeneMANIA web interface (Warde-Farley et al. 2010; Mostafavi et al. 2008). *Cel-ivp-3*, known now as *ivp-3*, was input as a query to GeneMANIA, which queried against the *C. elegans* organism database. Network weighting was based on biological processes as in GO. Association types included genetic interactions, predicted interactions, co-expression, physical interactions, other and shared protein domains.

| Locus | Oligo Name | Sequence (5' to 3') | Use |
|---|---|---|---|
| Cbr-ivp-3 | GL1119 | TGTCTATCGCTGCGACTTC | |
| | GL1120 | CCGTTCTCGAGCTGATTTGAT | |
| | GL1121 | CTGTATTCTGTCGTTCTCCGTG | |
| | GL1122 | GTGCGGAAAGCTGACGAAATC | |
| | GL1124 | GCATACAGTTCAGTGGAACG | Sequencing |
| | GL1125 | GCCCTACAGAAGCATCGAGAAG | |
| | GL1082 | CATTCTGCTCGTGTTGAGGTC | |
| | GL1083 | CCGGGTAACAAGCGAAATC | |
| Cel-ivp-3 | GL1228 | CGGATTCAGAAGATACGTCAGC | Constructing rescu |
| | GL1229 | GCTGTCGAAGAACTCGATGATC | fragment |
| | GL1287 | CCTTCTGGCAATCGTCGTAGC | Genotyping gk369 |
| | GL1284 | GTTGCATCACCTTCACCCTCTC | allele |
| | GL1327 | GGCTTGTCTGTGAAATTTGGGG | |
| Cbr-lin-3 | GL1242 | CGGCTGCAGTGTCTCGTTATTCGGTTCCAG | Constructing RNA |
| | GL1243 | AGACTCTCGAGCGTGCTGCTCATCGTGATC | plasmid |
| | GL911 | GTGGTTCCTTCTTGCCATTGTCC | |
| | GL912 | GAACGAAGAGTTGCGCCGTG | qRT-PCR |
| Cbr-lag-2 | GL1189 | CAACGGATACACCGGCTCC | |
| | GL1190 | GAGCACCATTCAGACACGC | qRT-PCR |
| *Cbr-pmp-3* | GL767 | CGGAATCGTTTCGAGGAATGC | |
| | GL768 | CGATGCGTGACTCCAGCAAG | qRT-PCR |
| Cbr-nhr-7 | GL1311 | AGTGTAGAAGACAAGAGTGCCC | |
| | GL1312 | CAGATCCTCCAATCCTGGTGT | qRT-PCR |
| Cbr-cwn-2 | GL1313 | CGAGAAAAAGAGCACGATCCG | |
| | GL1314 | TCGGTTTTCGATGGCGTTTC | qRT-PCR |
| Cbr-spin-2 | GL1315 | GTGGATATCTTGGGGACCGA | |
| | GL1316 | CCAGAAATGATTTGCCGGGAC | qRT-PCR |
| Cbr-daf-7 | GL1317 | GTCTCTACGACCTGATCGTCG | |
| | GL1318 | CGTTGAGAAGATGATGTGCGT | qRT-PCR |
| Cbr-sel-7 | GL1319 | CCCGATCAGAGGATACCCTC | |
| | GL1320 | GTCGGATGTCGAATTGGTGG | qRT-PCR |
| Cbr-gsa-1 | GL1321 | GCGATGCGATGCAGGTAATG | |
| | GL1322 | GCTCATCACGTAGTCTCTGCT | qRT-PCR |
| Cbr-mpk-1 | GL1323 | GTGGCATCCGCACTCGATAC | |
| | GL1324 | GATCTCTCGAAGCGTGCGTT | qRT-PCR |

TABLE 2.1: List of oligonucleotide primers used in this study

# Chapter 3

# Characterization of a novel vulva development gene *ivp-3*

I aimed to gain an in-depth understanding of the structure and function of *ivp-3* gene that had not been characterized prior to this study. Possible target genes of *Cbr-ivp-3* were identified in order to gain a deeper understanding of how this gene negatively regulates organ development through controlling cell proliferation and cell fate specification. A comparative analysis of the *ivp-3* gene in both *C. briggsae* and *C. elegans* was carried out to facilitate in understanding the evolution of gene function and developmental mechanisms. The findings of this thesis, outlined in this chapter, provide background for future comparative studies with *C. elegans* to understand how developmental processes change during evolution by investigating differences in the mechanism of reproductive system development.

## 3.1   Molecular Genetic Analysis of Cbr-ivp-3

Prior to this study, the *Cbr-ivp-3* gene had not been characterized. It was speculated that this gene had a role in the negative regulation of vulval development in *C. briggsae*, but the structure and function of this gene was largely unknown. A thorough molecular genetic analyses of *Cbr-ivp-3* was necessary to set the basis for experiments to determine its function and role in vulval development.

### 3.1.1 Expression of *Cbr-ivp-3* throughout larval development

The larval expression profiles of all genes in *C. briggsae* have previously been determined, providing a means to identify the expression levels of *Cbr-ivp-3* during the developmental processes (Grün et al. 2014). Grün et al. (2014), carried out a genome-wide comparative analysis of the evolution of transcript and protein abundance during development, and mRNA quantification by mRNA sequencing was used to complement the protein data. This dataset has provided a gene profile for *Cbr-ivp-3* for the embryonic, L1, L2, L3, L4, late L4 and the young adult stages (Figure 3.1).

The transcript expression levels appear to be relatively uniform throughout larval development and undergo pronounced changes at the embryo to larval transition and after completion of the final larval stage to the young adult stage. The data shows that expression levels are highest during the embryonic stage (4.8, Figure 3.1). The expression then drops drastically to 3.5 during the L1 stage and drops even lower to 2.5 at the L2 stage where it remains relatively stable for the remainder of the larval stages, L3, L4 and late L4 (2.8, 2.6, 2.7 respectively). The expression level increases to 3.8 during the young adult stage (Figure 3.1).

### 3.1.2 Determination of the open reading frame of *Cbr-ivp-3*

Much like the *C. elegans* genes, the genes in the *C. briggsae* genome were predicted using programs which combined various gene prediction methodologies such as protein-based comparisons and sequence conservation metrics. One such program is Genefinder, which requires a genomic DNA sequence and defined parameters of experimental gene sets (Stein et al. 2003). The quality of coding-sequence predictions is improving as better experimental sets are being confirmed and improved versions of Genefinder became available. As a result, correlating newly experimentally confirmed coding sequences with gene predictions is always underway.

Since *Cbr-ivp-3* had not been characterized prior to this study, the gene structure available through WormBase (http://www.wormbase.org/), had only been predicted and not experimentally confirmed. A wildtype copy of cDNA of the entire *Cbr-ivp-3* gene was sequenced to confirm the accuracy of the gene predictions provided by WormBase. The sequencing results indicated that the intron-exon boundaries predicted by WormBase slightly differed. The first exon of *Cbr-ivp-3*, was 20bp less than predicted by WormBase. Intron 1 was found to be smaller (48bp) than predicted (736bp) and the second exon fell within the previously predicted Intron 1. Furthermore, WormBase predicted that the second intron was 48bp in length but the sequencing results indicated Intron 2 was very large, 742bp. The boundary between Intron 2 and Exon 3 and the gene structures downstream of this boundary were predicted correctly by WormBase (Figure 3.2). This information was useful in carrying out further experiments involving this gene.

### 3.1.3   Identification of *Cbr-ivp-3* mutant alleles

A previous student from the Gupta Lab, Devika Sharanya, determined the locations and nature of mutations present in *Cbr-ivp(sy5216)* and *Cbr-ivp(sy5392)*, the two mutant alleles of *Cbr-ivp-3* known at the time. Unpublished data shows that a point mutation in *Cbr-ivp(sy5216)* is present in exon 7 of *Cbr-ivp-3*, which also happens to be within the RNase H-like domian, (Figure 3.2). The mutation was found to be a nonsense mutation in the sequence TGG, where the third guanine was replaced with an adenine (TGA). The TGA sequence is transcribed and translated as UGA stop codon (Figure 3.4), resulting in a truncated protein. In *Cbr-ivp(sy5392)*, the first adenine in the sequence AAA was replaced with a thymine (TAA), once again resulting in a truncated protein (Figure 3.5). This mutation also was located in exon 7 but just past the region where the RNase H-like domain ends (Figure 3.2).

Complementation tests conducted in Dr. Chamberlin's lab on the Muv mutant *Cbr-ivp(gu236)*, indicated a failure to complement with *Cbr-ivp(sy5216)*, strongly suggesting that *Cbr-ivp(gu236)* and *Cbr-ivp(sy5216)* are allelic mutations on the same gene, *Cbr-ivp-3*. To confirm this, I sequenced the *Cbr-ivp(gu236)* mutant.

The sequencing results indicated that a nonsense mutation was introduced at the fourth exon (exon intro map fig) of the *Cbr-ivp-3* DNA sequence (CGA), causing the cytosine to be replaced with thymine, yielding TGA in the DNA sequence. The TGA is transcribed and translated as UGA stop codon (Figure 3.3), resulting in in a truncated protein. The nonsense mutation found in *Cbr-ivp(gu236)* is located just upstream of where the RNase H-like domain commences, (Figure 3.2) thus the protein generated by this mutant likely does not contain the RNase H-like domain.

The sequencing results indicate that all three alleles of *Cbr-ivp-3* are nonsense mutations resulting in a truncated protein product. The mutation found in *Cbr-ivp(sy5216)*, however is the only allele where the mutation is present within the domain. The *Cbr-ivp(gu236)* and *Cbr-ivp(sy5392)* mutations are located just before and after the domain respectively (Table 3.1). Because all three mutants, *Cbr-ivp(sy5216)*, *Cbr-ivp(sy5392)* and *Cbr-ivp(gu236)*, are present on the same gene, and all mutations have been found to display the Muv phenotype, it is evident that *Cbr-ivp-3* is a gene, that plays a role in inhibiting inappropriate division of vulval tissue in *C. briggsae*.

### 3.1.4 Vulva morphology and cell differentiation analysis of *C. briggsae* Muv mutants

L4 animals were examined using Nomarski optics to observe and characterize the inappropriate division of VPCs in the *Cbr-ivp-3* mutant alleles, *(Cbr-ivp(sy5216)*, *Cbr-ivp(sy5392)* and *Cbr-ivp(gu236)*. All mutants showed ectopic division of VPCs as well as an increased percentage of induced VPCs (Figure 3.6). In all three alleles, P5.p, P6.p, and P7.p were induced 100% of the time, with the exception of *Cbr-ivp(sy5216)* where the % induction for P7.p was 97.40% (Table 3.2). In all strains, the P3.p cell was capable of adopting a vulval cell fate. In *Cbr-ivp(sy5216)* P3.p and P4.p had slightly higher percentages of induction and the highest induction score, 4.95 (Table 3.2), and P8.p was induced 94.87% of the time. The results were in accordance with what was reported of *Cbr-ivp(sy5216)* by Sharanya et al. (2015). The allele *Cbr-ivp(sy5392)* seemed to be the least potent of the three mutants, with an induction score of 4.80 (Table 3.2). The percentages of induced P3.p, P4.p and

P8.p cells were lower compared to *Cbr-ivp(sy5216)* and *Cbr-ivp(gu236)*. Sharanya et al. (2015) found that P8.p was induced 100% of the time and both P3.p and P4.p were induced 29% of the time in *Cbr-ivp(sy5392)*. These results differed from the results reported here and are likely due to the small data set used by Sharanya et al. (2015), where only 7 animals were observed. The third allele, *Cbr-ivp(gu236)*, which had not been previously quantified, had an induction score of 4.90. The percentages of induced VPCs were similar to those observed in *Cbr-ivp(sy5216)* with the exception of P.p.3. In this allele, the P3.p cell was induced 12.20% of the time in comparison to 17.95% in *Cbr-ivp(sy5216)* (Table 3.2).

Along with increased percentage of induced VPCs, severe variations in the gonad morphology and guidance in all three mutants were observed (Figure 3.7). The various defects in arm morphology included length, size, and migration defects. The posterior and anterior arms of the gonad were equally affected. Together, the results of this analysis indicate that all three of the mutant alleles of *Cbr-ivp-3* display severe Muv phenotypes with serious defects in VPC induction.

## 3.2 Molecular Genetic Analysis of *ivp-3* in *C. elegans*

The *C. elegans* ortholog of *Cbr-ivp-3* had been identified in Wormbase. It was found that *ivp-3* had also been uncharacterized in *C.elegans*. The nucleotide sequences of the two genes were blasted and resulted in 65% identity, indicating that differences have accrued over time. A molecular genetic analyses of was carried out in order to provide an avenue in which comparative studies to understand evolution of gene function and developmental mechanisms could take place. Comparative studies to understand species-specific function of orthologous genes can reveal evolutionary similarities and differences in the signalling and regulation of genes as well as developmental processes.

### 3.2.1   Expression of *ivp-3* throughout larval development

The larval expression profiles of all genes in *C. elegans* have previously been determined, providing a means to identify the expression levels of *ivp-3* during the developmental processes (Grün et al. 2014). This dataset has provided a gene profile for *ivp-3* in *C. elegans* for the embryonic stage, L1, L2, L3, L4, late L4 and the young adult stage (Figure 3.8).

Similar to the expression profile of *Cbr-ivp-3*, the transcript expression levels of *ivp-3* in *C. elegans* appear to be relatively uniform throughout larval development and undergo pronounced changes at the embryo to larval transition and after completion of the final larval stage to the young adult stage. The expression levels are highest during the embryonic stage (4.6, Figure 3.8). The expression then drops to 3.1 during the L1 stage and remains remains relatively stable for the L2, L3, L4 stages (2.8, 2.5, and 2.8 respectively). During late L4, the expression level slightly decreases to 2.3 followed by a drastic to increase 4.0 in the young adult stage (Figure 3.8).

The expression levels of *ivp-3* throughout larval development in both *C. elegans* and *C. briggsae* appear to have virtually no difference in expression patterns. Temporal regulation does not seem to play a role given the similarities in the levels of gene expression. It may, however, be possible that there are differences in the spatial patterns of *ivp-3* between the two species and that these differences may affect downstream signalling.

### 3.2.2   Predicted interactors of *ivp-3*

The GeneMANIA server (www.genemania.org) was used to assess and identify the confirmed and predicted interactions of *ivp-3* with other genes. These interactions are helpful in identifying genes that interact with *ivp-3* and thus provide an understanding of the role of *ivp-3*. Because they share a similar protein domain, the results suggest that 19 genes seem to be correlated with *ivp-3*. A gene functional network was constructed for these 19 genes and *ivp-3* (Figure 3.9).

GeneMANIA searches a large number of publicly available biological data sets to find related genes, including protein-protein, protein-DNA and genetic interactions, pathways, gene and protein expression data, protein domains and phenotypic screening profiles. Due to lack of information available for *ivp-3*, the genes associated with *ivp-3* were found based on shared protein domains only.

Of the 19 genes found to have a shared protein domain with ivp-3, three of these genes were uncharacterized, one (*T23E1.2*) is a pseudogene and another is dead according to Wormbase.org and is now believed to be part of the 3'UTR of an upstream gene (Table 3.3). Further analysis of the remaining 14 genes mainly showed enrichment of nucleic acid binding activity, 3'-5' exonuclease activity, exonuclease activity and nuclease activity, which are associated with transcriptional regulation.

### 3.2.3 Phenotypic analysis of *ivp-3* genes generated by the MMP Project

The million mutation project (MMP) consists of a library of mutagenized *C. elegans* strains to provide the research community with mutant alleles for more than 20,000 genes. Examining mutants of *C.elegans ivp-3* would provide insight into the gene's role in the sister species. The library did not contain any null alleles, however, twelve missense alleles of *ivp-3* were present in the MMP collection. In attempt to identify functionally relevant mutations from the twelve alleles, a comparative blastn analysis of the RNAse H-like domains of *C. elegans*, *C. brenneri*, *C. briggsae* and *C. remanei* was carried out in hopes of identifying specific regions conserved among the four species. Finding an allele with a missense mutation within this conserved region would make for an excellent candidate for analysis however, no such region was found. The strains *VC20274(gk197262)*, *VC40151(gk486330)*, and *VC40672(gk756793)* were then selected based on the hydrophobic to hydrophilic transitions of their mutations namely, phenylalanine to leucine, isoleucine to phenylalanine, and methionine to isoleucine respectively, which may cause loss of or reduced RNAse-H domain function (Table 3.4) (Figure 3.10). Analysis of these mutants showed no Muv phenotype and all three strains

were observed to be wild type. The functional integrity of the domains were not compromised with the mutations that were assessed. Discovery of a phenotype in MMP alleles that have not been analyzed could indicate structural importance of key residues.

### 3.2.4 Molecular analysis of *ivp-3(gk3691)*

The *C. elegans* Gene Knockout Lab at the University of British Columbia has generated a CRISPR allele, *VC3731(gk3691)*, for *C. elegans ivp-3* which was provided as a gift from Donald Moerman's lab. The cassette contains Myo-2 GFP, which allows for the identification of the allele. The strain has since been validated by PCR and Sanger sequencing. Phenotypic analysis of the strain indicated that there were three distinct populations of animals within the strain; wild type animals that did not express GFP, wild type animals expressing GFP, and animals that expressed GFP and possessed a Pvl phenotype and were sterile (See section 3.2.5).

It was hypothesized that Pvl sterile animals, expressing GFP may be homozygous for the deletion site whereas the wild type animals expressing GFP may be heterozygous. To test this hypothesis, genomic DNA of a single worm of each category was extracted and used to PCR amplify bands using two primer sets. The first primer set consisted of a primer (P1) located just before the *Y67D8C.3ab* upstream homology arm of the inserted repair template and in intron 2 of the *ivp-3* gene (Figure 3.14A). The reverse primer (P2) was located in the GFP gene of the the inserted repair template (Figure 3.14A).

As expected, a band was not observed in the PCR product of the animal not expressing GFP as it did not contain a GFP/drug selection cassette (Figure 3.14B). A band of the desired size (2034bp) was observed in both the sample containing the gDNA of the wild type animal expressing GFP and the sample containing gDNA of the sterile, Pvl animal expressing GFP (Figure 3.14B). This was also expected since both animals contained at least one copy of the cassette. Furthermore, the gel indicated that the band of the PCR product containing the gDNA of the wild type animal expressing GFP was not as bright as the band of the sterile, Pvl

animal expressing GFP. The brighter band is indicative of the presence of two copies of the cassette and suggests that the gDNA was that of a heterozygous and a homozygous animal respectively (Figure 3.14B).

The second primer set consisted of the same forward primer (P1) used in set 1, and a reverse primer (P3), located in the *Y67D8C.3ab* downstream homology arm and exon 6 the *ivp-3* gene (Figure 3.14A). Amplification of the the cassette would not occur since a band that is 6383bp in size, would not form under the thermocycling conditions that were set. Only samples containing at least one copy of the original *ivp-3* gene, would result in a band, 1596bp in size. As expected, a band of the desired size was observed in both the sample containing the gDNA of the animal not expressing GFP and sample of the the wild type animal that expressed GFP. A brighter band was observed in the sample containing the gDNA of the animal not expressing GFP in comparison to the band containing the gDNA of the wild type, GFP expressing animal (Figure 3.14B). This suggests that the wild type, GFP sample contained only one copy of the original *ivp-3* gene and thus is heterozygous. Furthermore, for the sample containing the gDNA of the Pvl, sterile animal expressing GFP, no band was observed (Figure 3.14B), indicating that it only contained copies of the cassette. The results of this experiment indicated that the the animals displaying the wild type phenotype while expressing GFP are heterozygous for the deletion site and animals which are Pvl, and sterile and expressing GFP are homozygous for the deletion site.

### 3.2.5 Phenotypic analysis of *ivp-3(gk3691)*

As mentioned previously, initial observations of *ivp-3(gk3691)* led to the identification of three populations of animals; wild type animals that did not express GFP, wild type animals expressing GFP, and sterile, Pvl animals that expressed GFP (Figure 3.11).

Since the PCR results indicate that the three populations of animals were observed because they were either homozygous for the original copy of the *ivp-3* gene, heterozygous, containing one copy of the cassette and one copy of the original the *ivp-3* gene, or homozygous with two copies of the cassette, then it is expected that

the Mendelian ratios of these phenotypes should be 25%, 50% and 25% respectively. The observed phenotypic ratios for these three phenotypes was determined. The analysis was carried out by allowing a young adult hermaphrodite, heterozygous for the deletion site, to mature and lay eggs for 24 hours. The hermaphrodite was then transferred to a new plate to lay eggs for another 24 hours and this was repeated, 24 hours later, for a third time. The F1 progeny were scored when they reached adulthood and all homozygous Pvl animals were cloned onto individual plates and monitored to observe if they produced F2 progeny. The populations from two hermaphrodites were analyzed. It was found that 100% of the Pvl, GFP-expressing progeny, homozygous for the deletion site, had been sterile and unable to produce eggs. The observed ratios of animals homozygous for the original copy of the *ivp-3* gene, heterozygous for the deletion site and homozygous for the deletion site were 29%, 55% and 16% respectively (Figure 3.12). This ratio differed slightly from the expected Mendelian ratio. It was then hypothesized that this deviation from the expected ratio may have been due to embryonic or larval lethality occurring in some animals that are homozygous for the deletion site.

To test embryonic and larval lethality, a young adult hermaphrodite, heterozygous for the deletion site, was allowed to lay eggs for 24 hours. The hermaphrodite was then transferred to a new plate to lay eggs for another 24 hours and this was repeated, 24 hours later for a third time. The eggs were counted once before hatching and then again 24 hours later. A large number of eggs, remaining unhatched is indicative of embryonic lethality. The populations from two hermaphrodites were analyzed. The results indicate that the percentage of eggs hatched in the *ivp-3(gk3691)* strain was similar to that of the N2 control (Figure 3.13), suggesting that animals homozygous for the deletion site are not embryonic lethal. The hatched animals were then scored when they reached adulthood. Furthermore, nearly all of the larval progeny reached adulthood and thus larval lethality did not occur (Figure 3.13). The results suggest that the reduced ratio of Pvl, sterile, homozygous animals may have been a result of problems that occur prior to the formation of the embryo, such as defects in germline development, oogenesis, spermatogenesis, ovulation or fertilization. Another possible explanation for difference between observed and expected ratios could invoke selection. For example, one allele may be selected against for the other.

The findings from the analysis of the *ivp-3(gk3691)* suggest that animals homozygous for the deletion site, which results in a complete loss of function of the *ivp-3* gene, possess a protruding vulva phenotype and are sterile. It is likely that loss of function of *ivp-3* in *C.elegans* prevents the production of fertilized eggs, and that in *C.elegans*, the *ivp-3* is an important gene necessary for growth to a fertile adult.

## 3.3 Genetic Pathway of *Cbr-ivp-3* Function in Vulval Development

I have attempted to understand the genetic pathway of *Cbr-ivp-3* and its function in vulval development through the identification of target genes. Since a severe Muv phenotype was observed in *C. briggsae*, I focused on identifying the mechanism in which *Cbr-ivp-3* negatively regulates organ development through controlling cell proliferation and cell fate specification. The characterization of *ivp-3* in *C. briggsae* will set the stage for comparing the function of the *C. elegans* ortholog in order to understand similarities and differences.

### 3.3.1 Overview of *Cbr-ivp-3* targets identified by RNAseq analysis

With the RNA sequence data from the staged L3 *Cbr-ivp(sy5216)* animals, we were able to obtain gene expression profiles of all of the genes that were differentially regulated. A global view of these genes is presented and described in Figure 3.15. A total of 6999 genes were found to be significantly altered. Initially targets were filtered by eliminating 155 genes that were involved in molting and collagen and cuticle development. This was done because the RNA sequence data is from the RNA of animals that was isolated at the L3 stage, where oscillations of gene expression, important for molting, are readily observed in the developing larvae (Hendriks et al. 2014). A GO analysis was then performed on the remaining genes. These results showed enrichment in terms associated with a number of biological

processes, including genes involved in ATP hydrolysis coupled proton transport to genes associated with nucleoside triphosphate biosynthetic processes (Figure 3.16). This suggests that Cbr-ivp-3 might play a role in biochemical or metabolic processes.

Since the process of vulva formation involves a great deal of cell signalling, signal transduction and cell communication, the focus was to investigate the expression profiles of target genes involved in such processes. Genes associated with the following GO terms were were selected: signalling, regulation of cell proliferation, cell surface receptor signalling pathway involved in cell-cell signalling, signal transduction, regulation of signalling, cell communication, regulation, of cell communication and animal organ development. The results of the GO analysis indicated a higher fold enrichment in gene involved in regulation of cell communication, regulation of signalling, and animal organ development (Figure 3.17). Genes that exhibited a fold change in $\log_2$ expression of >1.5 in either direction on a scale were selected and WormMine was used to identify genes that were associated with the development of the vulva. The search resulted in the selection of seven candidate target genes: *Cbr-nhr-7*, *Cbr-cwn-2*, *Cbr-spin-2*, *Cbr-daf-7*, *Cbr-sel-7*, *Cbr-gsa-1*, and *Cbr-mpk-1* (Table 3.6).

### 3.3.2 RT-qPCR validation of *Cbr-ivp-3* targets identified by RNAseq approach

The Go Term enrichment analysis allowed for the identification of seven candidate target genes, four of which were shown to be upregulated in the RNAseq dataset and three were downregulated. The following genes were selected for initial validation of RNAseq results using RT-qPCR : *Cbr-nhr-7*, *Cbr-cwn-2*, *Cbr-spin-2*, *Cbr-daf-7*, *Cbr-sel-7*, *Cbr-gsa-1*, and *Cbr-mpk-1* (Table 3.6).

Many of the candidate target genes returned in the (GO) terms analysis, were from the nuclear hormone receptor (nhr) family. A majority of the genes were found to be upregulated according to the RNAseq data. Given that the top hits inclusive of the nuclear hormone receptor family all carry similar attributes related

to sequence-specific DNA binding activity and transcription factor activity, the gene with the highest fold change in expression was selected (Wrombase). *Cbr-nhr-7* is an ortholog of *C. elegans nhr-7*. The RNAseq data revealed that *nhr-7* had a fold change of 3.8 (Table 3.6).

*Cbr-cwn-2* is an ortholog of *C.elegans cwn-2*. In *C. elegans, cwn-2* is one of the five genes that encode Wnt ligands along with *lin-44, cwn-1, egl-20, cwn-2* and *mom-2* (Eisenmann et al. 1998). It is known that Wnt signalling has a role in maintaining VPC competence and preventing VPCs from the fusing with the surrounding hypodermal syncytium (Myers and Greenwald 2007). In, *C.elegans, cwn-2* is involved in a number of functions such as its involvement in embryo development, anterior/posterior axis specification, vulval development, cell fate specification, and anterior/posterior axon guidance (Wormbase). It has also been found that CWN-2 appears to function redundantly with LIN-44 and MOM-2. In double mutants of *lin-44* and *mom-2*, the VPCs divide normally and are properly specified, but P7.p divides in reversed polarity, resulting in a vulva only derived from P5.p and P6.p, and a second pseudovulva is derived from P7.p (Inoue et al. 2004). The involvement of *cwn-2* in the wnt pathway and and evidence of its involvement in vulval development and cell fate specification has made this a good candidate for further investigation.

*Cbr-spin-2* is an ortholog of *C. elegans* spin-2. In *C.elegans*, *spin-2* is largely involved in reproductive development such as gonad development and oogenesis (Wrombase). It is also involved in cell migration, a key component of vulval development (Wrombase). According to the RNAseq data, the expression of *Cbr-spin-2* increased 1.9 fold. As such, its potential implication warranted investigation.

*Cbr-daf-7* is an ortholog of *C. elegans daf-7*. In *C. elegans*, *daf-7*, is a member of the transforming growth factor beta (TGF-$\beta$) superfamily and functions as part of a signalling pathway that interprets environmental conditions (Wormbase). Based on protein domain information, *Cbr-daf-7* is predicted to have growth factor activity. It has been found that the *daf-7* TGF-$\beta$ signal is produced by the ASI sensory neuron during reproductive development (Ren et al. 1996). In *C.elegans*, *daf-3* is a transcriptional regulator required for formation of the alternative dauer larval stage (Patterson et al. 1997). Its activity is antagonized by signalling through

the DAF-7/TGF-beta pathway, promoting reproductive growth (Patterson et al. 1997). The RNAseq results indicated that *Cbr-daf-7* was being up-regulated, with a fold change of 1.7 (Table 3.6).

*Cbr-sel-7* is an ortholog of *C. elegans sel-7* where its is involved in the negative regulation of transcription from RNA polymerase II promoter, the regulation of mesodermal cell fate specification, and lateral inhibition. *sel-7* is a nuclear protein and is associated with both *lin-12* and *glp-1*, receptors orthologous to Notch (Lambie and Kimble 1991). Notch signaling, along with other signalling events, is known to specify VPC fates (Greenwald 1998). It has been found that alleles reducing or eliminating the activity of *sel-7* lead to reduced levels of *lin-12* activity, suggesting that *sel-7* is a positive regulator of *lin-12* activity (Chen et al. 2004). *C. elegans glp-1* is required by various cell fate specification processes including vulval cell fate determination and it has been reported that *sel-7* plays a role in cell fate decisions mediated by *glp-1* (Tax et al. 1997).

*Cbr-gsa-1* was shown to be down-regulated by the RNAseq data, with a fold change of -2.3 (Table 3.6). *Cbr-gsa-1* is an ortholog of *C. elegans gsa-1*. According to Wormbase, *C. elegans gsa-1* encodes a subunit of G proteins and is involved in a number of process including receptor-mediated endocytosis, hermaphrodite genitalia development, and regulation of establishment of cell polarity (Wormbase). Based on protein domain information, *Cbr-gsa-1* is also involved in G-protein coupled receptor signalling pathway and signal transducer activity. Preoteomics data suggests that *C.elegans gsa-1* interacts with *glp-1*, a Notch receptor required during VPC determination, and acts to suppress it. The Go term analysis only returned a small number of candidate genes that were found to be down-regulated by the RNAseq data. The fold changes of the first three genes in this list were sufficiently different from the remaining genes in the list. For example, almost an entire fold change difference was observed between the third and the fourth down-regulated gene. *Cbr-gsa-1* was second on that list and had fold change of -2.3, significantly down-regulated in comparison to the other genes in the list.

*Cbr-mpk-1*, an ortholog of *C. elegans mpk-1* is commonly known its involvement in the Map kinase cascade, following stimulation by *let-60* during vulval development (Lackner et al. 1994; Wu and Han 1994). The RAS/MAPK activity

results in the specification of a 1° cell fate. It has been shown that mutations resulting in loss of *mpk-1* activity result in Vul animals whereas gain-of-function mutations exhibit a Muv phenotype (Lackner and Kim, 1998). Two likely targets of the MAPK pathway, are the transcription factors, LIN-31 and LIN-1 (Tan et al. 1998). It has been shown that inactivation of either *lin-1* or *lin-31* leads to a Muv phenotype.

The seven candidate target genes, identified from the RNAseq experiments based on GO term enrichment analysis and fold changes in expression were validated using RT-qPCR for confirmation (Table 3.6). The RT-qPCR data indicated that only two of the seven genes followed the same trend in expression observed in the RNAseq analysis. The RNAseq data suggested that the expression of *Cbr-spin-2* experienced a fold change of 1.9 in *Cbr-ivp(sy5216)* in comparison to the AF16 control. The RT-qPCR results indicated that there is a significant increase in *Cbr-spin-2* in comparison to AF16, showing a fold change of 1.7 (Figure 3.18). The RNAseq data suggested that *Cbr-sel-7* was being down-regulated in *Cbr-ivp(sy5216)* and experienced a fold change of -2.3. Though the fold changes varied compared to the RNAseq results, the RT-qPCR results also suggested that *Cbr-sel-7* was significantly down-regulated but with a fold change of -4.2 (Figure 3.18).

The RT-qPCR data also found that two of the seven genes followed the opposite trend in expression in comparison to the RNAseq data. *Cbr-nhr-7* was shown to be up-regulated with a fold change of 3.6, according to the RNAseq data (Figure 3.18). The RT-qPCR results indicated that *Cbr-nhr-7* is being significantly down-regulated with a fold change of -0.8. Furthermore, the RNAseq data suggested that *Cbr-mpk-1* was down-regulated, with a fold change of -1.9 (Figure 3.18). The RT-qPCR results indicated that this gene was being up regulated 1.5 fold with respect to AF16. There were three genes (*Cbr-cwn-2, Cbr-daf-7*, and *Cbr-gsa-1*) that did not show any significant change with respect the control, according the the RT-qPCR results (Figure 3.18). Conversely, the RNAseq data suggested that both *Cbr-cwn-2* and *Cbr-daf-7* were being up-regulated, with fold changes of 2.2 and 1.7 respectively and that *Cbr-gsa-1* was being down-regulated with a fold change of -2.3 (Figure 3.18).

The RT-qPCR data indicates that only two of the seven (29%) genes followed the same trends in expression observed in the RNAseq analysis. The number of genes tested for validation is very small and thus conclusions cannot yet be made on the accuracy of the RNAseq data. Further validation of additional mRNA targets in *Cbr-ivp(sy5216)* such as those presented in Table 3.6 will allow for a greater understanding of the extent of accuracy of the RNAseq results.

### 3.3.3 Analysis of expression levels of *lin-3* and *lag-2* in Muv mutants

It is known that *lin-3* encodes the inductive signal from the anchor cell and is necessary for vulval induction (Hill and Sternberg 1992). In *C. elegans*, *lin-3* signalling plays a role in maintaining VPC competence by preventing their fusion with hyp7 and many Class A and B SynMuv genes are likely to function within the hyp7 syncytium to repress ectopic expression of *lin-3* (Cui et al. 2006). Cui et al. (2006) have found that the absence of SynMuv function leads to the over secretion of *lin-3* from the hypodermis, resulting in a Muv phenotype through induction of P3.p, P4.p, and P.8p. To ask whether the *Cbr-ivp(sy5216)* mutant exhibits similar expression of *Cbr-lin-3*, RT-qPCR was utilized to measure *Cbr-lin-3* expression levels during the early L3 stage, the stage at which vulval induction occurs. The *bhEx31* transgenic strain, which carries a *hs::lin-3* plasmid from *C. elegans*, was used as a control. Following heat-shock, animals of the *bhEx31* strain confer a Muv phenotype due to increased levels of *lin-3*. The *bhEx3* transgenic animals were heat-shocked prior to isolation of RNA (Materials and Methods 2.5). It was found that the *Cbr-lin-3* transcript levels in *Cbr-ivp(sy5216)* were significantly increased (∼4-fold, Figure 3.19) in comparison to the wild type, AF16. In line with these results, RNAseq data showed a fold change of 3.5 (data not shown). An investigation in expression levels of *lin-3* carried out in *C. elegans* SynMuv double mutants, also demonstrated an increase in *C. elegans lin-3* transcript abundance (Cui et al. 2006). As expected, the *lin-3* levels in *bhEx31(hs::lin-3)* exhibited a modest but statistically significant increase (∼1.5-fold, Figure 3.19). One reason for not observing a higher level of *lin-3* expression following heat-shock of *bhEx31(hs::lin-3)*

may be due to the temperature, duration and stage at which heat shock was performed, although all three parameters were kept consistent throughout batches. It has been found that different doses of *lin-3* could be produced depending on the duration and temperature and stage at which heat-shock is performed and that a high dose results in 1° fates, an intermediate dose results in 2° fates, and a low dose in 3° fates (Sternberg 2005).

Sharanya et al. (2015) examined *Cbr-ivp(sy5216)* mutant animals at L3 and L4 stages using Nomarski optics containing 1° and 2° lineage markers to determine defects in VPCs of the mutants and found that P3.p, P4.p and P8.p cells were induced to take on a secondary cell fate in 5%, 48.8% and 42.5% of the mutants respectively (Sharanya et al. 2015). Since VPC induction of the secondary cell fate is regulated by Notch signalling, there was some evidence suggesting that *Cbr-ivp-3* may play a role in regulating Notch signalling. Furthermore, the work carried out in the Chamberlin Lab suggested that *C. briggsae* Muv mutants are less sensitive to pathway interference than *C. elegans.* Notch was tested as an alternative signalling pathway to identify the source of differences in EGF suppression seen between *C. elegans* and *C. briggsae.* The results suggested that the Notch pathway may be responsible for these differences.

It is known that LAG-2 activates LIN-12/Notch during VPC fate patterning and its expression occurs in all VPCs prior to the inductive signal that initiates vulval development. In response to this inductive signal, *lag-2* is transcribed in P6.p (Zhang and Greenwald 2011). The main effect is to induce neighbours to confer a 2° cell fate, thereby inhibiting them from adopting a 1° fate (Zhang and Greenwald 2011). To ask whether the increased levels of *Cbr-lag-2* in neighbouring cells had a role in P3.p, P4.p and P8.p acquiring 2° cell fates, the expression level of *Cbr-lag-2* was quantified using RT-qPCR during the early L3 stage, the stage at which vulval induction occurs. The data shows that the *Cbr-lag-2* transcript levels in *Cbr-ivp(sy5216)* were increased ($\sim$1.2-fold, Figure 3.19) but not significantly in comparison to the wild type, AF16. The results suggest that *lag-2* does not have a significant role in forming the Muv phenotype of *Cbr-ivp(sy5216).*

### 3.3.4   RNAi knockdown of *Cbr-lin-3* in a *Cbr-ivp(sy5216)*

Since the RT-qPCR results indicated high levels of *Cbr-lin-3* expression in *Cbr-ivp(sy5216)*, it was worth investigating the consequences of knocking down *Cbr-lin-3* expression in the mutant. It was hypothesised that knockdown of *Cbr-lin-3* should reduce the elevated levels of *Cbr-lin-3* in the mutant and thus rescue the Muv phenotype.

Reduced *Cbr-lin-3* expression was found to suppress the Muv phenotype of *Cbr-ivp(sy5216)* (Figure 3.20, Table 3.7). Upon feeding RNAi bacteria containing the *Cbr-lin-3* plasmid, to the *Cbr-ivp(sy5216)* mutant, sensitive to environmental RNAi, the induction score of the rescued mutant was determined to be $3.6 \pm 0.08$. When *Cbr-ivp(sy5216)* animals, sensitive to environmental RNAi were exposed to only the vector control L4440, the induction score was determined to be $4.8 \pm 0.08$, a score which is consistent with the data previously obtained from the penetrance analyses (Figure 3.7). When wild type *C.briggsae* animals, sensitive to environmental RNAi were exposed to the vector control L4440, an induction score of $3 \pm 0$ was observed (Figure 3.7). The induction score of the Muv mutant has been significantly reduced in comparison to that of the L4440 control, and shares a similar induction score to wild type animals.

The results of the RNAi experiment indicate that *Cbr-lin-3* is required for the Muv phenotype in the *Cbr-ivp-3* mutant. The suppression of the Muv phenotype by *Cbr-lin-3(RNAi)* is similar to the strong suppression of the SynMuv phenotype observed by using *lin-3(RNAi)* in several SynMuv strains (Cui et al. 2006). Furthermore, loss-of-function mutations of *lin-3* or in *let-23* lead to a Vul phenotype (Hill and Sternberg 1992). Both the RT-qPCR data and the RNAi data suggest that elevated levels of *Cbr-lin-3* play a significant role in the Muv phenotype observed in *Cbr-ivp(sy5216)*. The results suggest that *Cbr-ivp-3* appears to work through a well established model in which *Cbr-lin-3* is overexpressed.
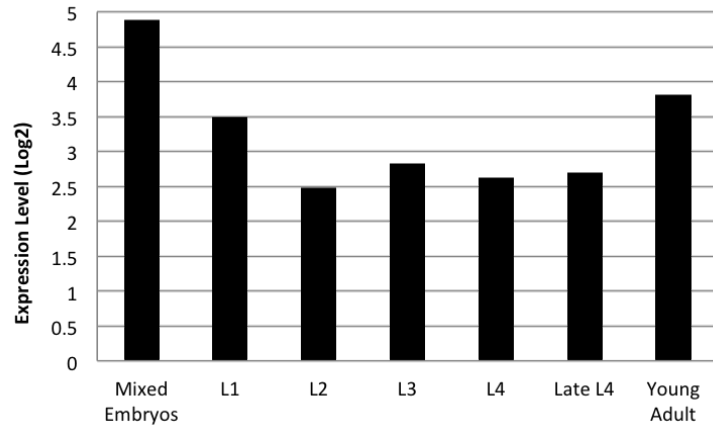
Figure 3.1: The gene expression profile for *Cbr-ivp-3* for the embryonic, L1, L2, L3, L4, late L4 and the young adult stages in *C. briggsae*. Description of developmental stages and raw data can be derived from Grun et al., 2014.
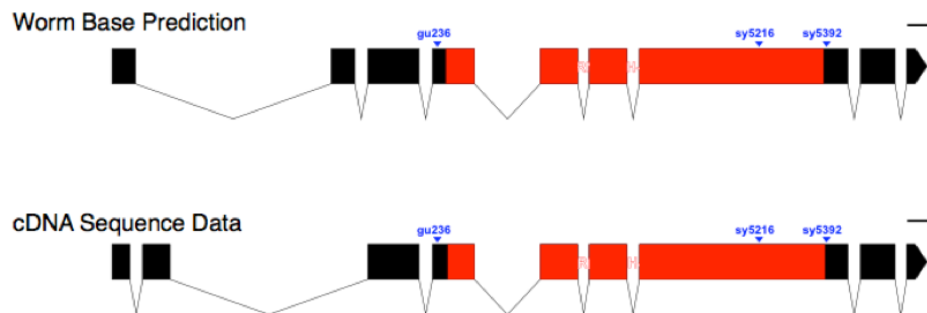


Figure 3.2: An intron-exon map illustrates the locations of the introns and exons, predicted by WormBase (a), (b) the boundaries identified after sequencing *Cbr-ivp-3* cDNA. The location of where the *Cbr-ivp(sy5216)*, *Cbr-ivp(sy5392)* and *Cbr-ivp(gu236)* mutations are also indicated. The position of the RNAse H-like domain is indicated in red.
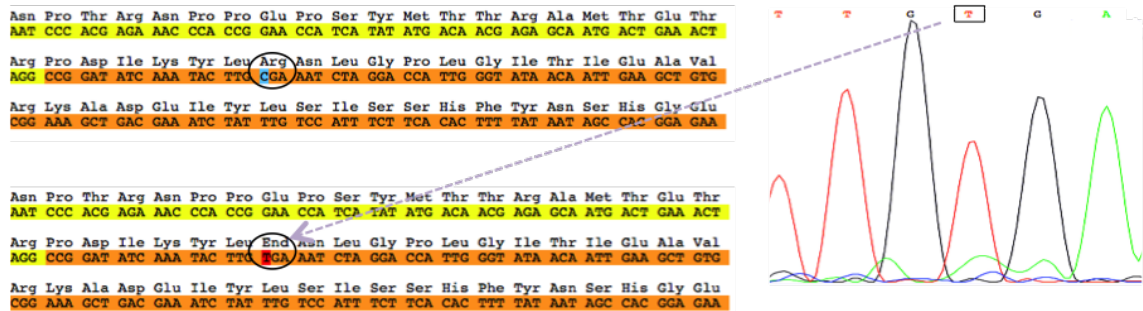
FIGURE 3.3: Sequencing results verified the presence of a point mutation in *Cbr-ivp-(gu236)*, indicated by the circled nucleotide. The point mutation was identified as a nonsense mutation where the cytosine in CGA was replaced by thymine, resulting in a TGA sequence.
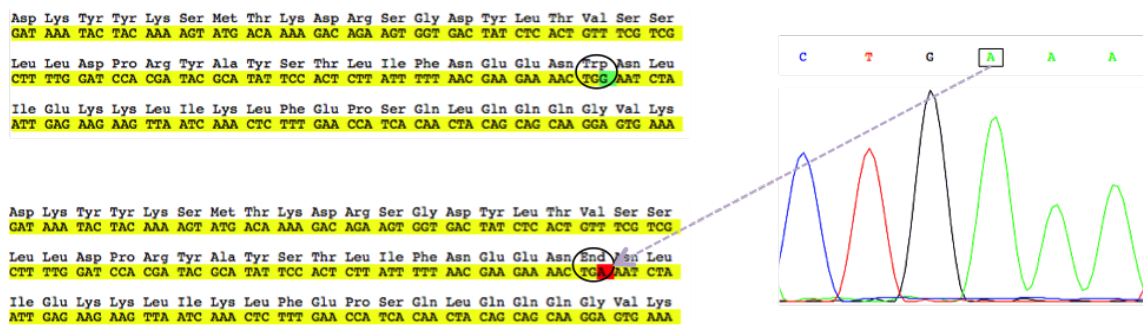


FIGURE 3.4: Sequencing results verified the presence of a nonsense mutation in *Cbr-ivp(sy5216)*, indicated by the circled nucleotide. In the sequence TGG, the third guanine was found to be replaced with an adenine (TGA)
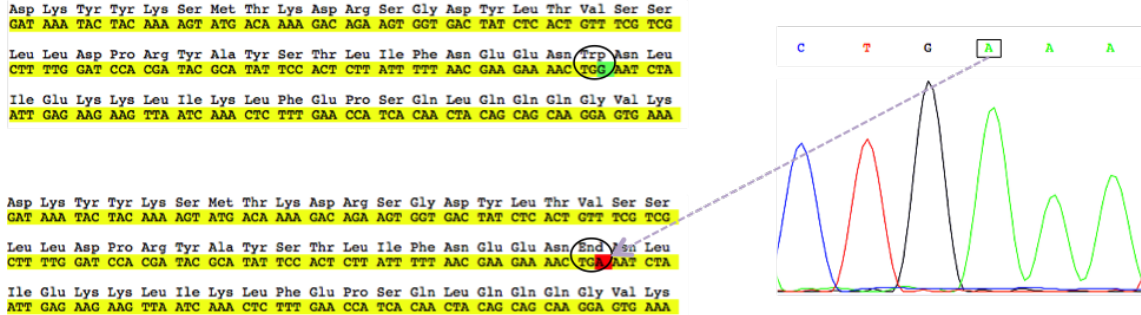
FIGURE 3.5: Sequencing results verified the presence of a nonsense
mutation in *Cbr-ivp(sy5392)*, indicated by the circled nucleotide.
The first adenine in the sequence AAA was replaced with a thymine
(TAA).

| Mutant | Type Of Mutation | Location Of Mutation | Mutation within RNase H-like domain? | Nucleotide change | Codon change | Amino acid change |
|---|---|---|---|---|---|---|
| *Cbr-ivp(sy5216)* | Nonsense | Exon 7 | Yes | G → A | TGG → TGA | Trp → STOP |
| *Cbr-ivp(sy5392)* | Nonsense | Exon 7 | No | A → T | AAA → TAA | Lys → STOP |
| *Cbr-ivp(gu236)* | Nonsense | Exon 4 | No | C → T | CGA → TGA | Arg → STOP |

TABLE 3.1: The table summarizes the nature of the three *Cbr-ivp-3*
mutants; *Cbr-ivp(gu236)*, *Cbr-ivp(sy5216)*, and *Cbr-ivp(sy5392)*.
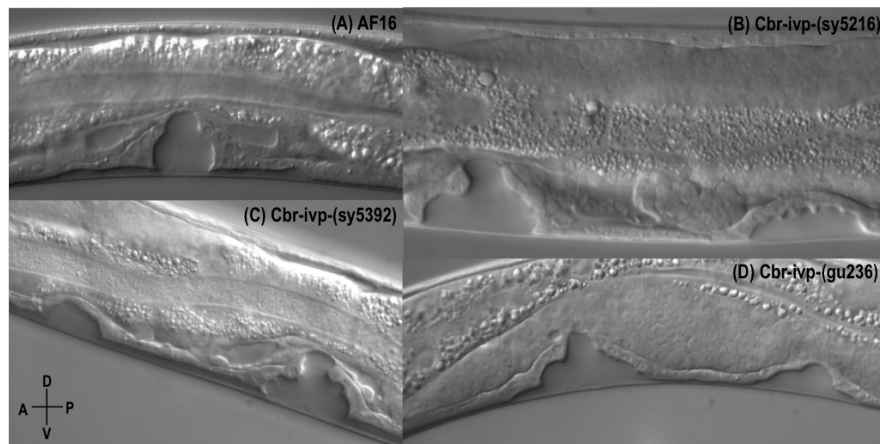
FIGURE 3.6: Vulval induction defects in *Cbr-ivp3* mutants. Animals were examined at mid-L4 stage. (A) Wild type, AF16 animal in which the formation of a single vulva can be observed with correct VPC induction and divisions. (B) In the *Cbr-ivp(sy5216)* animal, the formation of two vulvae can be observed. This is due to the induction of multiple VPCs. (C) The formation of multiple vulvae due to improper induction of VPCs in *Cbr-ivp(sy5392)*. (D) Similar to the other two mutants, the formation of two vulvae can be observed in *Cbr-lin(gu236)*. In all three mutants, it is common to observe the formation of three vulvae (not shown) due to the induction of P.4p and P.8p in addition to P.6p, P.5p and P.7p.

| | % Induction of VPCs | | | | | | | |
|---|---|---|---|---|---|---|---|---|
| Genotype | P3.p | P4.p | P5.p | P6.p | P7.p | P8.p | Average Ind | N |
| *Cbr-ivp(sy5216)* | 18.0 | 84.6 | 100.0 | 100.0 | 97.4 | 94.9 | 4.9 | 39 |
| *Cbr-ivp(sy392)* | 12.2 | 78.1 | 100.0 | 100.0 | 100.0 | 90.2 | 4.8 | 41 |
| *Cbr-ivp(gu236)* | 15.0 | 85.0 | 100.0 | 100.0 | 100.0 | 97.5 | 4.9 | 40 |

TABLE 3.2: *Cbr-ivp(gu236),Cbr-ivp(sy5216)*, and *Cbr-ivp(sy5392)* mutant animals were examined at the L4 stage under Normarski optics. The developing vulva was examined and the VPC induction scores were determine. Average ind is average VPC induction of each strain; N is number of animals.



FIGURE 3.7: Gonad abnormalities observed in *Cbr-ivp-3* mutant alleles. (A) a directionality defect observed in the gonad of in Cbr-ivp(sy5216); (B) bulging at the anterior end and directionality defects at the posterior end of the is unusually short gonad in Cbr-ivp(sy5392); (C) improper turning of the posterior arm in Cbr-ivp(gu236). A - Anterior; P - Posterior; D - Dorsal; V - Ventral.
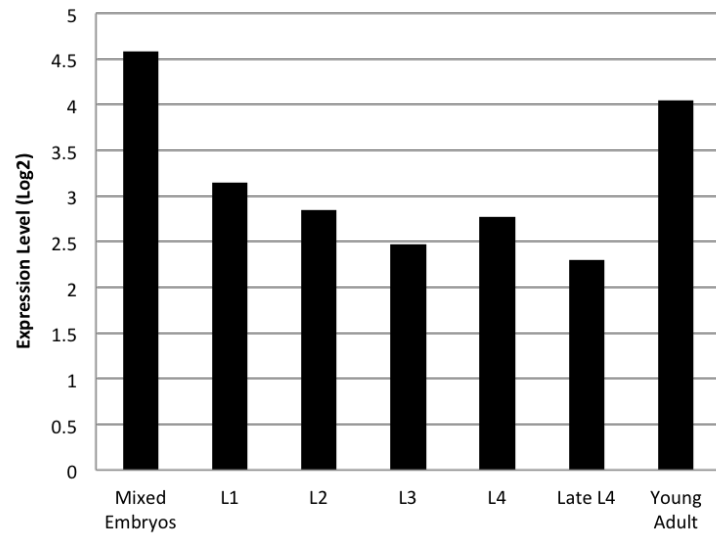
FIGURE 3.8: The gene expression profile for *ivp-3* for the embryonic, L1, L2, L3, L4, late L4 and the young adult stages in *C. elegans.* Description of developmental stages and raw data can be derived from Grun et al., 2014.

Figure 3.9: Gene network of *ivp-3* derived from GeneMANIA
(http://genemania.org). A gene network from GeneMANIA shows
the interactions between *C. elegans ivp-3* and 19 other genes ac-
cording to the functional association networks from the databases.
Interactions were found based on shared protein domains only.
Nodes represent proteins and links represent networks.

| Gene | Function |
|------|----------|
| C25F9.2 | -predicted to have 3'-5' exonuclease activity, DNA binding activity, DNA-directed DNA polymerase activity, endonuclease activity, and nucleotide binding activity, based on protein domain information |
| C10A4.1 | -an ortholog of human ZBED6 (zinc finger BED-type containing 6) and ZBED4 (zinc finger BED-type containing 4)<br>-predicted to have nucleic acid binding activity and protein dimerization activity, based on protein domain information |
| C09E7.4 | -an ortholog of human ZBED4 and ZBED1<br>-predicted to have nucleic acid binding activity and protein dimerization activity, based on protein domain information |
| B0545.4 | - involved in embryo development and reproduction<br>-predicted to have nucleic acid binding activity and protein dimerization activity, based on protein domain information |
| C53D6.6 | -an ortholog of human ZBED6 and ZBED4<br>-predicted to have nucleic acid binding activity and protein dimerization activity, based on protein domain information |
| W05H12.2 | -an ortholog of human EXD3 (exonuclease 3'-5' domain containing 3)<br>-predicted to have 3'-5' exonuclease activity and nucleic acid binding activity, based on protein domain information |
| Y57A10A.13 | - predicted to have 3'-5' exonuclease activity and nucleic acid binding activity, based on protein domain information |
| C03D6.1 | -an ortholog of members of the human AGO, PIWIL (Argonaute/PIWI) family including AGO4<br>-involved in body morphogenesis, embryo development, hermaphrodite genitalia development, nematode larval development and receptor-mediated endocytosis<br>-predicted to have nucleic acid binding activity, based on protein domain information<br>-expressed in the hypodermis, tail, and the intestine |
| F19F10.11 | - encodes a protein with a THAP or THAP-like domain (other proteins with such domains include LIN-15A, LIN-15B, LIN-36, and HIM-17 |
| egal-1 | -an ortholog of human EXOSC10 (exosome component 10)<br>-involved in locomotion, the molting cycle and reproduction<br>-predicted to have 3'-5' exonuclease activity and nucleic acid binding activity, based on protein domain information |
| W04A8.4 | - involved in striated muscle myosin thick filament assembly<br>- predicted to have 3'-5' exonuclease activity and nucleic acid binding activity, based on protein domain information<br>-localized to the endoplasmic reticulum |
| ZK662.5 | - predicted to have nucleic acid binding activity, based on protein domain information |
| F46F2.4 | - predicted to have nucleic acid binding activity, based on protein domain information |
| K05G3.1 | - predicted to have nucleic acid binding activity, based on protein domain information |
| rnh-1.0 | - one of four C. elegans genes that can encode an RNase H ribonuclease<br>-when expressed in vitro, isoforms exhibit RNase H activity<br>-transcripts are expressed throughout development |
| ZK1098.2 | Uncharacterized protein |
| F42H10.5 | Uncharacterized protein |
| ZK1098.3 | Uncharacterized protein |
| T23E1.2 | isoform a, pseudogene |
| F53G12.11 | -This gene is dead<br>-Appears to be part of the 3' UTR of the upstream gene |

Table 3.3: The functions of the 19 genes predicted by GeneMania to be associated with *ivp-3* based on shared protein domains. Information obtained from http://www.wormbase.org.

| Strain Name | Allele | Mutation | Amino Acid Changes |
|---|---|---|---|
| VC20274 | gk197262 | Proline to Leucine | Hydrophobic to hydrophobic, removal of proline ring |
| VC40151 | gk486330 | Isoleucine to Phenylalanine | Hydrophobic to hydrophobic + aromatic ring in RnaseH domain region |
| VC40672 | gk756793 | Methionine to Isoleucine | Neutral to hydrophobic in RnaseH domain region |

TABLE 3.4: The million mutation project (MMP) library contained twelve missense alleles of *ivp-3* were present in the MMP collection. Three of these strains, *VC20274, VC40151*, and *VC40672*, were selected for analysis based on their changes in the amino acid sequence.
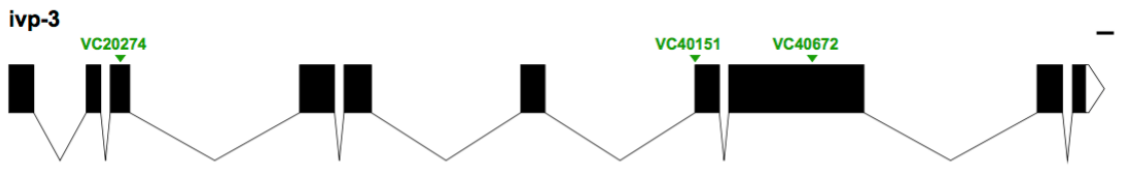


FIGURE 3.10: An intron-exon map illustrates the locations of the mutations of the three *C.elegans ivp-3* missense alleles that were selected for analysis from the MMP collection.
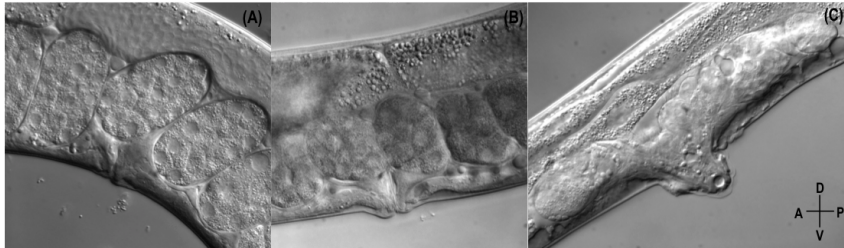
FIGURE 3.11: Phenotypic analysis of the CRISPR allele, *ivp-3(gk3691)*, for *c. elegans ivp-3* indicated that there were three populations of animals within the strain; (A) wild type animal-sthat did not express GFP (B) wild type animals expressing GFP, believed to be heterozygous for the deletion site and (C) sterile animals that expressed GFP and had a Pvl phenotype. The animals were found to be homozygous for the deletion site.



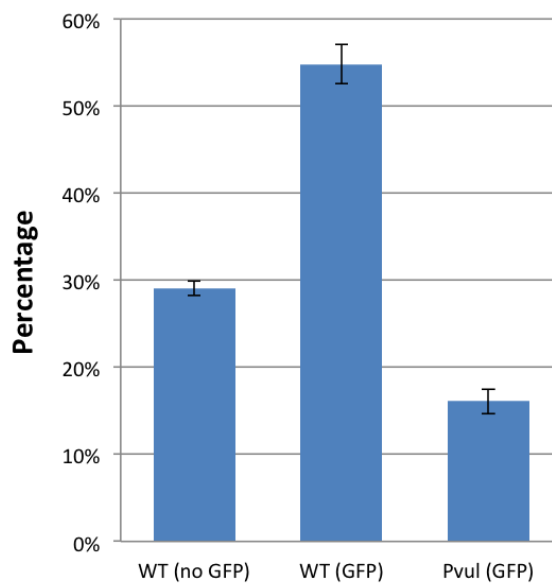FIGURE 3.12: Initial observations of *ivp-3 (gk3691)* led to the identification of three populations of animals; wild type animals that did not express GFP, wild type animals expressing GFP, and sterile, Pvl animals that expressed GFP. The observed phenotypic ratios for these three phenotypes were determined by scoring the progeny of two heterozygous hermaphrodites. Error bars represent standard error of the mean.
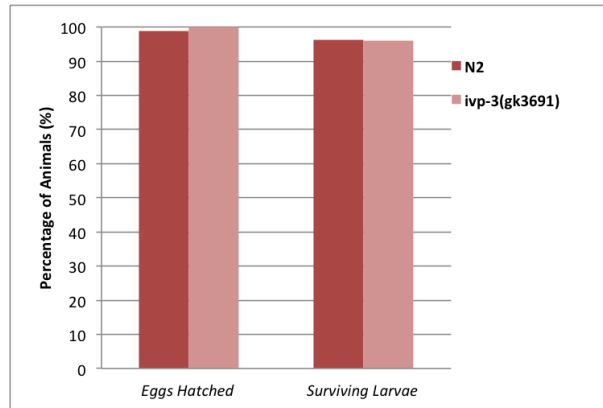
FIGURE 3.13: The eggs of two *ivp-3 (gk3691)* heterozygous hermaphrodites were counted once before hatching and again 24 hours later. A large number of eggs, remaining unhatched is indicative of embryonic lethality. The hatched animals were then scored when they reached adulthood. A reduced number of adults in comparison to the number of eggs hatched is indicative of larval lethality.

| Gene ID | Log$_2$ Fold Change |
|---------|---------------------|
| Cbr-nhr-7 | 3.64 |
| Cbr-cwn-2 | 2.21 |
| Cbr-spin-2 | 1.90 |
| Cbr-daf-7 | 1.73 |
| Cbr-sel-7 | -2.32 |
| Cbr-gsa-1 | -2.25 |
| Cbr-mpk-1 | -1.93 |

TABLE 3.5: The Go Term enrichment analysis allowed for the identification of seven candidate target genes, four of which were shown to be upregalated (green) in the RNAseq dataset and three were downregulated (red). The genes were selected for validation by RT-qPCR.
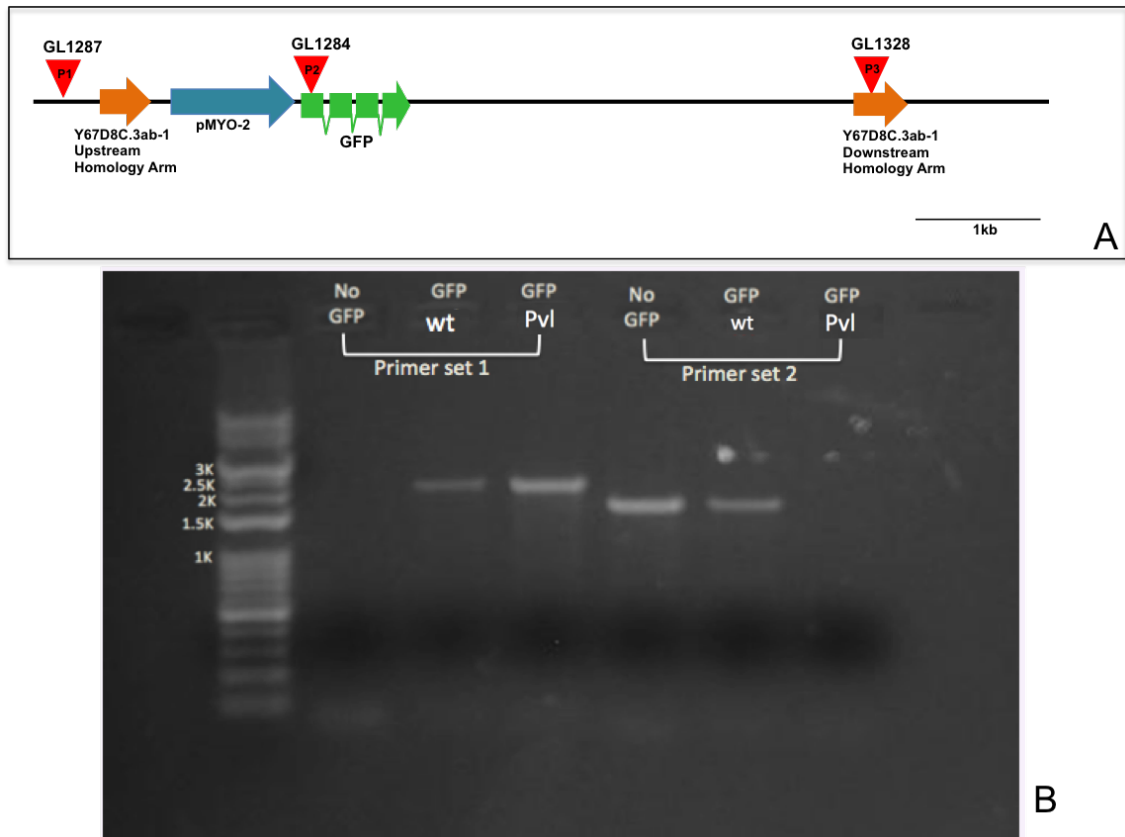
Figure 3.14: A PCR reaction was set up to determine whether the Pvl, sterile animals were homozygous for the deletion site. (A) A schematic drawing of a portion of the inserted template. The genomic validation primers are labeled P1, P2, and P3. Primer set 1, containing P1 and P2 were used to amplify a band 2034bp in size. Primer set 2, containing P1 and P3 would amplify a band 6383bp in size if amplified form the inserted template or 1596bp from the original, undeleted *ivp-3* gene. (B) Agarose gel of PCR fragments obtained from amplification of the insertion template. Genomic DNA of a single worm was extracted from each of the three populations of animals within *ivp-3(gk3691)*: wild type animalsthat did not express GFP (No GFP), wild type animals expressing GFP (GFP wt), and animals that expressed GFP and Pvl sterile animals (GFP Pvl). Two PCR reactions were set up with the genomic DNA, one with primer set 1 and the other with primer set 2.
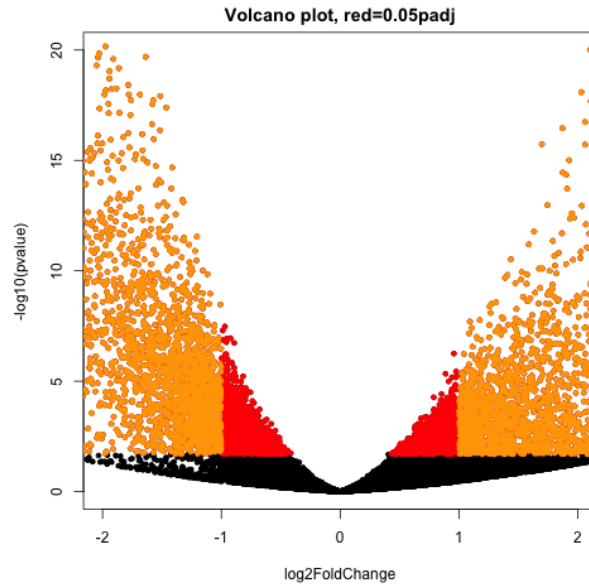
Figure 3.15: The fold change of transcripts from *Cbr-ivp(sy5216)* mutant animals plotted against their p-values. Each point represents an individual gene. Data points to the right of 0 represent upregulated genes, while data points to the left of 0 represent downregulated genes.



Figure 3.16: A Gene Ontology (GO) enrichment analysis was performed on the gene expression profiles of genes obtained from the RNAseq data. Genes associated with ATP hydrolysis coupled proton transport, energy coupled proton transmembrane transport, and ATP synthesis coupled proton transport showed the greatest enrichment.
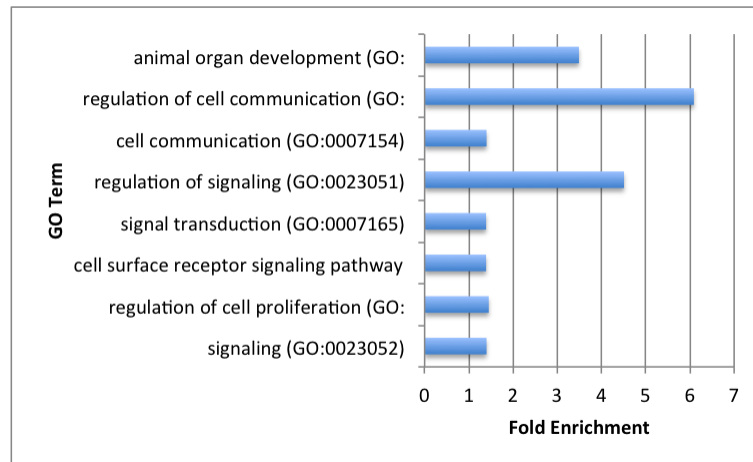
FIGURE 3.17: Following a GO enrichment analysis, genes associated with the following GO terms were selected: signalling, regulation of cell proliferation, cell surface receptor signalling pathway involved in cell-cell signal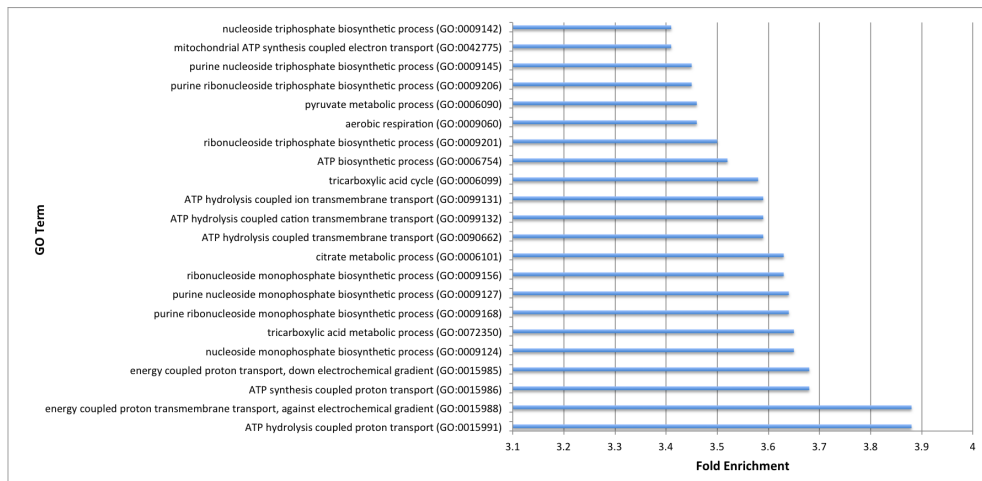ling, signal transduction, regulation of signalling, cell communication, regulation, of cell communication and animal organ development.

| Gene ID | Log$_2$ Fold Change |
|---------|---------------------|
| Cbr-nhr-7 | 3.64 |
| Cbr-cwn-2 | 2.21 |
| Cbr-spin-2 | 1.90 |
| Cbr-daf-7 | 1.73 |
| Cbr-sel-7 | -2.32 |
| Cbr-gsa-1 | -2.25 |
| Cbr-mpk-1 | -1.93 |

TABLE 3.6: The Go Term enrichment analysis allowed for the identification of seven candidate target genes, four of which were shown to be upregalated (green) in the RNAseq dataset and three were downregulated (red). The genes were selected for validation by RT-qPCR.
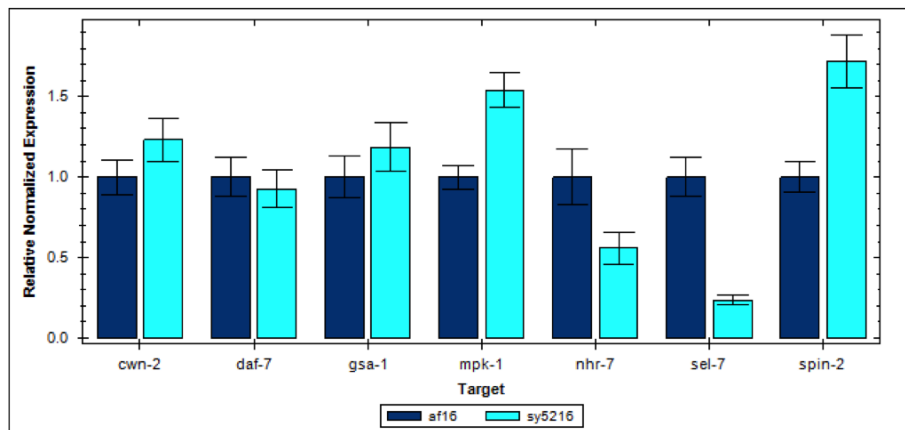
FIGURE 3.18: Validation by RT-qPCR of the seven target genes selected from the Go Term enrichment analysis. All trials are normalized to internal reference gene *Cbr-pmp-3*. Error bars represent standard error of the mean.
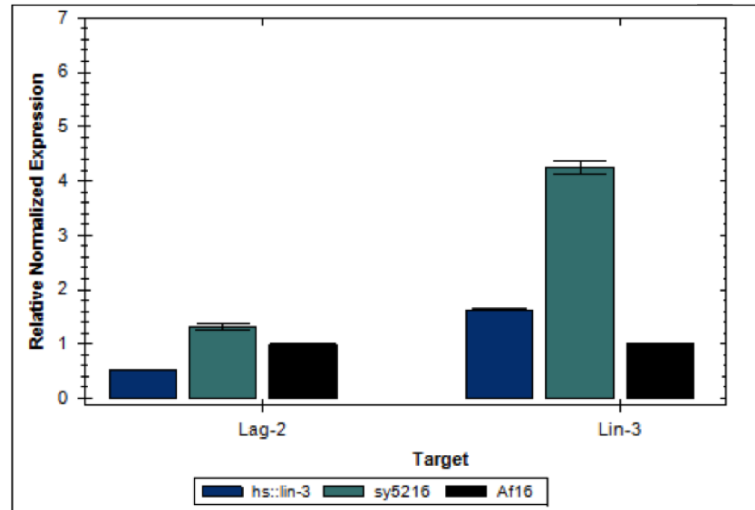
FIGURE 3.19: The expression of Cbr-lin-3 transcripts in Cbr-ivp(sy5216) determined by RT-qPCR. Relative fold changes of Cbr-lin-3 transcripts have been plotted. Error bars represent standard error of the mean. AF16 and HS::lin-3 were used as controls.
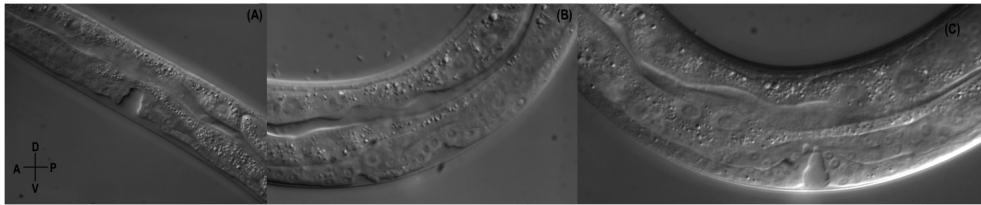
FIGURE 3.20: The affects of RNAi knockdown of *Cbr-lin-3* in the *Cbr-ivp-3* mutant, Cbr-ivp(sy5216). (A)The VPC induction of mfIs42[sid-2::GFP; myo-2::dSRed]; L4440(RNAi), a wildtype C. briggsae strain, sensitive to environmental RNAi, was exposed to RNAi bacteria containing the L4440 empty vector. VPC induction and vulval formation looks normal. (B)Multiple vulvae were observed to be forming in *Cbr-lin(sy5216)*; *mfIs42[sid-2::GFP; myo-2::dSRed]; L4440(RNAi)*. The *Cbr-ivp(sy5216)* strain, sensitive to environmental RNAi, was exposed to RNAi bacteria containing the L4440 empty vector. VPC induction and vulval formation is abnormal, similar to vulva development of the *Cbr-ivp-3* mutnat alleles. (C) Vulval induction appears normal in *Cbr-lin(sy5216)*; *mfIs42[sid-2::GFP; myo-2::dSRed]; Cbr-lin-3(RNAi)*. The *Cbr-ivp(sy5216)* strain, sensitive to environmental RNAi, was exposed to RNAi bacteria containing the *Cbr-lin-3* RNAi vector. The knockdown of *Cbr-lin-3* appears to have rescued the Muv phenotype.

| Genotype | VPC Induction score ± SE | N |
|---|---|---|
| mfIs42[sid-2::GFP; myo-2::dSRed] ; L4440(RNAi) | 3 ± 0.00 | 60 |
| Cbr-lin(sy5216); mfIs42[sid-2::GFP; myo-2::dSRed] ; Cbr-lin-3(RNAi) | 3.6 ± 0.08 | 61 |
| Cbr-lin(sy5216); mfIs42[sid-2::GFP; myo-2::dSRed] ; L4440(RNAi) | 4.76 ± 0.08 | 60 |

Table 3.7: A comparison of the induction scores of *Cbr-ivp(sy5216)* RNAi sensitive animals, that were fed RNAi bacteria containing the *Cbr-lin-3* plasmid and *Cbr-ivp(sy5216)* RNAi sensitive animals and wild type RNAi sensitive animals that were exposed to the empty vector, L4440. The induction score of the Muv mutant has been significantly reduced in comparison to that of the L4440 control, and shares a similar induction score to wild type animals. N is number of animals.

# Chapter 4

# Conclusions, Significance and Future Directions

## 4.1    Conclusions

In this section, I will summarize my findings and will highlight the significance of my work. I will discuss the functional differences in the *ivp-3* gene, by comparing the results of the molecular genetic analyses of the gene in both *C. elegans* and *C. briggsae*. Lastly, I will attempt to uncover the role of *ivp-3* in vulval development based on the findings of this study.

### 4.1.1    Summary of findings

In this thesis, I have carried out a molecular genetic analyses of *ivp-3* in both *C. briggsae* and *C. elegans* and have begun to characterize the functional role of *Cbr-ivp-3*.

For the analysis of the *Cbr-ivp-3* gene, I have identified the gene expression profile for the embryonic, L1, L2, L3, L4, late L4 and the young adult stages from the larval gene expression dataset in *C. briggsae* (Grün et al. 2014). I have found that the transcript expression levels appear to be relatively uniform throughout larval development and undergo pronounced changes at the embryo to larval transition and after completion of the final larval stage to the young adult stage. I

have sequenced the cDNA of the *Cbr-ivp-3* gene to confirm the accuracy of the gene predictions provided by WormBase and found that the intron-exon boundaries were not correctly predicted upstream of the third exon. The third of the three mutants of *Cbr-ivp-3*, *Cbr-ivp(gu236)*, was sequenced and I have found that a nonsense mutation is present at the fourth exon of the *Cbr-ivp-3* gene. The mutation is located just upstream of where the RNase H-like domain begins, thus the truncated protein generated by this mutant does not contain the RNase H-like domain. Furthermore, the inappropriate divisions of VPCs in the *Cbr-ivp-3* mutant alleles (*Cbr-ivp(sy5216)*, *Cbr-ivp(sy5392)* and *Cbr-ivp(gu236)* have been observed and characterized. All mutants showed ectopic division of VPCs as well as increased percentage of induced VPCs. Along with increased percentage of induced VPCs, severe variations in the gonad morphology and guidance in all three mutants were observed.

I have also carried out molecular genetic analyses of *ivp-3* in *C. elegans* and have identified the gene expression profile for *ivp-3* for the embryonic, L1, L2, L3, L4, late L4 and the young adult stages, using the larval gene expression dataset in *C. elegans* (Grün et al. 2014). Similar to the expression profile of *Cbr-ivp-3*, the transcript expression levels are relatively uniform throughout larval development and pronounced changes are observed at the embryo to larval transition and after completion of the final larval stage to the young adult stage. My findings from the proteomics data show that 19 genes share a similar protein domain with *ivp-3* and are involved in processes such as nucleic acid binding activity, 3'-5' exonuclease activity, and nuclease activity. The phenotypic analysis of the *ivp-3(gk3691)* strain has indicated that there are three distinct populations of animals within the strain, the ratios have been determined, and the genotypes associated with these phenotypes have been identified. It has been found that there is no embryonic lethality or larval lethality associated with the strain and that animals homozygous for the deletion site confer a protruding vulva phenotype and are sterile.

I have begun to analyze the genetic pathway of *Cbr-ivp-3* and its function in vulval development. An RNAseq analysis was carried out to identify genes that may be differentially expressed in *Cbr-ivp(sy5216)*. With the RNA sequence data from the staged L3 *Cbr-ivp(sy5216)* animals, we were able to obtain gene

expression profiles of thousands of genes. Using the Gene Ontology (GO) terms associated with vulval development, the following genes were selected for initial validation of RNA-seq results using RT-qPCR: *Cbr-nhr-7*, *Cbr-cwn-2*, *Cbr-spin-2*, *Cbr-daf-7*, *Cbr-sel-7*, *Cbr-gsa-1*, *Cbr-mpk-1*. The RT-qPCR data indicated that two of the seven genes followed the same trend in expression observed in the RNA-seq analysis. Also using RT-qPCR, the expression levels of *Cbr-lin-3* and *Cbr-lag-2* in *Cbr-ivp(sy5216)* were measured at the early-L3 stage. It was found that the *Cbr-lin-3* transcript levels in *Cbr-ivp(sy5216)* was significantly higher than the wild type and that the *Cbr-lag-2* transcript levels did not significantly change in the Muv mutant. Since the RT-qPCR results indicated high levels of *Cbr-lin-3* expression in *Cbr-ivp(sy5216)*, RNAi was utilized to knockdown *Cbr-lin-3* expression in *Cbr-ivp(sy5216)*. It was found that reduced levels of *Cbr-lin-3* expression suppressed the Muv phenotype of *Cbr-ivp(sy5216)* as the induction score of the mutant was significantly reduced in comparison the L4440 control.

## 4.1.2   Significance of findings

The work described in this thesis focuses on the identification of *ivp-3*, a gene involved in vulval development in *C. briggsae*, with an emphasis on comparative evo-devo analysis using *C. elegans*.

I have characterized a novel gene in *C. briggsae* which can now be used in future experiments to determine its function and role in vulval development. I have validated *Cbr-ivp-3* by determining its expression profile throughout larval development, identifying its gene structure (i.e. the open reading frame and nature of mutations in alleles), and analyzing the inappropriate division of VPCs in the three *Cbr-ivp-3* mutant alleles (*Cbr-ivp(sy5216)*, *Cbr-ivp(sy5392)* and *Cbr-ivp(gu236)*).

Furthermore, I have provided an avenue in which comparative studies to understand evolution of gene function and developmental mechanisms can take place, by characterizing *ivp-3*, the ortholog in *C.elegans*. The expression profile of this gene throughout larval development has been determined and literature reported interactions of *ivp-3* with other genes have been identified. A thorough phenotypic analysis of *ivp-3(gk3691)*, an allele that that lacks the entire coding sequence of

the gene, has been carried out. The analysis reveals significant differences in *ivp-3* function between the two species, supporting the notion that there is evolutionary functional divergence within the gene.

I have also attempted to identify target genes that may be involved in the vulva development pathway associated with *Cbr-ivp-3*. The data from the RNAseq analysis has identified gene expression profiles of thousands of genes that can be used to identify target genes that are differentially expressed in *Cbr-ivp(sy5216)*.

Furthermore, I have attempted to understand the genetic pathway of *Cbr-ivp-3* and its function in vulval development. Through RT-qPCR, I have determined that *Cbr-lag-2* transcript levels are not significantly changed in the Muv mutant, providing evidence against the hypothesis that *Cbr-ivp-3* may play a role in regulating Notch signalling. I have found that *Cbr-lin-3* is expressed in significantly high levels and that reduced levels of *Cbr-lin-3* expression, by RNAi knockdown, suppressed the Muv phenotype of *Cbr-ivp(sy5216)*. Despite previous speculation that this may not be the case (Sharanya et al. 2015), the findings in this thesis suggest that *Cbr-ivp-3* appears to work through a well established model in which *Cbr-lin-3* is overexpressed. My findings strongly suggest that *Cbr-ivp-3* is functioning in a manner similar to some SynMuv genes.

### 4.1.3  Functional differences in *ivp-3*

The phenotypic analyses carried out for the *ivp-3* mutants in both *C. briggsae* and *C. elegans* can help determine functional differences in the gene between the two species. The *Cbr-ivp-3* mutants, all of which produce a truncated version of the protein, are Muv mutants with multiple pseudovulvae present on the ventral surface of the animal. In these mutants, a greater number of VPCs are induced than usual. These animals are fertile and various abnormalities in the gonad have been observed. In the *ivp-3(gk3691)* strain, the animals homozygous for the deletion site confer a protruding vulva phenotype and are sterile. It is likely that loss of function of *ivp-3* in *C. elegans* prevents the production of fertilized eggs, and that in *C. elegans*, the *ivp-3* is an important gene, required for growth into a fertile adult. It is possible that the Pvl phenotype may be a result of multiple

VPCs inducing to form a single protrusion, similar to a Muv phenotype. Thus, the idea that the role of *ivp-3* in vulval development may be conserved between *C. elegans* and *C. briggsae* cannot be ruled out. It is possible that the underlying developmental mechanism may be conserved, despite the differences in phenotype. Nomarski optics can be used to identify VPC induction patterns in *ivp-3(gk3691)* animals to determine if this is the case.

The gene structure of *ivp-3* gene differs slightly between the two species. In *C. elegans*, the gene consists of 10 exons and is 6231bp in length, in the unspliced gene. In *C. briggsae*, the gene consists of 9 exons and is much smaller in size (3060bp unspliced). This larger gene may be a result of gene duplications which are common among *Caenorhabditis* species (Stein et al. 2003). The duplication of genes is important in providing raw materials for the evolution of genetic diversity. In some cases, a change in a gene can lead to a new function of that gene. For example, it was found the acquisition of an additional domain in the *lin-17* receptor in *Pristionchus pacificus* resulted in a novel wiring of the Wnt signalling pathway (Wang and Sommer 2011). This observation reveals that the evolution of vulva induction can involve molecular changes that may shift signalling pathways. The nucleotide sequences of the two genes were blasted and revealed a 65% identity, indicative of changes in both the *C. elegans* and *C. briggsae* lineages since their divergence.

Both *Cbr-ivp-3* and *ivp-3* have an RNase H-like domain, both approximately 300 amino acids in length. The presence of the RNase H-like domain can provide clues about gene function. Several transferases contain this catalytic domain including ribonuclease H class I (RNase HI) and class II (RNase HII), HIV RNase (reverse transcriptase domain), retroviral integrase (catalytic domain), Mu transposase (core domain), transposase inhibitors, 3'-5' exonucleases (exonuclease domains), and mitochondrial resolvases (catalytic domain) (InterPro). Based on the protein domain information, *ivp-3* in both *C. briggsae* and *C. elegans* are predicted to have nucleic acid binding activity. Furthermore, the GeneMANIA search used to identify genes associated with *C. elegans ivp-3* matched 19 genes based on shared protein domains. These genes mainly showed enrichment of nucleic acid

binding activity, 3'-5' exonuclease activity, exonuclease activity and nuclease activity, which are associated with transcriptional regulation. Together, these findings infer the possibility that the IVP-3 translocates into the nucleus, likely to regulate gene expression in both species.

In this study, I found that *Cbr-ivp(sy5216)*, a mutant of *Cbr-ivp-3*, has significantly high expression levels of *Cbr-lin-3* and that this increased expression of the inductive signal in the Muv mutant is the cause of ectopic vulval development. A Muv phenotype can result in either species from overexpression of *lin-3* from the anchor cell (Katz et al. 1996). The results suggest that *Cbr-ivp-3* appears to work through a well established model in which *Cbr-lin-3* is overexpressed, however, more work must be done to determine whether the shared mechanism is conserved downstream of *lin-3*. Thus far, only a molecular genetic analysis of *ivp-3* in *C. elegans* has been determined. The role of *lin-3* in the formation of the protruding vulva in homozygotes of *ivp-3(gk3691)* can be looked at to determine if *lin-3* is also overexpressed in *C. elegans*.

The expression levels of *ivp-3* throughout larval development in both *C. elegans* and *C. briggsae* have been investigated and appear to have virtually no difference in expression patterns. The translational expression levels of *ivp-3* in both species are relatively uniform throughout larval development and undergo pronounced changes at the embryo to larval transition and after completion of the final larval stage to the young adult stage. Temporal regulation does not seem to play a role given the similarities in the levels of gene expression. It may be possible that there are differences in the spatial patterns of *ivp-3* between the two species and that these differences may affect downstream signalling. Transcriptional fusion of *ivp-3* in both species may help determine if this is the case. Without further experimentation, we cannot preclude spatial regulation.

### 4.1.4   The role of *ivp-3* in vulval development

Based on the findings of this study, it seems as though *Cbr-ivp-3* is functioning in a manner similar to some SynMuv genes. Despite previous speculation that this may not be the case (Sharanya et al. 2015), the findings of this thesis strongly

suggest otherwise. *Cbr-ivp-3* is a negative regulator of vulval differentiation by inhibiting the inappropriate division of vulval precursors. In all three *Cbr-ivp-3* mutant animals, additional VPCs were observed to adopt vulval fates, leading to a Muv phenotype. Furthermore, it was found that *Cbr-lin-3* expression is increased in *Cbr-ivp(sy5216)* and knockdown of *Cbr-lin-3* in *Cbr-ivp(sy5216)* results in rescue of the muv phenotype. Thus, *Cbr-ivp-3* functions to negatively regulate the *Cbr-lin-3* inductive pathway. Defects associated with the Lin-3/EGF pathway, such as overexpressed or constitutively activated EGFRs or misregulated EGF ligands are commonly associated with cancer (Normanno et al. 2006). Genes that negatively regulate such proteins might serve to inhibit inappropriate signalling, and thus act similar to tumour suppressor genes. It is possible that *Cbr-ivp-3* functions as a tumour suppressor by preventing over-expression of *Cbr-lin-3* and thus cell proliferation and possibly cell fate specification. Based on the presence of the RNase H-like domain, Cbr-IVP-3 is predicted to have nucleic acid binding activity. It is possible that Cbr-IVP-3 translocates into the nucleus to regulate gene expression.

All of the characteristics of *Cbr-ivp-3* identified in this study are also characteristics of SynMuv genes. As previously discussed, the Muv phenotype observed in SynMuv mutants are caused by the dysregulation of *lin-3*, indicating that SynMuv genes negatively regulate vulval development by means of repressing *ivp-3* expression. Molecular characterization of SynMuv genes, commonly indicates their involvement in chromatin-level transcriptional regulation. Since the protein domain information predicts that *Cbr-ivp-3* is involved in nucleic acid binding activity, it is possible that Cbr-IVP-3 may translocate into the nucleus and regulate gene expression, similar to the SynMuv genes. Further studies can be done to confirm if this is indeed the case.

The role of *C. elegans ivp-3* in vulval development is yet to be determined. The findings in this study suggest that *ivp-3* is an important gene necessary for growth to a fertile adult and may play a role in germline development, oogenesis, spermatogenesis, ovulation or fertilization. It is possible that the Pvl phenotype observed in animals homozygous for the deletion site in the *ivp-3(gk3691)* strain, may caused by the induction of multiple VPCs to form a single protrusion. Thus,

83

*ivp-3* may play a role in vulval development. Further experimentation is required in order to determine the role of *ivp-3* in *C. elegans.* This can then allow for an in-depth comparison with *Cbr-ivp-3.*

## 4.2 Future Directions

The findings of this thesis have contributed to an understanding of a novel gene involved in the negative regulation of the vulva. A thorough molecular genetic analyses of *ivp-3* in *C. briggsae* and *C. elegans* has provided a platform for future experiments to further understand the function of *ivp-3* and its role in vulval development. Although the phenotypes and molecular identities of *Cbr-ivp-3* have been identified, more work must be carried out in order to determine the exact role of *ivp-3* during development in both nematode species.

### 4.2.1 Validating genes identified by RNAseq data

Validation of the 7 target genes selected from the RNA-seq dataset, indicated that only two of the seven (29%) genes followed the same trends in expression, observed in the RNA-seq analysis. Further validation of additional mRNA targets in *Cbr-ivp(sy5216)* will allow for a greater understanding of the extent of accuracy of the RNA-seq results.

Once the accuracy of the RNA-seq results has been confirmed, those putative target genes that are successfully validated by RT-qPCR could be analyzed for further identification of their involvement in the Muv phenotype observed in *Cbr-ivp(sy5216).* One way to do this may be to knockdown such genes using RNAi. A *Cbr-ivp(sy5216)* mutant in an RNAi hypersensitive background has already been built to investigate RNAi-mediated reduction of *Cbr-lin-3.* This mutant can also be used determine the effects of knockdown of overexpressed genes identified by RNA-seq and RT-qPCR. A similar experiment could be done in parallel in the wild type *C. briggsae* RNAi hypersensitive background to determine whether the knockdown of the gene alone has any effect on vulval development. A comparative

analysis of the target gene of interest can also be carried out if the gene has an ortholog in *C. elegans*. Using RNAi the gene could be knocked down in *C. elegans* to determine if the mechanism is conserved. This comprehensive and comparative analysis of the putative target genes established in this study will allow us to further elucidate the mechanism for the Muv phenotype in *ivp-3* mutants.

### 4.2.2 Generating a translational fusion reporter construct for *Cbr-ivp-3*

The larval expression profile for *Cbr-ivp-3* has previously been determined (Grün et al. 2014). In order to visualize the active location of the *Cbr-ivp-3* throughout development in wild type animals, a translational reporter plasmid can be constructed. The translational *Cbr-ivp-3::GFP* fusion would include the entire genomic region, allowing observation of *Cbr-ivp-3* expression in live animals. In SynMuv double mutants, *lin-3* is ectopically expressed throughout the animal whereas in wild type animals, *lin-3* expression is restricted to certain tissues, specifically the pharynx, anchor cell, gonad and tail (Cui et al. 2006). In addition, the expression of *lin-3* from the AC, in *C. elegans* wild type animals, requires the function of the transcription factor HLH-2/E/Daughterless and an unidentified nuclear hormone receptor (NHR) (Hwang and Sternberg 2004). Gonad ablation experiments demonstrate that *Cbr-ivp(sy5216)* can bypass the requirement of the inductive signal from the AC (Sharanya et al. 2015). It is likely that *Cbr-ivp-3* does not function to negatively regulate *Cbr-lin-3* at the level of transcription within the AC but it may function in the hyp7 syncytium to keep *lin-3* repressed. This is commonly observed in SynMuv genes. Identifying the spatial expression of *Cbr-ivp-3* in wild type animals through the use of a translational reporter, can determine if *Cbr-ivp-3* is also present in the tissues where SynMuv genes are found to restrict *lin-3*. Furthermore, if *Cbr-ivp-3* is present in the hyp7 syncytium, it shows that *ivp-3* functions to regulate *lin-3* in a similar manner to SynMuv genes, providing further evidence that *Cbr-ivp-3* may be a SynMuv gene.

### 4.2.3 The phenotypic rescue of *Cbr-ivp-3* using *C. elegans ivp-3*

A rescue experiment in which the wild type copy of *C. elegans ivp-3* is injected into *Cbr-ivp(sy5216)* can be carried out to determine whether the *C. elegans* copy of *ivp-3* would compensate for and rescue the mutant phenotype. A 9kb fragment was amplified and includes introns as well as 1899bp of the 5'UTR and 1227bp of 3'UTR. The fragment has been confirmed via sequencing and an injection mix, containing Myo-2::GFP along with the *Cel-ivp-3* fragment has been prepared. Injections into young adult *Cbr-ivp(sy5216)* hermaphrodite animals has been unsuccessful thus far. The generation of rescue lines would provide insight into the functional differences and/or similarities in *ivp-3* in both species. Since transgenic rescues are not always complete in the nematode species, it will be necessary to generate multiple lines to determine the capacity of the *C. elegans* gene to rescue the vulva defect in *C. briggsae.*

### 4.2.4 Identifying functional components of *Cbr-ivp-3* using suppressor screens

Suppressor screens can be used to to identify components that function in a genetic pathway. A mutagen, such as EMS, is used to induce mutations in the sperm and oocytes of mutant hermaphrodites. Second-site mutations that either enhance (worsen) or suppress (rescue) that phenotype can then be screened for (Jorgensen and Mango 2002). Second-site mutations can help identify proteins involved in the same process as that disrupted in the starting strain. Such screens have led to monumental discoveries in the vulval development pathway. For example, identification of proteins in the MAP kinase signalling pathway were identified by screening for mutations that suppress the vulval defects caused by an activated *let-60* gene (Lackner et al. 1994). Another example can be seen in the the *lin-15* operon that negatively regulates the RAS pathway. EGF- receptor signaling is found to be constitutively active in loss-of-function mutations of this operon, thus resulting in a Muv phenotype (Han et al. 1990). Screens for second-site mutations

that suppressed the Muv phenotype of *lin-15* mutations allowed for the identification of components both upstream and downstream of RAS, including mutations in the EGF tyrosine-kinase receptor LET-23 (Han et al. 1990).

Because such a screen involves a strain whose genetic composition causes a defined phenotypic defect, *Cbr-ivp(sy5216)* would make an excellent candidate for this type of experiment. The second-site mutations, generated by such a screen, can help identify proteins that are involved in the same process as *Cbr-ivp-3*. *Cbr-ivp(sy5216)* mutants can be mutagenized using EMS and second-site mutations that suppress the Muv phenotype can then be screened for. Outcrossing and genetic mapping of the suppressed Muv mutant can then be performed to determine the identity of the second-site mutations. The second-site mutations can help identify components involved in the same process as that disrupted in *Cbr-lin(sy5216)*.

### 4.2.5  Further validation of *ivp-3(gk3691)*

The Pvl phenotype, found in animals homozygous for the deletion site, has been observed in adult hermaphrodites at the plate level only. Examination under Nomarski optics at the L4 stage, can be used to identify VPC induction patterns in these animals. It is possible that the Pvl phenotype may be due to multiple VPCs inducing to form a single protrusion, indicative of a Muv phenotype. This would suggest that the role of *ivp-3* in vulval development may be conserved between *C. elegans* and *C. briggsae*.

The results suggest that embryonic and larval lethality are not the cause of the reduced ratio of Pvl, sterile, homozygous animals. The observed phenotypic ratio may be a result of problems that occur prior to the formation of the embryo, such as defects in germline development, oogenesis, spermatogenesis, ovulation or fertilization. These fertility defects can be investigated by examining morphological events during oocyte growth, maturation, and ovulation which can be directly observable using Nomarski microscopy in living animals (Ward and Carrel 1979). McCarter et al. (1999) have developed a timeline of morphological events during oocyte growth, maturation, and ovulation in *C. elegans*. For example, oocyte

development can be observed when the the nucleolus disappears, meiotic maturation can be seen when the nuclear envelope begins to breakdown, ovulation can be noted when the oocyte begins to enter the spermatheca, the presence of polar bodies signify meiotic divisions, and embryogenesis can be seen when the pronuclei fuse (McCarter et al. 1999). Examining such morphological events in *ivp-3(gk3691)* animals using Normarki microscopy, may be helpful in determining the cause of the reduced ratio of Pvl, sterile, homozygous animals and thus provide insight into the role of *Cel-ivp-3*.

Lastly, a rescue experiment in which the wild type copy of *Cbr-ivp-3* is injected into *ivp-3(gk3691)* animals, homozygous for the deletion site can be carried out to determine whether the *C. briggsae* copy of *ivp-3* would compensate for and rescue the mutant phenotype. The generation of rescue lines would shed light on the functional conservation of domains throughout evolution.

# Bibliography

Abel, E. V., Kim, E. J., Wu, J., Hynes, M., Bednar, F., Proctor, E., Wang, L., Dziubinski, M. L., and Simeone, D. M. (2014). The Notch pathway is important in maintaining the cancer stem cell population in pancreatic cancer. *PloS one* 9(3), e91983.

Alper, S. and Podbilewicz, B. (2008). Cell fusion in Caenorhabditis elegans. *Cell Fusion: Overviews and Methods*, 53–74.

Ambros, V. (1999). Cell cycle-dependent sequencing of cell fate decisions in Caenorhabditis elegans vulva precursor cells. *Development* 126(9), 1947–1956.

Andersson, E. R., Sandberg, R., and Lendahl, U. (2011). Notch signaling: simplicity in design, versatility in function. *Development* 138(17), 3593–3612.

Artavanis-Tsakonas, S., Rand, M. D., and Lake, R. J. (1999). Notch signaling: cell fate control and signal integration in development. *Science* 284(5415), 770–776.

Bird, R. C. (2003). Role of cyclins and cyclin-dependent kinases in G1 phase progression. *G1 Phase Progression. Kluwer Academic/Plenum, New York*, 40–57.

Blencowe, B. J. (2006). Alternative splicing: new insights from global analyses. *Cell* 126(1), 37–47.

Blomen, V. and Boonstra, J. (2007). Cell fate determination during G1 phase progression. *Cellular and Molecular Life Sciences* 64(23), 3084–3104.

Boxer, L. M. and Dang, C. V. (2001). Translocations involving c-myc and c-myc function. *Oncogene* 20(40), 5595.

Bray, S. J. (2016). Notch signalling in context. *Nature Reviews Molecular Cell Biology* 17(11), 722–735.

Brenner, S. (1974). The genetics of Caenorhabditis elegans. *Genetics* 77(1), 71–94.

Ceol, C. J. and Horvitz, H. R. (2001). dpl-1 DP and efl-1 E2F act with lin-35 Rb to antagonize Ras signaling in C. elegans vulval development. *Molecular cell* 7(3), 461–473.

Ceol, C. J. and Horvitz, H. (2004). A new class of C. elegans synMuv genes implicates a Tip60/NuA4-like HAT complex as a negative regulator of Ras signaling. *Developmental cell* 6(4), 563–576.

Chamorro, M. N., Schwartz, D. R., Vonica, A., Brivanlou, A. H., Cho, K. R., and Varmus, H. E. (2005). FGF-20 and DKK1 are transcriptional targets of β-catenin and FGF-20 is implicated in cancer and development. *The EMBO journal* 24(1), 73–84.

Chen, J., Li, X., and Greenwald, I. (2004). sel-7, a positive regulator of lin-12 activity, encodes a novel nuclear protein in Caenorhabditis elegans. *Genetics* 166(1), 151–160.

Church, D. L., Guan, K.-L., and Lambie, E. J. (1995). Three genes of the MAP kinase cascade, mek-2, mpk-1/sur-1 and let-60 ras, are required for meiotic cell cycle progression in Caenorhabditis elegans. *Development* 121(8), 2525–2535.

Clark, S. G., Lu, X., and Horvitz, H. R. (1994). The Caenorhabditis elegans locus lin-15, a negative regulator of a tyrosine kinase signaling pathway, encodes two different proteins. *Genetics* 137(4), 987–997.

Coghlan, A. and Wolfe, K. H. (2002). Fourfold faster rate of genome rearrangement in nematodes than in Drosophila. *Genome research* 12(6), 857–867.

Cui, M., Chen, J., Myers, T. R., Hwang, B. J., Sternberg, P. W., Greenwald, I., and Han, M. (2006). SynMuv genes redundantly inhibit lin-3/EGF expression to prevent inappropriate vulval induction in C. elegans. *Developmental cell* 10(5), 667–672.

Cutter, A. D. (2008). Divergence times in Caenorhabditis and Drosophila inferred from direct estimates of the neutral mutation rate. *Molecular biology and evolution* 25(4), 778–786.

Deshpande, R., Inoue, T., Priess, J. R., and Hill, R. J. (2005). lin-17/Frizzled and lin-18 regulate POP-1/TCF-1 localization and cell type specification during C. elegans vulval development. *Developmental biology* 278(1), 118–129.

Dhillon, A. S., Hagan, S., Rath, O., and Kolch, W. (2007). MAP kinase signalling pathways in cancer. *Oncogene* 26(22), 3279–3290.

Eisenmann, D. M., Maloof, J. N., Simske, J. S., Kenyon, C., and Kim, S. K. (1998). The beta-catenin homolog BAR-1 and LET-60 Ras coordinately regulate the Hox gene lin-39 during Caenorhabditis elegans vulval development. *Development* 125(18), 3667–3680.

Fay, D. S. and Yochem, J. (2007). The SynMuv genes of Caenorhabditis elegans in vulval development and beyond. *Developmental biology* 306(1), 1–9.

Félix, M.-A. and Wagner, A. (2008). Robustness and evolution: concepts, insights and challenges from a developmental model system. *Heredity* 100(2), 132–140.

Ferguson, E. L. and Horvitz, H. R. (1985). Identification and characterization of 22 genes that affect the vulval cell lineages of the nematode Caenorhabditis elegans. *Genetics* 110(1), 17–72.

Ferguson, E. L. and Horvitz, H. R. (1989). The multivulva phenotype of certain Caenorhabditis elegans mutants results from defects in two functionally redundant pathways. *Genetics* 123(1), 109–121.

Ferguson, E. L., Sternberg, P. W., and Horvitz, H. R. (1987). A genetic pathway for the specification of the vulval cell lineages of Caenorhabditis elegans. *Nature* 326(6110), 259–267.

Ferrando, A. A. (2009). The role of NOTCH1 signaling in T-ALL. *ASH Education Program Book* 2009(1), 353–361.

Galluzzo, P. and Bocchetta, M. (2011). Notch signaling in lung cancer. *Expert review of anticancer therapy* 11(4), 533–540.

Gartner, A., Milstein, S., Ahmed, S., Hodgkin, J., and Hengartner, M. O. (2000). A conserved checkpoint pathway mediates DNA damage–induced apoptosis and cell cycle arrest in C. elegans. *Molecular cell* 5(3), 435–443.

Goodspeed, A., Heiser, L. M., Gray, J. W., and Costello, J. C. (2016). Tumor-derived cell lines as molecular models of cancer pharmacogenomics. *Molecular Cancer Research* 14(1), 3–13.

Gowen, L. C., Johnson, B. L., Latour, A. M., Sulik, K. K., and Koller, B. H. (1996). Brca1 deficiency results in early embryonic lethality characterized by neuroepithelial abnormalities. *Nature genetics* 12(2), 191–194.

Greenwald, I. (1998). LIN-12/Notch signaling: lessons from worms and flies. *Genes & development* 12(12), 1751–1762.

Greenwald, I. S., Sternberg, P. W., and Horvitz, H. R. (1983). The lin-12 locus specifies cell fates in Caenorhabditis elegans. *Cell* 34(2), 435–444.

Gross, K., Wronski, A., Skibinski, A., Phillips, S., and Kuperwasser, C. (2016). Cell Fate Decisions During Breast Cancer Development. *Journal of developmental biology* 4(1), 4.

Grün, D., Kirchner, M., Thierfelder, N., Stoeckius, M., Selbach, M., and Rajewsky, N. (2014). Conservation of mRNA and protein expression during development of C. elegans. *Cell reports* 6(3), 565–577.

Gupta, B. P., Johnsen, R., and Chen, N. (2007). Genomics and biology of the nematode Caenorhabditis briggsae.

Han, M., Aroian, R. V., and Sternberg, P. W. (1990). The let-60 locus controls the switch between vulval and nonvulval cell fates in Caenorhabditis elegans. *Genetics* 126(4), 899–913.

Han, M., Golden, A., Han, Y., and Sternberg, P. W. (1993). C. elegans lin-45 raf gene participates in let-60 ras-stimulated vulval differentiation. *Nature* 363(6425), 133.

He, G., Siddik, Z. H., Huang, Z., Wang, R., Koomen, J., Kobayashi, R., Khokhar, A. R., and Kuang, J. (2005). Induction of p21 by p53 following DNA damage inhibits both Cdk4 and Cdk2 activities. *Oncogene* 24(18), 2929–2943.

He, T.-C., Sparks, A. B., Rago, C., Hermeking, H., Zawel, L., Da Costa, L. T., Morin, P. J., Vogelstein, B., and Kinzler, K. W. (1998). Identification of c-MYC as a target of the APC pathway. *Science* 281(5382), 1509–1512.

Hendriks, G.-J., Gaidatzis, D., Aeschimann, F., and Großhans, H. (2014). Extensive oscillatory gene expression during C. elegans larval development. *Molecular cell* 53(3), 380–392.

Hill, R. J. and Sternberg, P. W. (1992). The gene lin-3 encodes an inductive signal for vulval development in C. elegans. *Nature* 358(6386), 470.

Hirsh, D., Oppenheim, D., and Klass, M. (1976). Development of the reproductive system of Caenorhabditis elegans. *Developmental biology* 49(1), 200–219.

Hoffmann, I. (2000). The role of Cdc25 phosphatases in cell cycle checkpoints. *Protoplasma* 211(1), 8–11.

Holland, J. D., Klaus, A., Garratt, A. N., and Birchmeier, W. (2013). Wnt signaling in stem and cancer stem cells. *Current opinion in cell biology* 25(2), 254–264.

Hunter, T. and Pines, J. (1994). Cyclins and cancer II: cyclin D and CDK inhibitors come of age. *Cell* 79(4), 573–582.

Hwang, B. J. and Sternberg, P. W. (2004). A cell-specific enhancer that specifies lin-3 expression in the C. elegans anchor cell for vulval development. *Development* 131(1), 143–151.

Inoue, T., Oz, H. S., Wiland, D., Gharib, S., Deshpande, R., Hill, R. J., Katz, W. S., and Sternberg, P. W. (2004). C. elegans LIN-18 is a Ryk ortholog and functions in parallel to LIN-17/Frizzled in Wnt signaling. *Cell* 118(6), 795–806.

James, R. G., Conrad, W. H., and Moon, R. T. (2008). $\beta$-catenin-independent Wnt pathways: signals, core proteins, and effectors. *Wnt signaling: Pathway methods and mammalian models*, 131–144.

Jorgensen, E. M. and Mango, S. E. (2002). The art and design of genetic screens: Caenorhabditis elegans. *Nature Reviews Genetics* 3(5), 356–369.

Katoh, M. (2008). WNT signaling in stem cell biology and regenerative medicine. *Current drug targets* 9(7), 565–570.

Katz, W. S., Lesa, G. M., Yannoukakos, D., Clandinin, T. R., Schlessinger, J., and Sternberg, P. W. (1996). A point mutation in the extracellular domain activates LET-23, the Caenorhabditis elegans epidermal growth factor receptor homolog. *Molecular and cellular biology* 16(2), 529–537.

Khanna-Gupta, A., Chen, J., Silver, M., Sun, H., Abayasekara, N., Halene, S., Sportoletti, P., Pandolfi, P. P., and Berliner, N. (2009). Nucleophosmin-1 Interacts with CCAAT Enhancer Binding Protein Alpha (C/EBP$\alpha$) to Facilitate Granulocyte Maturation: Implications in MDS and AML. *Blood* 114(22), 2768–2768.

Kim, J. and Orkin, S. H. (2011). Embryonic stem cell-specific signatures in cancer: insights into genomic regulatory networks and implications for medicine. *Genome medicine* 3(11), 75.

Kimble, J. and Hirsh, D. (1979). The postembryonic cell lineages of the hermaphrodite and male gonads in Caenorhabditis elegans. *Developmental biology* 70(2), 396–417.

Kiontke, K. and Sudhaus, W. (2006). Ecology of Caenorhabditis species. *WormBook* 9, 1–14.

Kitagawa, K., Kotake, Y., and Kitagawa, M. (2009). Ubiquitin-mediated control of oncogene and tumor suppressor gene products. *Cancer science* 100(8), 1374–1381.

Knudsen, E. S. and Knudsen, K. E. (2006). Retinoblastoma tumor suppressor: where cancer meets the cell cycle. *Experimental Biology and Medicine* 231(7), 1271–1281.

Kobet, R. A., Pan, X., Zhang, B., Pak, S. C., Asch, A. S., and Lee, M.-H. (2014). Caenorhabditis elegans: a model system for anti-cancer drug discovery and therapeutic target identification. *Biomolecules & therapeutics* 22(5), 371–383.

Krause, M., Harrison, S. W., Xu, S.-Q., Chen, L., and Fire, A. (1994). Elements regulating cell-and stage-specific expression of the C. elegans MyoD family homolog hlh-1. *Developmental biology* 166(1), 133–148.

Lackner, M. R., Kornfeld, K., Miller, L. M., Horvitz, H. R., and Kim, S. K. (1994). A MAP kinase homolog, mpk-1, is involved in ras-mediated induction of vulval cell fates in Caenorhabditis elegans. *Genes & development* 8(2), 160–173.

Lambie, E. J. (2002). Cell proliferation and growth in C. elegans. *Bioessays* 24(1), 38–53.

Lambie, E. J. and Kimble, J. (1991). Two homologous regulatory genes, lin-12 and glp-1, have overlapping functions. *Development* 112(1), 231–240.

Lange, C. A. and Yee, D. (2008). Progesterone and breast cancer. *Women's Health* 4(2), 151–162.

Leuken, R. van, Clijsters, L., and Wolthuis, R. (2008). To cell cycle, swing the APC/C. *Biochimica et Biophysica Acta (BBA)-Reviews on Cancer* 1786(1), 49–59.

Lodish, H., Berk, A., Zipursky, S., Matsudaira, P., Baltimore, D., and Darnell, J. (2000). Tumor cells and the onset of cancer. *Molecular Cell Biology*.

Lu, X. and Horvitz, H. R. (1998). lin-35 and lin-53, two genes that antagonize a C. elegans Ras pathway, encode proteins similar to Rb and its binding protein RbAp48. *Cell* 95(7), 981–991.

Maduro, M. F. (2010). Cell fate specification in the C. elegans embryo. *Developmental Dynamics* 239(5), 1315–1329.

Marshall, C. (1995). Specificity of receptor tyrosine kinase signaling: transient versus sustained extracellular signal-regulated kinase activation. *Cell* 80(2), 179–185.

McCarter, J., Bartlett, B., Dang, T., and Schedl, T. (1999). On the Control of Oocyte Meiotic Maturation and Ovulation inCaenorhabditis elegans. *Developmental biology* 205(1), 111–128.

Mello, C., Kramer, J., Stinchcomb, D., and Ambros, V. (1991). Efficient gene transfer in C. elegans after microinjection of DNA into germline cytoplasm: extrachromosomal maintenance and integration of transforming sequences. *EMBO J* 10, 3959–3970.

Miyamoto, S. and Rosenberg, D. W. (2011). Role of Notch signaling in colon homeostasis and carcinogenesis. *Cancer science* 102(11), 1938–1942.

Moon, B.-S., Jeong, W.-J., Park, J., Kim, T. I., Min, D. S., and Choi, K.-Y. (2014). Role of oncogenic K-Ras in cancer stem cell activation by aberrant Wnt/$\beta$-catenin signaling. *JNCI: Journal of the National Cancer Institute* 106(2).

Mostafavi, S., Ray, D., Warde-Farley, D., Grouios, C., and Morris, Q. (2008). GeneMANIA: a real-time multiple association network integration algorithm for predicting gene function. *Genome biology* 9(1), S4.

Myers, T. R. and Greenwald, I. (2007). Wnt signal from multiple tissues and lin-3/EGF signal from the gonad maintain vulval precursor cell competence in Caenorhabditis elegans. *Proceedings of the National Academy of Sciences* 104(51), 20368–20373.

Narasimha, A. M., Kaulich, M., Shapiro, G. S., Choi, Y. J., Sicinski, P., and Dowdy, S. F. (2014). Cyclin D activates the Rb tumor suppressor by monophosphorylation. *Elife* 3, e02872.

Neidich, J. A. (2005). Inborn Errors of Development: The Molecular Basis of Clinical Disorders of Morphogenesis. *American journal of human genetics* 76(2), 368.

Nevins, J. R. (2001). The Rb/E2F pathway and cancer. *Human molecular genetics* 10(7), 699–703.

Nishikawa, S.-I., Osawa, M., Yonetani, S., Torikai-Nishikawa, S., and Freter, R. (2008). Niche required for inducing quiescent stem cells. In: *Cold Spring Harbor symposia on quantitative biology*. Vol. 73. Cold Spring Harbor Laboratory Press, 67–71.

Normanno, N., De Luca, A., Bianco, C., Strizzi, L., Mancino, M., Maiello, M. R., Carotenuto, A., De Feo, G., Caponigro, F., and Salomon, D. S. (2006). Epidermal growth factor receptor (EGFR) signaling in cancer. *Gene* 366(1), 2–16.

Nuez, I. and Félix, M.-A. (2012). Evolution of susceptibility to ingested double-stranded RNAs in Caenorhabditis nematodes. *PLoS One* 7(1), e29811.

Nusse, R., Fuerer, C., Ching, W., Harnish, K., Logan, C., Zeng, A., Ten Berge, D., and Kalani, Y. (2008). Wnt signaling and stem cell control. In: *Cold Spring Harbor symposia on quantitative biology.* Vol. 73. Cold Spring Harbor Laboratory Press, 59–66.

Okabe, H., Lee, S.-H., Phuchareon, J., Albertson, D. G., McCormick, F., and Tetsu, O. (2006). A critical role for FBXW8 and MAPK in cyclin D1 degradation and cancer cell proliferation. *PloS one* 1(1), e128.

Pandolfi, P., Grignani, F., Alcalay, M., Mencarelli, A., Biondi, A., LoCoco, F., and Pelicci, P. (1991). Structure and origin of the acute promyelocytic leukemia myl/RAR alpha cDNA and characterization of its retinoid-binding and trans-activation properties. *Oncogene* 6(7), 1285–1292.

Patterson, G. I., Koweek, A., Wong, A., Liu, Y., and Ruvkun, G. (1997). The DAF-3 Smad protein antagonizes TGF-$\beta$-related receptor signaling in the Caenorhabditis elegansdauer pathway. *Genes & development* 11(20), 2679–2690.

Pellegrino, M. W., Farooqui, S., Fröhli, E., Rehrauer, H., Kaeser-Pebernard, S., Müller, F., Gasser, R. B., and Hajnal, A. (2011). LIN-39 and the EGFR/RAS/MAPK pathway regulate C. elegans vulval morphogenesis via the VAB-23 zinc finger protein. *Development* 138(21), 4649–4660.

Prior, I. A., Lewis, P. D., and Mattos, C. (2012). A comprehensive survey of Ras mutations in cancer. *Cancer research* 72(10), 2457–2467.

Queralt, E. and Uhlmann, F. (2008). Cdk-counteracting phosphatases unlock mitotic exit. *Current opinion in cell biology* 20(6), 661–668.

Rajalingam, K., Schreck, R., Rapp, U. R., and Albert, Š. (2007). Ras oncogenes and their downstream targets. *Biochimica Et Biophysica Acta (BBA)-Molecular Cell Research* 1773(8), 1177–1195.

Reedijk, M. (2012). Notch signaling and breast cancer. In: *Notch Signaling in Embryology and Cancer.* Springer, 241–257.

Ren, P., Lim, C.-S., Johsen, R., Albert, P. S., Pilgrim, D., and Riddle, D. L. (1996). Control of C. elegans. Larval Development by Neuronal Expression of b Homolog. *Science* 274, 1389–1391.

Ristorcelli, E. and Lombardo, D. (2010). Targeting Notch signaling in pancreatic cancer. *Expert opinion on therapeutic targets* 14(5), 541–552.

Rousselot, P., Hardas, B., Patel, A., Guidez, F., Gäken, J., Castaigne, S., Dejean, A., Degos, L., Farzaneh, F., et al. (1994). The PML-RAR alpha gene product of the t (15; 17) translocation inhibits retinoic acid-induced granulocytic differentiation and mediated transactivation in human myeloid cells. *Oncogene* 9(2), 545–551.

Saffer, A. M., Kim, D. H., Oudenaarden, A. van, and Horvitz, H. R. (2011). The Caenorhabditis elegans synthetic multivulva genes prevent ras pathway activation by tightly repressing global ectopic expression of lin-3 EGF. *PLoS Genet* 7(12), e1002418.

Schulze, W. X., Deng, L., and Mann, M. (2005). Phosphotyrosine interactome of the ErbB-receptor kinase family. *Molecular systems biology* 1(1).

Schumacher, B., Hofmann, K., Boulton, S., and Gartner, A. (2001). The C. elegans homolog of the p53 tumor suppressor is required for DNA damage-induced apoptosis. *Current biology* 11(21), 1722–1727.

Seydoux, G. and Greenwald, I. (1989). Cell autonomy of lin-12 function in a cell fate decision in C. elegans. *Cell* 57(7), 1237–1245.

Sharanya, D., Fillis, C. J., Kim, J., Zitnik, E. M., Ward, K. A., Gallagher, M. E., Chamberlin, H. M., and Gupta, B. P. (2015). Mutations in Caenorhabditis briggsae identify new genes important for limiting the response to EGF signaling during vulval development. *Evolution & development* 17(1), 34–48.

Sharanya, D., Thillainathan, B., Marri, S., Bojanala, N., Taylor, J., Flibotte, S., Moerman, D. G., Waterston, R. H., and Gupta, B. P. (2012). Genetic control of vulval development in Caenorhabditis briggsae. *G3: Genes| Genomes| Genetics* 2(12), 1625–1641.

Sherr, C. J. (2004). Principles of tumor suppression. *Cell* 116(2), 235–246.

Sherr, C. J. and McCormick, F. (2002). The RB and p53 pathways in cancer. *Cancer cell* 2(2), 103–112.

Sherr, C. J. and Roberts, J. M. (1999). CDK inhibitors: positive and negative regulators of G1-phase progression. *Genes & development* 13(12), 1501–1512.

Sherwood, D. R., Butler, J. A., Kramer, J. M., and Sternberg, P. W. (2005). FOS-1 promotes basement-membrane removal during anchor-cell invasion in C. elegans. *Cell* 121(6), 951–962.

Simske, J. S. and Kim, S. K. (1995). Sequential signalling during Caenorhabditis elegans vulval induction. *Nature* 375(6527), 142.

Sommer, R. J. (2005). Evolution of development in nematodes related to C. elegans.

Stein, L. D., Bao, Z., Blasiar, D., Blumenthal, T., Brent, M. R., Chen, N., Chinwalla, A., Clarke, L., Clee, C., Coghlan, A., et al. (2003). The genome sequence of Caenorhabditis briggsae: a platform for comparative genomics. *PLoS Biol* 1(2), e45.

Sternberg, P. W. (2005). Vulval development. *WormBook* 25, 1–28.

Sternberg, P. W. and Horvitz, H. R. (1986). Pattern formation during vulval development in C. elegans. *Cell* 44(5), 761–772.

Sternberg, P. W. and Horvitz, H. R. (1989). The combined action of two intercellular signaling pathways specifies three cell fates during vulval induction in C. elegans. *Cell* 58(4), 679–693.

Sulston, J. and White, J. (1980). Regulation and cell autonomy during postembryonic development of Caenorhabditis elegans. *Developmental biology* 78(2), 577–597.

Sulston, J. E. and Horvitz, H. R. (1977). Post-embryonic cell lineages of the nematode, Caenorhabditis elegans. *Developmental biology* 56(1), 110–156.

Sundaram, M. (2006). RTK/Ras/MAPK signaling. WormBook, ed. The C. elegans Research Community. *WormBook*.

Tamura, Y., Simizu, S., and Osada, H. (2004). The phosphorylation status and anti-apoptotic activity of Bcl-2 are regulated by ERK and protein phosphatase 2A on the mitochondria. *FEBS letters* 569(1-3), 249–255.

Tan, P. B., Lackner, M. R., and Kim, S. K. (1998). MAP kinase signaling specificity mediated by the LIN-1 Ets/LIN-31 WH transcription factor complex during C. elegans vulval induction. *Cell* 93(4), 569–580.

Tax, F. E., Thomas, J. H., Ferguson, E. L., and Horvitzt, H. R. (1997). Identification and characterization of genes that interact with lin-12 in Caenorhabditis elegans. *Genetics* 147(4), 1675–1695.

Towatari, M., Ciro, M., Ottolenghi, S., Tsuzuki, S., and Enver, T. (2004). Involvement of mitogen-activated protein kinase in the cytokine-regulated phosphorylation of transcription factor GATA-1. *The Hematology Journal* 5(3), 262–272.

Trent, C., Tsung, N., and Horvitz, H. R. (1983). Egg-laying defective mutants of the nematode Caenorhabditis elegans. *Genetics* 104(4), 619–647.

Uyar, B., Chu, J. S., Vergara, I. A., Chua, S. Y., Jones, M. R., Wong, T., Baillie, D. L., and Chen, N. (2012). RNA-seq analysis of the C. briggsae transcriptome. *Genome research* 22(8), 1567–1580.

Vasef, M. A., Brynes, R. K., Sturm, M., Bromley, C., and Robinson, R. A. (1999). Expression of cyclin D1 in parathyroid carcinomas, adenomas, and hyperplasias: a paraffin immunohistochemical study. *Modern pathology: an official journal of the United States and Canadian Academy of Pathology, Inc* 12(4), 412–416.

Wang, M. and Sternberg, P. W. (1999). Competence and commitment of Caenorhabditis elegans vulval precursor cells. *Developmental biology* 212(1), 12–24.

Wang, M. and Sternberg, P. W. (2000). Patterning of the C. elegans 1 degrees vulval lineage by RAS and Wnt pathways. *Development* 127(23), 5047–5058.

Wang, X. and Sommer, R. J. (2011). Antagonism of LIN-17/Frizzled and LIN-18/Ryk in nematode vulva induction reveals evolutionary alterations in core developmental pathways. *PLoS Biol* 9(7), e1001110.

Ward, S. and Carrel, J. (1979). Fertilization and sperm competition in the nematode. *Caenorhabditis elegans*, 304–321.

Warde-Farley, D., Donaldson, S. L., Comes, O., Zuberi, K., Badrawi, R., Chao, P., Franz, M., Grouios, C., Kazi, F., Lopes, C. T., et al. (2010). The GeneMANIA prediction server: biological network integration for gene prioritization and predicting gene function. *Nucleic acids research* 38(suppl 2), W214–W220.

Webb, C. T., Shabalina, S. A., Ogurtsov, A. Y., and Kondrashov, A. S. (2002). Analysis of similarity within 142 pairs of orthologous intergenic regions of

Caenorhabditis elegans and Caenorhabditis briggsae. *Nucleic acids research* 30(5), 1233–1239.

Weinstein, N. and Podbilewicz, B. (2016). Organogenesis of the C. elegans Vulva and Control of Cell Fusion. In: *Organogenetic Gene Networks*. Springer, 9–56.

Wend, P., Holland, J. D., Ziebold, U., and Birchmeier, W. (2010). Wnt signaling in stem and cancer stem cells. In: *Seminars in cell & developmental biology*. Vol. 21. 8. Elsevier, 855–863.

Whelan, J. T., Hollis, S. E., Cha, D. S., Asch, A. S., and Lee, M.-H. (2012). Post-transcriptional regulation of the Ras-ERK/MAPK signaling pathway. *Journal of cellular physiology* 227(3), 1235–1241.

Wilson-Sanders, S. E. (2011). Invertebrate models for biomedical research, testing, and education. *ILAR J* 52(2), 126–152.

Winston, W. M., Sutherlin, M., Wright, A. J., Feinberg, E. H., and Hunter, C. P. (2007). Caenorhabditis elegans SID-2 is required for environmental RNA interference. *Proceedings of the National Academy of Sciences* 104(25), 10565–10570.

Wu, Y. and Han, M. (1994). Suppression of activated Let-60 ras protein defines a role of Caenorhabditis elegans Sur-1 MAP kinase in vulval differentiation. *Genes & Development* 8(2), 147–159.

Yamasaki, L. (2004). Role of the RB tumor suppressor in cancer. In: *Signal Transduction in Cancer*. Springer, 209–239.

Yoo, A. S., Bais, C., and Greenwald, I. (2004). Crosstalk between the EGFR and LIN-12/Notch pathways in C. elegans vulval development. *Science* 303(5658), 663–666.

Zetterberg, A., Larsson, O., and Wiman, K. G. (1995). What is the restriction point? *Current opinion in cell biology* 7(6), 835–842.

Zhan, T., Rindtorff, N., and Boutros, M. (2016). Wnt signaling in cancer. *Oncogene*.

Zhang, X. and Greenwald, I. (2011). Spatial Regulation of lag-2 Transcription During Vulval Precursor Cell Fate Patterning in Caenorhabditis eleganslag-2. *Genetics* 188(4), 847–858.

Zhao, Y., Bjørbæk, C., and Moller, D. E. (1996). Regulation and interaction of pp90rsk isoforms with mitogen-activated protein kinases. *Journal of Biological Chemistry* 271(47), 29773–29779.